AN EXPERIMENTAL STUDY OF THE EFFECT OF TEMPERATURE, PRESSURE AND FLOW RATE ON MODIFIED ZADRA GOLD ELUTION PROCESS

**A THESIS SUBMITTED TO THE GRADUATE
SCHOOL OF APPLIED SCIENCES
OF
NEAR EAST UNIVERSITY**

**By
PHILLIP PHIRI**

**In Partial Fulfillment of The Requirements For
the Degree of Master of Science
in
Mechanical Engineering**

NICOSIA, 2019

PHILLIP
PHIRI

AN EXPERIMENTAL STUDY OF THE EFFECT OF
TEMPERATURE, PRESSURE AND FLOW RATE ON
MODIFIED ZADRA GOLD ELUTION PROCESS

NEU
2019

AN EXPERIMENTAL STUDY OF THE EFFECT OF TEMPERATURE, PRESSURE AND FLOW RATE ON MODIFIED ZADRA GOLD ELUTION PROCESS

**A THESIS SUBMITTED TO THE
GRADUATE SCHOOL OF APPLIED SCIENCES
OF
NEAR EAST UNIVERSITY**

**By
PHILLIP PHIRI**

**In Partial Fulfillment of the Requirements for
the Degree of Masters of Science
in
Mechanical Engineering**

NICOSIA, 2019

Phillip PHIRI: AN EXPERIMENTAL STUDY OF THE EFFECT OF TEMPERATURE, PRESSURE AND FLOW RATE ON MODIFIED ZADRA GOLD ELUTION PROCESS

Approval of Director of Graduate School of Applied Sciences

Prof. Dr. Nadire ÇAVUŞ

We certify this thesis is satisfactory for the award of the degree of Master of Science in Mechanical Engineering

Examination Committee in Charge

Assist. Prof. Dr. Devrim AYDIN	Committee Chairman, Mechanical Engineering Department, EMU
Assist. Prof. Dr. Youssef KASSEM	Mechanical Engineering Department, NEU
Assist. Prof. Dr. Ali EVCİL	Mechanical Engineering Department, NEU
Assist. Prof. Dr. Ali. ŞEFIK	Co-Supervisor, Mechanical Engineering Department, CIU
Assoc. Prof. Dr. Hüseyin ÇAMUR	Supervisor, Mechanical Engineering Department, NEU

I hereby declare that, all the information in this document has been obtained and presented in accordance with academic rules and ethical conduct. I also declare that, as required by these rules and conduct, I have fully cited and referenced all materials and results that are not original to this work.

Name, Last Name: Phillip Phiri
Signature:
Date:

ACKNOWLEDGEMENTS

I would like to express my great gratitude to Assoc. Prof. Dr. Ing. Hüseyin Çamur my supervisor, Assist. Prof. Dr. Ali Şefik my co-supervisor for their patience and encouragement throughout this research. I am very grateful to them for giving me this opportunity. I wish to extend my appreciation to Eng. John Ajusa (Metallurgist Newmetco Mining Zimbabwe), who has provided the constructive inputs and invaluable advice for the maturation of my thesis. The time he has allocated to me is greatly appreciated.

I extend my thanks to Mr. Witness Mutsata as well, who lent his assistance to me whenever I asked for it. I am equally very thankful to my dear friends, Eng. Clemence Maffoti, Eng. Nigel Babvu, for their never-ending support to always keep me enthusiastic. I would like to use this opportunity to deliver a deep sense of gratitude towards my beloved companion, Rejoyce Nyengera. Her encouraging attitude and belief in me provide me with appreciation and self-confidence. I feel fortunate to know that she will always be by my side.

My deepest thanks go to my sisters for always being there for me and making my life meaningful. Nevertheless, special thanks go to my dearest, mother and father, who have brought me to this earth by the grace of God, I wish you were here being proud of your son, nevertheless, I will make you proud where ever you are because I believe you can see me. Finally, I want to thank Mr Paji and Sr Elizabeth for your great job. You believed in me and your initiative has forever changed my life. Words alone will never explain how much grateful I am. Above all I give great praise to God almighty, the greatest Scientist, for all this is by your grace and I give it back to you.

To my fiancé and family…

ABSTRACT

An investigation was performed in order to determine functional effect of the parameters that affect gold elution in a modified Zadra gold elution process. Elution of gold is a process where gold is desorbed or eluted back into solution by the effect of chemical and mechanical factors. This study focused on the mechanical factors namely, temperature, pressure and flow rate. An experimental test rig that mimics the Zadra gold elution circuit was used. The novelty of the study was centred on fluidising the contents of the reactor bed namely, gold loaded carbon. All the experiments where conducted in a fluidised bed reactor. Experiments were conducted for 7 hours. From each test, 4 samples were obtained every 2 hours. It was observed that as pressure increases gold concentration decreases. Starting from a pressure of 1 bar, gold concentration change decreased with increase in pressure to 1.5 bar up to 2bar. Gold concentration change increased as temperature increased. From 110^0C to 120^0C, gold concentration increased in the solution. However, gold concentration at 110^0C, was comparable to that at 130^0C. As flow rate increased, gold concentration increased in the solution. Two flow diversions of 32403 Re and 37608 Re conformed to this tendency. At low flow rate 23892 Re gold concentration change was almost constant.

Keywords: Zadra gold elution process; gold concentration; fluidised bed reactor

ÖZET

Bir Zadra altın elüsyon işleminde, altın elüsyonunu etkileyen parametrelerin fonksiyonel etkisini belirlemek için bir araştırma yapılmıştır. Altının elüsyonu, altının kimyasal veya mekanik faktörlerin etkisiyle çözüldüğü veya çözelti haline getirildiği bir işlemdir. Bu çalışma mekanik faktörler yani, sıcaklık, basınç ve akış hızı. Zadra altın elüsyon devresini taklit eden deneysel bir test teçhizatı kullanıldı. Çalışmanın yeniliği, reaktör yatağının içeriğinin akışkanlaştırılması üzerine odaklandı. Altın yüklü karbon Akışkanlaştırılmış yataklı bir reaktörde yapılan tüm deneyler. Deneyler 7 saat boyunca yapıldı. Her testten, 2 saatte bir 4 numune elde edildi. Basınç arttıkça altın konsantrasyonunun azaldığı gözlendi. 1 barlık bir basınçtan başlayarak, altın konsantrasyonundaki değişim, basınçtaki 2 bar'a kadar 1,5 bar'a yükselerek azalmıştır. Altın konsantrasyonu değişimi sıcaklık arttıkça arttı. 110^0C ila 120^0C arasında, çözelti içinde altın konsantrasyonu arttı. Bununla birlikte, 110^0C 'deki altın konsantrasyonu, 130^0C 'deki ile karşılaştırılabilir idi. Akış hızı arttıkça, çözeltide altın konsantrasyonu arttı. 32403 Re ve 37608 Re'nin iki akış sapması bu eğilime uyuyordu. Düşük akış hızında 23892 Re altın konsantrasyonu değişimi neredeyse sabitti.

Anahtar Kelimeler: Zadra altın elüsyon süreci; altın konsantrasyonu; akışkan yataklı reaktör

TABLE OF CONTENTS

ACKNOWLEDGEMENTS ii
ABSTRACT iv
ÖZET v
TABLE OF CONTENTS vi
LIST OF TABLES x
LIST OF FIGURES xi
LIST OF ABBREVIATIONS xii
LIST OF SYMBOLS xiv

CHAPTER 1: INTRODUCTION

1.1 Overview 1
1.2 Thesis Problem 1
1.3 The Aim and Novelty of the Thesis 1
1.4 Thesis Overview 2

CHAPTER 2: LITERATURE REVIEW

2.1 Overview 4
2.2 Gold Recovery Process 4
  2.2.1 Cyanidation 5
  2.2.2 Comminution 6
  2.2.3 Thickening 6
  2.2.4 Leaching 7
  2.2.5 Elution/Desorption Process 8
2.3 Factors Affecting Elution Process 8
  2.3.1 Effect of Temperature and Pressure on Elution Process 9
    2.3.1.1 Effect of Temperature on Cyanide Decomposition 11
  2.3.2 Effect of Flow Rate on Elution Process 12

2.3.3 Effect of Activated Carbon Selection on Elution Process 15
2.3.4 Effects of Reagents on Elution Process 16
2.3.4.1 Effects of Cyanide on Elution Process 16
2.3.4.2 Effects of Sodium Hydroxide on Elution Process 17
2.3.5 Effects of Catalysts on Elution Process 17
2.4 Electrowinning Cell Design 20
2.4.1 Electrowinning Cell Predicted Extraction Efficiency 21
2.4.2 Extraction Efficiency Curves 22
2.4.3 Eluate Temperature against Cell Efficiency 22
2.4.3.1 Eluate Temperature and Solution Chemistry in the Electrowinning Cell 22
2.4.4 Gas Generation During Electrowinning 22
2.4.5 Summary 23

CHAPTER 3: EXPERIMENTAL DESIGN AND METHODOLOGY

3.1 Overview 24
3.2 Introduction 24
3.2.1 Elution Reactor 26
3.2.2 Electrowinning Cell 28
3.2.3 Complete Assembled View of the Test Rig 30
3.2.4 Electrical and Control Circuitry 32
3.3 Equipment Sizing 34
3.3.1 Heating Element 34
3.3.2 Insulation Blanket 36
3.3.3 Minimum Fluidization Velocity 38
3.3.4 Pump Selection 40
3.3.4.1 Friction Head Hf for Pipe 41

3.3.4.2 Head Loss due to Sudden Contraction Hc from Elution Reactor to Pipe 41
3.3.4.3 Head Loss due to Sudden Contraction from EWC to Pipe 41
3.3.4.4 Head Loss due to Sudden Enlargement He 42
3.3.4.5 Total Dynamic Head 42
3.5 Material for Experiment 43
3.6 Experimental Set Up Conditions for Elution System 43
3.6.1 Flow Rate Control 43
3.5.2 Temperature Control 46
3.5.3 Pressure Control 46
3.6 Experimental Conditions 47
3.7 Experimental Procedure 48
3.8 Summary 49

CHAPTER 4: RESULTS AND DISCUSSIONS

4.1 Overview 50
4.1.1 Repeatability of the Experiment 50
4.1.2 Effect of Pressure on Elution 51
4.1.3 Effect of Temperature on Elution 53
4.1.4 Effect of Flow Rate on Elution 55
4.2 Summary 58

CHAPTER 5: CONCLUSIONS AND RECOMMENDATIONS

5.1 Overview 59
5.2 Conclusion 59
5.3 Recommendations 61

REFERENCES 62

APPENDICES 65

Appendix 1a: Valves/ Fittings/ Head Losses 66
Appendix 1b: Warman pipe friction chart 67
Appendix 2: Characteristic curves and performance data 68
Appendix 3: Properties of saturated water 69
Appendix 4a: First pressure test results 70
Appendix 4b: Second pressure test results 71
Appendix 4c: Third pressure test results 72
Appendix 5a: First temperature test results 73
Appendix 5b: Second temperature test results 74
Appendix 5c: Third temperature test results 75
Appendix 6a: First flow rate test results 76
Appendix 6b: Second flow rate test results 77
Appendix 6c: Third flow rate test results 78
Appendix 7: Pressure linearity graphs 79
Appendix 8: Temperature linearity graphs 80
Appendix 9: Flow rate linearity graphs 81

LIST OF TABLES

Table 3.1: Flow rates results and corresponding Reynolds number 46
Table 3.2: Experimental conditions for temperature test.. 47
Table 3.3: Experimental conditions for pressure test 47
Table 3.4: Experimental conditions for flow rate test 47
Table 4.1: Repeatability test results.. 50

LIST OF FIGURES

Figure 2.1: Cyanidation gold recovery process (Mular et al., 2002)........................... 5

Figure 2.2: Range of bed-surface heat transfer coefficients (Rhodes, 2008).............. 10

Figure 2.3: Cyanide profiles for elutions at different temperatures (Merwe, 1993) 13

Figure 2.4: Pressure versus velocity for packed and fluidised beds (Rhodes, 2008)... 14

Figure 2.5: Elution by ethanol at 40, 60, and 80^0C (Ubaldini et al., 2006)................. 19

Figure 2.6: Elution by isopropanol at 40, 60, and 80^0C (Ubaldini et al., 2006).......... 19

Figure 2.7: Elution by ethylene glycol at 40, 60, and 80^0C (Ubaldini et al., 2006)..... 20

Figure 3.1: Elution pressurized vessel... 27

Figure 3.2: Section view of the elution vessel.. 28

Figure 3.3: Electrowinning cell design.. 29

Figure 3.4: Section view through electrowinning cell design..................................... 29

Figure 3.5: 3D model elution circuit complete.. 30

Figure 3.6: Fully assembled elution circui 31

Figure 3.7: Wiring diagram for the elution test rig. 33

Figure 3.8: Elution system circuitry... 34

Figure 3.9: Problem illustration (Incropera, et al 2011).. 36

Figure 3.10: Thermal circuit (Incropera, et al 2011)... 37

Figure 4.1: Pressure test graph 51

Figure 4.2: Gold concentration change versus pressure difference graph.................... 52

Figure 4.3: Temperature test graph 53

Figure 4.4: Gold concentration change versus temperature difference graph............. 55

Figure 4.5: Flow rate test graph.. 56

Figure 4.6: Gold concentration change versus flow rate difference graph.................. 57

LIST OF ABBREVIATIONS

AARL:	Anglo American Research Laboratory
AD:	Apparent Density
A:	Silver
Ar:	Argon
A_u $(CN)_2^-$:	Aurocyanide Complex
Au:	Gold
BD:	Bulk Density
CIL:	Carbon in Leach
CIP:	Carbon in Pulp
CN:	Cyanide
EW:	Electrowinning
EWC	Electrowinning Cell
GBC 933 AA:	Atomic Adsorption machine
H_2O:	Water
H_2O_2:	Hydrogen Peroxide
H_2SO_4:	Sulphuric Acid
HCl:	Hydrochloric Acid
HCN:	Hydrogen Cyanide
HDPE:	High-density polyethylene
Kr:	Krypton
NaCN:	Sodium Cyanide
NaOH:	Sodium Hydroxide
Nu:	Nusselt Number
O_2:	Oxygen
OH^-:	Hydroxide
PV:	Process Variable
Re:	Reynolds Number
RIL:	Resins in Leach
S.G.:	Specific Density
SV:	Set Value

VSD: Variable Speed Drive

LIST OF SYMBOLS

A_1:	Inlet pipe cross section
A_2:	Outlet pipe cross section
A_s:	Surface area
C:	Gold concentration
C_p:	Specific heat capacity
D:	Diffusion coefficient of gold
d:	Diameter
dC/dx:	Concentration gradient
E_{ad}:	Adsorption energy
E_{des}:	Desorption energy
f:	Frictional factor
H:	Height
H_c:	Head loss due to sudden contraction
H_e:	Head loss due to sudden enlargement
H_f:	Frictional head
H_m:	Total dynamic head
h_{gc}:	Gas or liquid convective heat transfer coefficient
h_i:	Internal overall convection coefficient
h_o:	Room overall convection coefficient
h_{pc}:	Particle convective heat transfer coefficient
h_r:	Radiant heat transfer coefficient
J:	Flux
K:	Adsorption desorption equilibrium constant
K_B:	Boltzmann constant
K_c:	Contraction factor
K'':	Kozeny's Constant
k:	Thermal conductivity coefficient
k_{ad}:	Adsorption coefficient
k_{des}:	Desorption coefficient

L:	Length
l:	Thickness
m:	Mass
N:	Rotational speed
P:	Power
p:	Pressure
p^0:	Saturation vapour pressure
Q:	Volumetric flow rate
q:	Heat transfer rate
q_i'':	Inside heat flux
q_o'':	Outside heat flux
R:	Gas constant
R''_{cd}:	Thermal resistance due to conduction
$R''_{cv,i,\,i}$:	Internal thermal resistance due to convection
$R''_{cv,o,\,o}$:	External thermal resistance due to convection
r_{ad}:	Rate of adsorption
r_{des}:	Rate of desorption
S:	Surface area per unit volume of particle
T:	System temperature
$T_{(\infty,i)}$:	Finial average solution temperature
$T_{(\infty,o)}$:	Room air temperature
$T_{(o,i)}$:	Initial average solution temperature
T_i:	Inside temperature
T_{mean}:	Mean temperature
T_o:	Outside temperature
t:	Time
U:	Superficial velocity
V:	Volume
v:	Flow line velocity
v_1:	Inlet pipe line velocity
x:	Distance of movement /particle size diameter

Greek Symbols

Δ:	Change in a quantity
υ_n:	Pre-exponential factor of the chemical process of order n
ε:	Voidage
η:	Efficiency
μ:	Fluid dynamic viscosity
ν:	Fluid kinematic viscosity
π:	Ratio of a circle’s perimeter to its diameter
ρ:	Density
ρ_f:	Fluid density
ρ_p:	Particle density
σ_0:	Areal density of sites or surface atoms

CHAPTER 1

INTRODUCTION

1.1 Overview

In gold mining, elution or desorption is the gold removal stage from carbon particles. Potable water (low ionic strength) is pumped through the reactor at high temperature and pressure. Activated carbon containing adsorbed gold from leach plant is subjected to high temperatures and pressure in the elution reactor. Gold is desorbed from carbon into the solution and further treated in the electrowinning chamber. Conventionally elution process takes about 24 hours or more. This current process runs with a packed bed of carbon inside the elution reactor. Developments are being investigated to have the process operate at low material and energy cost, yet achieving good stripping efficiencies by modifying process variables such as temperature, pressure and flow rates. As much as gold elution is a mechanically motivated process, it also depends on chemistry since it involves chemical reactions. Gold elution is driven by a both mechanical and chemical process. However, scope of this thesis is limited to the investigation of the effect of system parameters namely, temperature, pressure and flow rate.

1.2 Thesis Problem

Elution process takes about 20 hours or more to complete in Zadra elution process (Wang, 2017). The longer the elution process, more input materials required for the process, such as caustic soda, sodium cyanide, hydrochloric or sulphuric acid, depending on the technique being applied for elution. It also implies that more electrical energy is required since heat is a prerequisite of the process. Hence the current process is expensive to run.

1.3 The Aim and Novelty of the Thesis

The research on the effect of the process parameters of the Zadra elution process is being conducted in order to optimise the process parameters to minimise the energy consumption and to lower operation and design costs of the elution process. Such a move will advance the efficiency of the Zadra elution process. In that vein, the main aim of this research is to perform experiments for fluidized bed and test the effect of each system parameter namely, temperature, pressure and flow rate on the rate of gold elution. The research intends to fluidise the loaded carbon bed because of the nature of the reactiveness of the fluidised bed columns compared to packed bed columns. This will be achieved by varying one parameter while keeping other two constant during the elution process.

Two different ideas have been put forward by two scholars, the first is that at high temperatures with cyanide pre-treatment the elution of metal cyanides in a column is independent of flowrate (Van Deventer, et al, 2003). The second one is that at decreased flow velocities sharper elution patterns are obtained (Davidson, 1974). These are not opposing ideas, only that the first one says at high temperature elution is independent of flowrate, the second one just gives information on slow velocities not telling anything about temperature. Both of these two ideas do not mention fluidised bed columns for gold elution. For elution process, heat and mass transfer rates are proportional to the rate of reaction, therefore a novel idea to fluidise the carbon bed will tend to increase heat and mass transfer rates, in turn increasing rate of reaction. The long stripping time required for the process remains a problem on energy balance and material cost, and further investigation should be put in place to lead to the development of process with shorter stripping time (Gray, 1999). This takes into account of the process variables which include those directly affecting the rate of reaction from a mechanical and chemical standpoint. To enable fluidisation, the flow rate is the governing parameter, hence flow rate must be evaluated as a variable. Higher temperatures do not only expedite the process, but also increase the stripping efficiency to approximately 100%. To enable operation at an elevated temperature, the pressure is needed to keep the eluting media in the liquid phase. Finally, this justifies the need to investigate temperature, pressure and flow rates in the elution process.

1.4 Thesis Overview

This thesis is divided into 5 chapters, which are structured as follows.

Chapter 1 is an introduction to the thesis. In this chapter, a definition of the thesis is presented with a general overview, aims, justification and novelty of the study.

Chapter 2 introduces the literature review of gold mining process through several stages for clarity (in brief), the elution process in detail, factors affecting elution process in depth, and safety aspects to be considered during elution process.

Chapter 3 is a detailed explanation of the methodology employed on experimental setup, equipment sizing calculations and drawings.

Chapter 4 is a detailed explanation and discussion of the results obtained from the experiments.

Chapter 5 Concludes and gives recommendations on further studies on elution process.

CHAPTER 2
LITERATURE REVIEW

2.1 Overview

In this chapter, the researcher reviews the studies that have been undertaken on the elution process, and related topics that affect the rate of elution process. To begin with, the chapter will briefly explain the main building blocks of gold extraction process in a holistic approach in **heading 2.2**. Topics to be discussed include the gold recovery process, which will briefly explain cyanidation as the most popular approach in the gold industry. After briefly explaining the gold extraction process holistically, the chapter will focus on the factors that affect the rate of the elution process in **heading 2.3.** The factors will include temperature, pressure, cyanide decomposition, flow rate, activated carbon selection, reagents and catalyst. **Heading 2.3** will focus on heat transfer in a fluidised bed related to the particle size, film thickness of the fluid and convection heat transfer coefficient in a system. Necessary arguments are presented to show how better particle convection heat transfer coefficient is attained under fluidised bed compared to packed bed system. **Heading 2.4** focuses on the electrowinning design. This will include electrowinning cell predicted extraction efficiency, extraction efficiency curves and effect of eluate temperature versus cell efficiency. Finally, **heading 2.5** will be a summary of this chapter.

2.2 Gold Recovery Process

The process of recovering gold includes a set of related stages from ore size reduction to smelting. As highlighted above, there are different gold recovering processes such as amalgamation with mercury and chlorination. These two will not be covered in this study because amalgamation procedures are not in the scope of this study since they do not include elution as a building block. The process which will be focused on is called cyanidation and it includes the following steps, from the leading to the final, comminution, thickening, leaching, adsorption, desorption or elution, electrowinning, and finally smelting. Mular et al., (2002) describes cyanidation as a gold recovery process as shown in Figure 2.1 below.

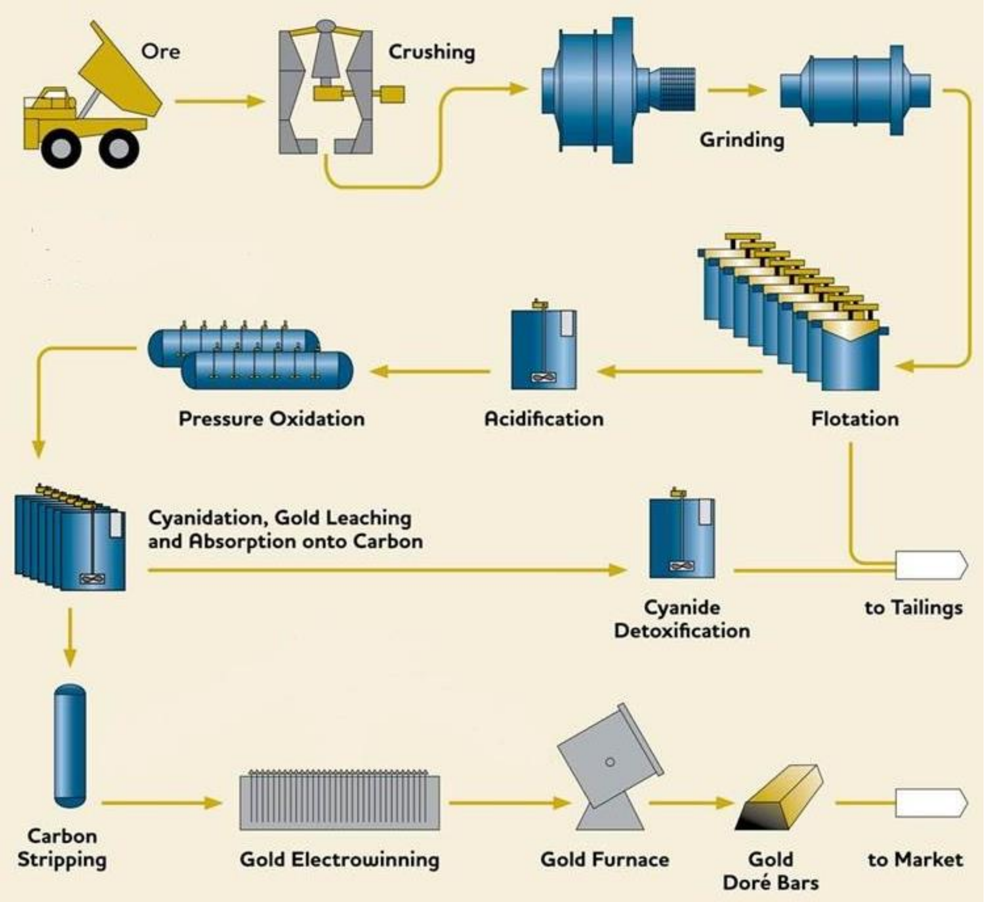

Figure 2.1: Cyanidation gold recovery process (Mular et al., 2002)

2.2.1 Cyanidation

Cyanidation is a process by which gold is dissolved into an aqueous alkaline cyanide solution and subsequent separation of the gold containing solution from finely ground ores. It must be noted that in general the process by which gold is dissolved in the alkaline cyanide solution gives that particular process a general term cyanidation. This is so because there is another process used to attain free gold from ores after comminution without need for cyanidation and its subsequent processes. This route is not covered since it is not scope of study, because it does not include elution as a building block (Van Den Berg, R., Petersen, 2000). All over the world this process has been used to treat ores and calcines and generally, it concentrates on a commercial scale (Mular et al., 2002). The fundamental chemistry of the cyanidation can be summarised as following; under oxidising conditions, cyanide and gold form a complex aurocyanide when dissolved in an alkaline solution. The cyanidation process comprises of the following stages (Stanley, 1987).

2.2.2 Comminution

Comminution is the process of decreasing a material, particularly a mineral ore, to small particles or fragments. This is a stage where the large primary gold ores are ground, transferred to next stage. The level of fineness of gold is greatly dependant on the mineralogy of the gold ore, grinding for adequate gold liberation, and the economically optimum extraction recovery. Ore hoisted from the shafts has to be first crushed, broken down into smaller pieces using a primary crusher. The secondary crusher breaks it down further to enable milling. The fine grinding of the ore is essential for the purposes of liberating the fine gold particles and maximise the reaction kinetics during the leaching process. The grinding occurs in an autogenous or semi-autogenous grinding (SAG) mill. This process requires very high ratios of liquids to solids (Van Den Berg, et al, 2000). The wet ground particles are further pumped to the thickening process.

2.2.3 Thickening

The reagent economics, size of the equipment, and the reaction contact time in the following stages require that the liquid content of the pulp must be low. This means the solids must be dewatered. This is done in a thickener or a dewatering cyclone which uses a fish tailed spigot to select the percent solids required for the process. At this juncture, most of the gold particles contained in the ore has been set free from the previous processes (Mular et al., 2002). Subsequently, if the proper water to solid percent ratio has been attained, the pulp is mixed with alkaline aqueous cyanide solution in the leaching plant.

2.2.4 Leaching

After dewatering of the pulp from the thickening stage, gold is dissolved into the aqueous solution through a process called leaching. This is achieved on sudden contact with dissolved cyanide salt such as sodium or calcine cyanide, which further dissolves gold particles. In both cases of a batch or continuous process of leaching, agitation is essential in order to avoid settling of pulp and increasing the rate of leaching reaction. This is done by both compressed air and mechanical agitation (Stanley, 1987). Compressed air provides oxygen which is essential for the chemistry of agitation while mechanical agitation is essential for both settling avoidance and contact. According to Van Den Berg, et al, (2000) Equation 2.1 below shows the route by which most of the gold is dissolved into aqueous form,

$$2Au + 4CN^- + O_2 + 2H_2O \leftrightarrows 2Au(CN)_2^- + 2OH^- + H_2O_2 \tag{2.1}$$

and a small but significant proportion dissolves via the Elsner reaction Equation 2.2:

$$4Au + 8CN^- + O_2 + 2H_2O \leftrightarrows 4Au(CN)_2^- + 4OH^- \tag{2.2}$$

After dissolving gold ores and concentrates in cyanide solution, we get a solution pregnant with ionic metal cyanide complexes. We further need to liberate gold from this solution. The aurocyanide complex may be removed from the solution by one of the following procedures (Van Den Berg, et al, 2000); Zinc cementation which involves adding zinc dust and lead nitrate to the clarified cyanide solution to precipitate the gold or adsorption which involves activated carbon adsorbing aurocyanides on to it. Both of these processes can be done in either of the following carbon-in-pulp (CIP) processes namely, fluidised bed, fixed or packed bed, multistage column, and moving bed packed column modes. The most popular method for removing the aurocyanide complex from the solution is adsorption under CIP. Using CIP adsorption procedure has become popular since carbon is cheap reusable.

2.2.5 Elution/Desorption Process

The elution process is based on the first law by Fick:

$$J = -D\frac{dC}{dx} \qquad (2.3)$$

Where; the flux in $\mathrm{g/cm^2s}$ is given by J, the coefficient of diffusion of gold in $\mathrm{cm^2/s}$ is given by D, $\mathrm{dC/dx}$ is concentration gradient, C is concentration of gold ($\mathrm{g/cm^3}$), and the movement perpendicular to the surface of the barrier is given by x in (cm). Since in principle diffusion takes place in the direction opposite to that of higher concentration, Fick's law has a negative sign. Mass transfer rate is directly proportional to the molar concentration different at high temperature (But, 1960). Elution is a process where gold that is on the activated carbon particles is desorbed into an aqueous solution. This gold containing solution further processes into smelting plant to recover solid bullion. It precedes the adsorption process, where the gold containing solution, dissolved in cyanide, is passed through activated carbon. The gold in solution is deposited onto activated carbon.

Currently, elution has two main processes being implemented amongst others, the Zadra process and the Anglo American Research Laboratories (AARL) process (Adams, 1994). The differences between the two are that with AARL, carbon has to be acid washed first before elution with Hydrochloric Acid, and immerse it in caustic cyanide solution at high temperatures. High temperature de-ionised water is then travelled through elution tank. In Zadra process, hot caustic cyanide solution is pumped through the column and then to an electrowinning cell for gold sedimentation (Sun, et al, 1995). Secondly, with AARL electrowinning process is done separately after the elution process, while with the Zadra process elution and electrowinning is done simultaneously (Mular et al., 2002).

2.3 Factors Affecting Elution Process

The factors highlighted in the section affect both Zadra and AARL elution processes. It must be noted that great attention and emphasis will be given in the Zadra elution process.

This is because the research experiments will be centred on the factors affecting the modified Zadra elution process.

2.3.1 Effect of Temperature and Pressure on Elution Process

Merwe, (1993) stated that temperature is the most essential parameter in the desorption process of gold cyanide from carbon, with approximately an order of magnitude increase in elution rate and efficiency of 100%. Elution rate at $180^0\mathrm{C}$ is 8 times faster than at $90^0\mathrm{C}$ at atmospheric pressure (Jeffrey, et al, 2009). The gold loading capacity on carbon decreases with increasing temperatures. At high temperature ($150^0\mathrm{C}$) and pressure (0.5MPa), the rate of desorption is approximately 96% (Xinhai Mining) for about 12 to 14 hours, faster than the conventional system that takes 20 hours (Wang, 2017). Modified high temperature and pressurised Zadra process has been implemented by other organisations, operating at $140^0\mathrm{C}$ and 600kPa decreasing the elution time to about 12 hours (Feng, et al, 2003). Operating at high temperatures to increase the elution efficiency and decreasing the elution time, requires operation at high pressures also in order to keep the eluting medium in its liquid phase. Consequently, elution systems have evolved into two classes:

1. operating at temperatures less than $100^0\mathrm{C}$ and atmospheric pressure and
2. operating at elevated pressures to allow operation at elevated temperatures above $100^0\mathrm{C}$ to achieve faster and efficient elution rates

With regards to this study which involves a fluidised bed, the idea of operating at high temperatures in a closed reactor has not been exploited. It is the purpose of this experimentally based thesis to investigate the effect of temperatures above $100^0\mathrm{C}$ under fluidised bed. Secondly, conventional elution takes 20 hours or more, and recent developments of high temperatures above $100^0\mathrm{C}$ and high pressure of 0.5MPa have managed to reduce the time to around 12 to 16 hours (Feng et al., 2003). Arguably the elution time still remains on the high side, and the higher the time required, the higher the energy consumption and material (chemicals) cost as well. In mining energy and process chemicals (cyanide, caustic soda, and acid) are the main driving costs, constituting about 56% (Snyders, et al., 2013).

In a fluidised bed, the convective heat transfer coefficient between bed and surface immersed is due to three properties. According to Botterill (1975), these properties are additive as follows,

$$\mathrm{h} = \mathrm{h_{pc}} + \mathrm{h_{gc}} + \mathrm{h_r} \tag{2.4}$$

Where $\mathrm{h_{pc}}$ is coefficient of particle convective heat transfer, this is heat transfer caused by movement of solid packets that carry heat to and from the surface, $\mathrm{h_{gc}}$ is the gas or liquid coefficient of convective heat transfer that describes the heat transfer by movement of the gas between particles, and $\mathrm{h_r}$ is the coefficient of radiant heat transfer. Figure 2.2, after Botterill, (1986), shows the range of coefficients against the effect of the size of the particle on the significant mechanism of heat transfer. By considering the idea of a volumetric basis, we realise that the particles in a fluidised bed have one thousand times higher heat capacity of the fluid.

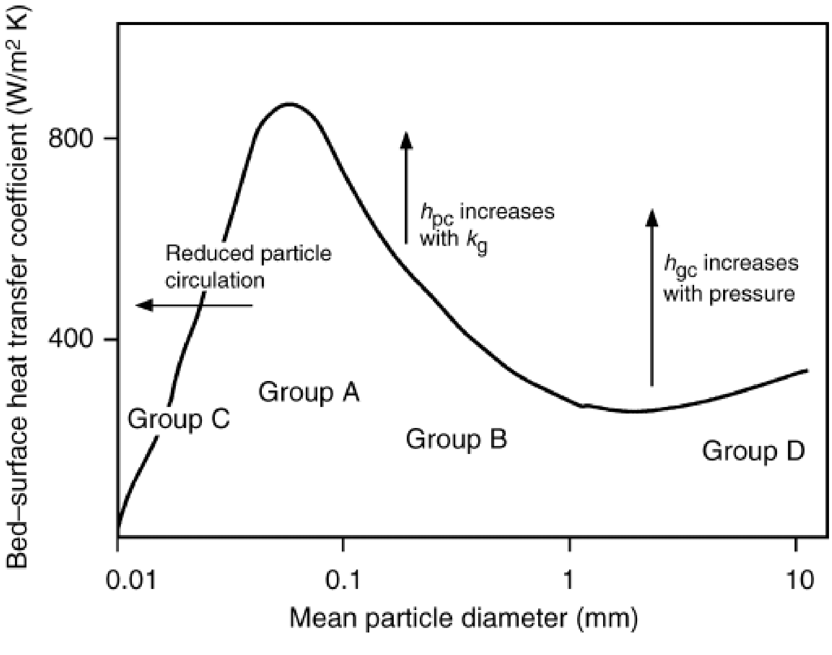

Figure 2.2: Range of bed-surface heat transfer coefficients (Rhodes, 2008)

This is dependent on the direction of heat flow. Considering the size of the particle, it is evident that the particle-surface contact area is too small to permit considerable heat transfer. The factors which affect the thickness of the fluid film or the film conductivity influence the heat transfer under particle convective conditions. If we decrease the size of the particle, for example, this will reduce the mean thickness of the gas/liquid film and so improves the h_{pc}. However, if we decrease the size of the particle into Group C range, we decrease the mobility of the particle thereby reducing the convective heat transfer for the particle. If fluid temperature is increased, this increases the conductivity of the fluid improving h_{pc}. Increasing fluid velocity to or above the minimum fluidization enhances the circulation of the particle which improves particle convective heat transfer. The conventional method for desorption currently in use is employing fluid flow through a packed bed. This entails the fluid to particle interaction is limited, not only in terms of contact, but also heat transfer and particle vibration. A fluidised system is good in that it keeps a uniform temperature throughout the bed. Their violent turbulent motion enables the absorption of heat from the fluid, due to increased heat transfer coefficient (Mickley, et al, 1949).

2.3.1.1 Effect of Temperature on Cyanide Decomposition

Cyanide is used to dissolve minerals into the aqueous solution. The cyanide and the metallic ion form an aurocyanide complex together. This happens during the adsorption process. This process is feasible under room temperatures. Further down the process, when the same conditions are reversed, desorption takes place (Merwe, 1993). At elevated temperatures and pressures, the elution process is faster and efficient in terms of percentage of gold stripping from carbon particles, but only to a certain optimum degree, since higher temperatures decompose the aurocyanide complex. The elution of the cyanide gold complex is done by soaking the gold loaded carbon into a solution, alkaline or non-alkaline, at elevated temperatures in a reactor by passing hot deionised water (Merwe, 1993). In this regard two reactions are predominant at high temperatures during elution. These cause aurocyanide decomposition as follows:

1. Hydrolysis

$$CN^- + 3H_2O \rightarrow [HCOONH_4] + OH^- \tag{2.5}$$

$$[HCOONH_4] + 0.5O_2 \rightarrow HCO_3^- + NH_4^+ \tag{2.6}$$

$$HCO_3^- + NH_4^+ + 2OH^- \xrightarrow{pH\ 10.5} NH_3 + CO_3^{2-} + 2H_2O \tag{2.7}$$

2. Oxidation

$$CN^- + 0.5O_2 \rightarrow [CNO^-] \tag{2.8}$$

$$[CNO^-] + H_2O \rightarrow CO_3^{2-} + NH_4^+ \tag{2.9}$$

The decomposition of cyanide happens at the same time as gold elution. It is essential to understand the effects of temperature on cyanide since cyanide decomposes at certain critical temperatures. This happens in two forms of reaction as shown above. According to Merwe (1993), cyanide decomposition is gradual at low temperature unless there is a presence of carbon. He also noted that carbon effect decreases with temperature increase. Therefore, at higher temperatures hydrolysis reaction is more significant, while at low temperatures the dominant reaction is that of catalytic oxidation. Hence hydrolysis becomes the main mechanism for cyanide loss in both main elution processes of Zadra and AARL (Merwe, 1993). Figure 2.3 shows that high temperature improves the degradation of cyanide, and therefore results in a lower maximum of the elution profile. Although elution is efficient at higher temperatures, cyanide critical operating temperature becomes the major limiting factor to further increase in temperature.

2.3.2 Effect of Flow Rate on Elution Process

Flowrate is more fundamental in the elution process during solution circulation in the circuit. The diffusivity of the aurocyanide ion within the micropores of carbon is greatly affected by the easy of flow (Sun, et al, 1995). In the column, as the solution flows through the carbon, gold is being eluted. If we dividing the column into sub-volumes, and assume the rate of the reaction to be spatially uniform within each sub-volume, we can derive Equation 2.10 by considering also the following assumptions.

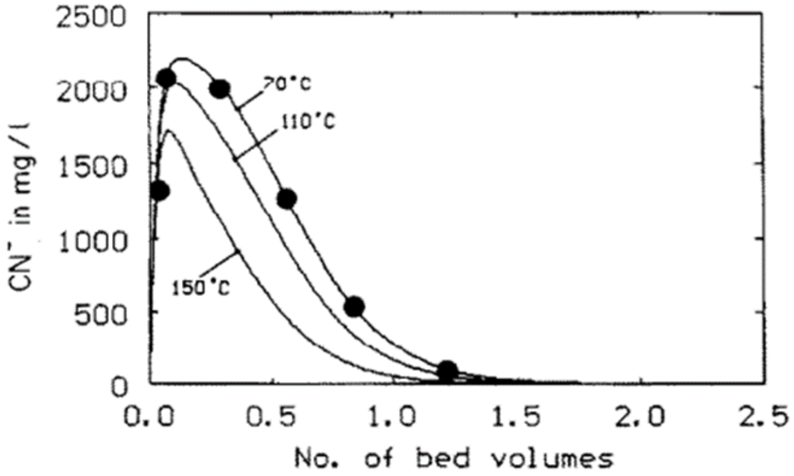

Figure 2.3: Cyanide profiles for elutions at different temperatures (Merwe, 1993)

If we assume that a sub-volume is located at point y from the inlet of the column, there will be three types of net mass changes: net bulk flow (in and out), net dispersion (in and out), and desorption of gold from carbon particles. This is explained by a general mass balance that explains diffusivity which is a factor of flowrate.

$$\begin{pmatrix}\text{rate of}\\ \text{bulk flow}\end{pmatrix}_{\text{in \& out}} + \begin{pmatrix}\text{rate of}\\ \text{axial dispersion}\end{pmatrix}_{\text{in \& out}} + \begin{pmatrix}\text{rate of gold}\\ \text{desorption from carbon}\end{pmatrix} = \begin{pmatrix}\text{rate of}\\ \text{accumulation}\end{pmatrix} \tag{2.10}$$

From research according to Davidson, (1974), elution has a sharp profile when flowrate is modelled as a plug flow i.e. approximately laminar flow through a porous media. According to Rhodes, (2008), if a fluid flew vertically upwards through a bed containing particle it experiences a pressure loss. This loss in pressure increases as the fluid flow velocity elevate due to increased frictional forces. As this persists, a point is reached when the drag force is exerted on the particle by the fluid is equal to the weight of the particle. At that moment the particles get elevated by the solution. In turn, this increases the separation distance between the particles and the bed becomes fluidised (Rhodes, 2008). By doing the force balance analysis it can be realised that the solution pressure through the bed of particles are equal to the particle weight per unit area.

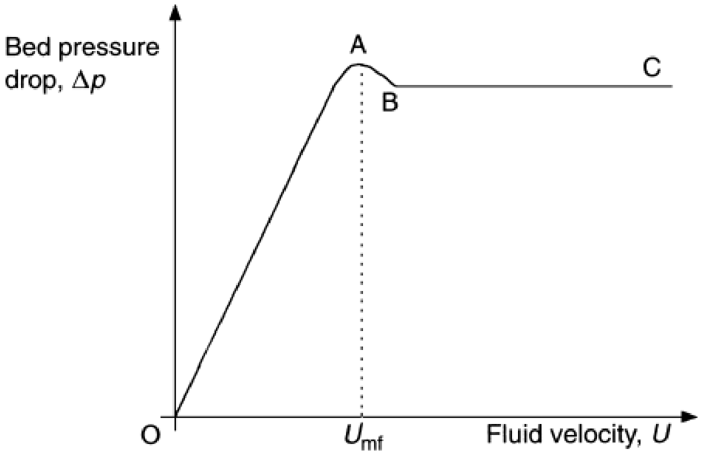

Figure 2.4: Pressure versus velocity for packed and fluidised beds (Rhodes, 2008)

A plot of fluid pressure loss across the bed versus the superficial fluid velocity through the bed is shown in Figure 2.4. Referring to Figure 2.4, portion OA represents the region of a packed bed. In this portion during fluid flow through particles, the particles do not move, and the distance of separation is constant. The Carman-Kozeny Equation 2.11 describes the linear relationship in the laminar flow regime and the Ergun Equation 2.12 in general.

$$\frac{(-\Delta p)}{H} = 180\frac{\mu U}{x^2}\frac{(1-\varepsilon)^2}{\varepsilon^3} \tag{2.11}$$

$$\frac{(-\Delta p)}{H} = 150\frac{\mu U}{x^2}\frac{(1-\varepsilon)^2}{\varepsilon^3} + 1.75\frac{\rho_p U^2}{x}\frac{(1-\varepsilon)}{\varepsilon^3} \tag{2.12}$$

Where $-\Delta\mathrm{p}$ is the pressure drop of fluid with a superficial velocity U, over a bed column of height H, and of viscosity μ. ε is the particle voidage and particle density ρ_p.

The portion BC represents the fluidised region. We use Equation 2.13 to describe this portion. It can be noticed that the pressure at point A raised above the one predicted by Equation 2.13. This is more significant in more compacted particles in a column.

Primarily it is due to the increase in force required to separate the particles by breaking through the adhesive forces between them, and wall frictional force between bed and distributor.

$$(-\Delta p) = H(1 - \varepsilon)(\rho_p - \rho_f)g \tag{2.13}$$

Where ρ_f is fluid density, ρ_p is particle density, ε is voidage, H is column height and Δp is a pressure drop. The reason to study the mechanism of fluidised bed under the effects on flow rate is because of its benefits to reactions as compared to a packed bed. Conventional elution systems use packed bed system. It is important to note that the fundamental advantage of a fluidised bed over a packed bed is that it can maintain a uniform temperature distribution across the fluid and the bed Rhodes, (2008). This enables uniform heat transfer from the fluid to the bed (Barker, 1965; Mickley, et al, 1949). As discussed in **Section 2.3.1** under the effect of temperature and pressure on elution process, it is also shown that fluidised beds have high convection heat coefficient. This results in a better rate of reaction. Two different ideas have been put forward by two scholars, the first is that at high temperatures with cyanide pre-treatment the elution of metal cyanides in a column is independent of flowrate (Van Deventer, et al, 2003). The second one is that at decreased flow velocities sharper elution patterns are obtained (Davidson, 1974). These are not opposing ideas, only that the first one says at high temperature elution is independent of flowrate, the second one just gives information on slow velocities not telling anything about temperature. This can be applicable to both the Zadra and AARL processes. Therefore, it is important to investigate the effect of flow rate under high temperatures in order to marry the two ideas on the elution under fluidised bed system.

2.3.3 Effect of Activated Carbon Selection on Elution Process

Activated carbon is the most common material used for gold adsorption. The common size used is about 3.36 mm (Rogans, 2012). This is relatively large when considering the kinetics of desorption after gold has been loaded during the adsorption process. Generally, elution requires at most 48 hours to complete, depending on the method being used. The main reason for the long elution time is due to the gradual rate of diffusion of the aurocyanide ion within micropores of large activated carbon when compared to aurocyanide species size (Sun, et al, 1995). The aurocyanide complex, as very small as it is compared to the carbon granule, it occupies the micropores of the carbon granule. The pore size is in micro range. Therefore, it can be concluded that, the smaller the carbon particle used for adsorption, the greater the adsorption due to surface area, and the greater elution efficiency also for gold recover, since the aurocyanide particles need to diffuse through a short distance to elution sub-volume area (Sun & Yen, 1995). In this study we will consider the standard size of carbon for selection which is in the range.

2.3.4 Effects of Reagents on Elution Process

The two main important reagents to elution process are sodium cyanide (NaCN) and Caustic soda (sodium hydroxide-NaOH). These two have been thoroughly studied and documented on their role and effects on gold elution both in the AARL and Zadra elution processes (Snyders, Bradshaw, Akdogan, & Eksteen, 2015).

2.3.4.1 Effects of Cyanide on Elution Process

According to (Snyders et al., 2015), with increase in cyanide in the solution, so does an increase in the rate of elution. From their study, an increase in the elution was noted from an increase of 1 to 2% of cyanide, but further increase from 2% to 4% results in a decrease in elution rate. The main two points of discussion are the issue of either or not there is partial degradation of the NaAu $(CN)_2$ to AuCN on the activated carbon surface. If the discussion point of degradation is to hold, this would suggest that cyanide is essential since it can be converted back to aurocyanide ion that is easily absorbable. Authors who suggested partial degradation are McDougall et al. (1980), Cook et al. (1989) and Cook et al. (1990). Experiments done with free cyanide contradicted with the earlier results mainly by Jones et al. (1989), Adams and Fleming (1989). Adams, (1991) suggested that no activated carbon is sufficient enough to be a reducing agent to reduce Aurocyanide ion unless the medium is acidic, as this can lead to decomposition of the aurocyanide ion.

Although this contradiction may hold, Van Deventer and Van der Merwe (1993) ascribed to the conflict as a result of using different kinds of carbon samples during the experiments from the scholars. In conclusion, cyanide is necessary during elution for ion formation since the process will involve electrowinning. For this, it ensures strong anion that electroplates on the cathode during electrowinning.

2.3.4.2 Effects of Sodium Hydroxide on Elution Process

The effects of sodium hydroxide are seen to increase the rate of elution as its concentration is increased in the solution. The rate of gold loading is seen to be enhanced by lowering the pH of the eluate (McDougall, et al. 1980). Experiments conducted by (Snyders et al., 2015) show that the increase in elution rate happens in the lower ranges of concentration of the sodium hydroxide of approximately up to 1%. An increase from 1% to about 20% of sodium hydroxide will result in a decrease in the rate of elution as shown by Davidson and Duncanson (1977), which he attributed to the stability of nickel, copper and silver cyanide complexes being lower at high pH values. Sodium hydroxide also reacts exothermically with the solution. This, in turn, enhances a spike in temperature increase during elution, since elution requires high temperatures for gold loading to occur. Thus, sodium hydroxide also gives in energy to the eluate.

2.3.5 Effects of Catalysts on Elution Process

Conventionally desorption of gold using the Zadra process would include a solution with relative concentrations; 0.1% NaCN and 1% NaOH, at about 93^0C. Different elution technologies for precious metals (Au, or Ag) do exist. These also include hot elution or pressure desorption with a hydro-alcoholic solution before electrowinning (Ubaldini, et al., 1998). From the referenced work, the efficiency of alcohol was investigated. The main parameters investigated were elution time and temperatures on the rate of desorption in the presence of different hydro-alcoholic eluents with NaOH excluding HCN.

These eluents are isopropanol, ethylene glycol and ethanol (Espiell, Roca, Cruells, & Núñez, 1988) (Ubaldini, et al., 2006). The following reagents were used in the elution test works; sodium hydroxide, demineralised water, ethylene glycol, ethanol, and isopropanol. The test works for the elution for all three main reagents were done under the following conditions: pH 12, time 8 hours, extraction temperature; $40^0\mathrm{C} - 60^0\mathrm{C} - 80^0\mathrm{C}$; and a flow rate of 4ml/min. The demineralised water contained 20% v/v of ethanol, isopropanol or ethylene glycol, 1% by weight of NaOH was added, excluding Cyanide (Ubaldini et al., 2006). In all cases, NaOH was present. This was done to achieve both good extents and high desorption rates. This is mainly because preliminary all experiments show with the absents of NaOH, gold extraction decreases by about 30% Au. Figure 2.5 shows the results from the test works. From the graph obtained it shows generally that with an increase in temperature, better results are obtained. At $80^0\mathrm{C}$, after 5 hours $> 95\%$ of gold was extracted. Figure 2.6 shows the results for isopropanol. It is clear that with an increase in temperature better results were obtained again. Isopropanol exhibits faster elution rates than ethanol with more than 98% Au eluted after an hour at $80^0\mathrm{C}$. In Figure 2.7 results for ethylene glycol are shown. Most interestingly is the fact that about 77% Au was extracted after 8 hours elution at $40^0\mathrm{C}$. Gold concentrations obtained after 8 hours with relative temperatures were 16 mg/L Au at $40^0\mathrm{C}$, 19.4 mg/L Au at $60^0\mathrm{C}$, and 32.8 mg/L Au at $80^0\mathrm{C}$. It can be positively concluded that temperature plays a significant role in elution. The activation energy was more than 57kJ/mol. This shows that desorption is the rate determining factor. We can arrange the results by order of estimated kinetic constants at any temperature as follows $\mathrm{K}_{\mathrm{isopropanol}} > \mathrm{K}_{\mathrm{ethyl\ glycol}} > \mathrm{K}_{\mathrm{ethanol}}$. Isopropanol was the best organic compound for the elution process. From a pragmatic standpoint, if we were to consider using a catalyst, we would select ethylene glycol or ethanol due to their non-flammability property which conforms to (Ubaldini et al., 2006)'s selection. Since the study is focusing on the mechanical faculty of the process which include effects of pressure, temperature and flow rate on elution, we will not consider catalysts in our study. This can the exploited under chemistry studies.

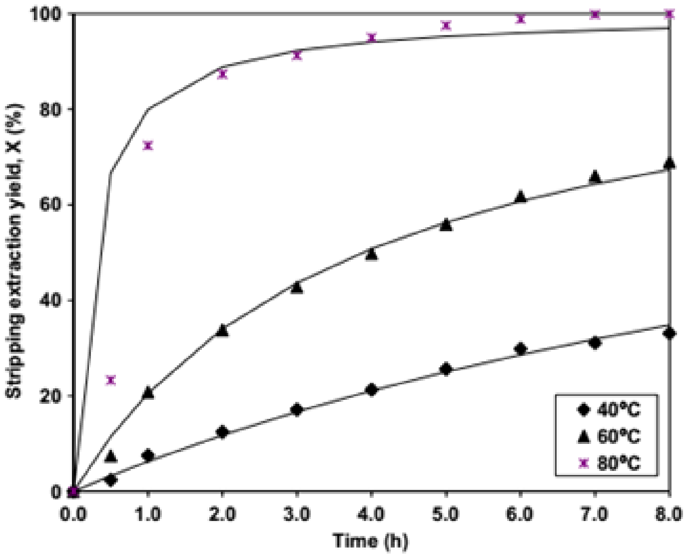

Figure 2.5: Elution by ethanol at 40, 60, and 80^{0}C (Ubaldini et al., 2006)

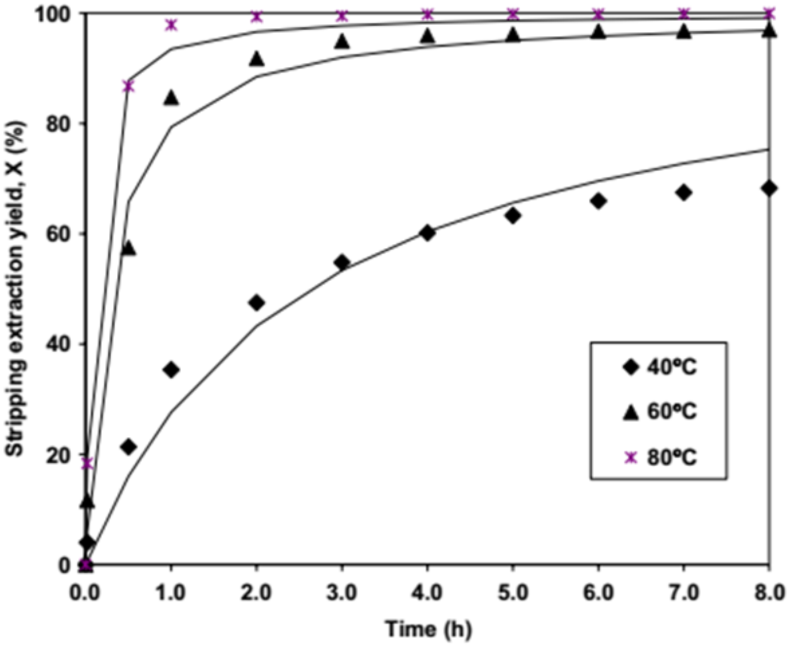

Figure 2.6: Elution by isopropanol at 40, 60, and 80^{0}C (Ubaldini et al., 2006)

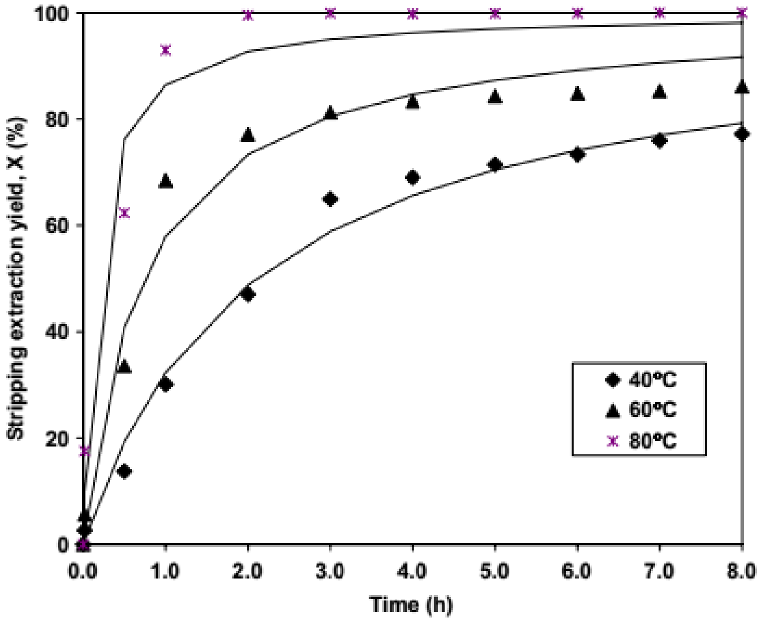

Figure 2.7: Elution by ethylene glycol at 40, 60, and 80^0C (Ubaldini et al., 2006)

2.4 Electrowinning Cell Design

According to Mular et al., (2002) elution and electrowinning forms significant part of the gold extraction process. Two methods exist which incorporate elution/desorption and electrowinning, the Zadra process: which involves the simultaneous circulation of eluate through desorption column and electrowinning cell, and the AARL (Anglo American Research Laboratories Method) which involves decoupling of the two into two separate processes. These configurations have an effect on the process time and economies of the resources used. Coupling the two-means relating the elution temperature to the EW process yet decoupling the processes also means the need for extra heat exchanger if need be to elevate the temperature for eluate into the EWC. Since desorption and electrolysis do not require different temperatures, it is not necessary to decouple the components for elution (Wang Monica, 2017). Like any other electrowinning process, oxidation reaction taking place at the anode Equation 2.16 generates electrons, which are consumed at the cathode Equation 2.15 to deposit the metal.

Electrode reactions which takes place during electrolysis of an alkaline gold cyanide solution can be seen in the equation below;

At Anode

$$2H_2O \rightarrow 4H^+ + O_2 + 4e^- \qquad (2.14)$$

At Cathode

$$Au(CN)_2^- + e^- \rightarrow Au + 2CN^- \qquad (2.15)$$

In cyanide solutions, gold is present as a stable auro-cyanide complex anion with a comparatively high cathodic potential (E_0). This cathodic shift demands high cell voltage and consequently, other cathodic reactions like the evolution of H_2 by the discharge of H^+ and the reduction of O_2 can also take place. These extra reactions consume current and decrease the current efficiency of the gold electrowinning process.

Originally, most cells were designed and operated to electroplate the precious metals onto the cathodes. The cathodes were periodically removed and either digested in hydrochloric acid to remove most of the steel wool or simply calcine and smelted. The harvesting and maintenance of these cells can take 4 to 24 hours of operating time per week, depending on the gold production rate. Presently, most new operations favour operating cells so as to promote the deposition of gold as sludge rather than plating. The electrodeposited gold forms as fine grains on the cathode surface and are readily dislodged by the cogenerated hydrogen gas bubbles and the velocity of the eluate solution and accumulates at the bottom of the tank below the cathodes as a black sludge. The bottom of a sludging cell is sloped to a drain point. The harvesting and maintenance of these cells typically take 30 minutes to 1 hour of operation time per week, depending on the gold production rate and the extent of metal bonding to the cathodes.

2.4.1 Electrowinning Cell Predicted Extraction Efficiency

The main variations in operating parameters between the above two described modes are current density and fluid superficial velocity. Operating in sludging mode generally requires higher levels of both, as higher current density enhances a random growth of electrodeposits where loosely adhere to the cathodes and are readily dislodged by the greater evolution of hydrogen gas. Higher fluid superficial velocities in the cell reduce the metal ion depleted zone in the immediate vicinity of the cathodes and reduce the thickness of the electrical double layer of the cathodes. If the superficial velocity is too low, the reduction reaction is limited by the diffusion rate of the metal through the electrical double layer.

2.4.2 Extraction Efficiency Curves

Typical curves for extraction efficiency versus effective cell retention time are shown in Figure 2.4 below and demonstrates the general improvement in extraction efficiency attained as the cell design and operation of the cell has been improved.

2.4.3 Eluate Temperature against Cell Efficiency

Other important operating variables that significantly affect the performance of the EWC are temperature and solution chemistry.

2.4.3.1 Eluate Temperature and Solution Chemistry in the Electrowinning Cell

The electrolyte temperature is not critical as long as the solution is cooled below the boiling point prior to passing through the electrowinning cell. Where plastics are used, the solution may require further cooling to 60^0C. According to (Mular et al., 2002), eluate temperature should significantly be in excess of 70^0C to enable higher significant extraction efficiencies. At this temperature, efficiency is high because of a combination of lower dissolved oxygen content, decreased solution viscosity and increased ionic mobility at the high temperature. Generally, at the elevated pH ranges, solution conductivity is not a problem. It is important to maintain eluate pH in the range of 12-13 to achieve ionic mobility and electrolyte conductivity in the electrowinning cell (Mular et al., 2002).

2.4.4 Gas Generation During Electrowinning

As shown from the Equations 2.15 and 2.16 above a by-product of hydrogen cyanide (HCN) is formed (Mular et al., 2002). This is a poisonous and hazardous gas. The gas should be vented out through a pressure relief valve. This reduces and maintains required pressure in the circuit. HCN skin and eye irritation. It is dangerous if inhaled. It is highly flammable, and thus it should be quickly evented out as soon as there is an increase in pressure.

2.4.5 Summary

The chapter had three main sections. The first section looked at the general processes leading to elution process. These were briefly, but concisely explained to give an idea of the study background. The second section dealt with factors that affect elution process. The section looked at all factors, even those that require faculty of chemistry and metallurgy. This was done in order to understand the behaviour of the material under study when subjected to various condition. This enables the researcher to give a better discussion and conclusion of the experiment’s outcome further in the study. Finally, the researcher looked at the electrowinning cell design. It is not the main focus of the study, but needs proper design attention in order not to spoil the outcomes of the experiments.

CHAPTER 3

EXPERIMENTAL DESIGN AND METHODOLOGY

3.1 Overview

This chapter of the study serves to inform the tasks taken and completed during the fabrication, commissioning and experiments with the elution rig, the system which involves gold elution in a fluidized bed column under high temperature and pressure. Under **heading 3.2,** the details on the mechanical design of the major two tanks, the elution vessel and the electrowinning cell are presented. Under **heading 3.3** is the electrical and control circuitry details which give the sizes of the electronic components, with pictures and diagrams. Under **heading 3.4**, the details related to the sizing of the solution heater, insulation blanket, and the pump are presented step by step. The conditions required for the experiment are tabulated under **heading 3.5**. The setup of the experimental procedure is explained under **heading 3.6** which includes control procedures for the system flow rate, temperature and pressure. Finally, **heading 3.7** is a summary of chapter 3.

3.2 Introduction

The elution test rig consists of the elution reactor, the electrowinning cell and pipe line and fittings. In this chapter is a detailed description of each component in the system. This includes what each component is made up of and the design technical approach on each in order to achieve desired operations of the integrated system.

Below is a flow chart summery of the methodology steps taken to achieve the full design. The flow chart shows that there are two main methods for gold elution in practice at commercial level. The researcher chose to delve into the Zadra elution process, the AARL method was mentioned in order to show how useful it is in commercial industry. But the Zadra elution process was used because of its familiarity in African mines. The researcher modified the circuitry of the Zadra elution process following the summarised steps below.

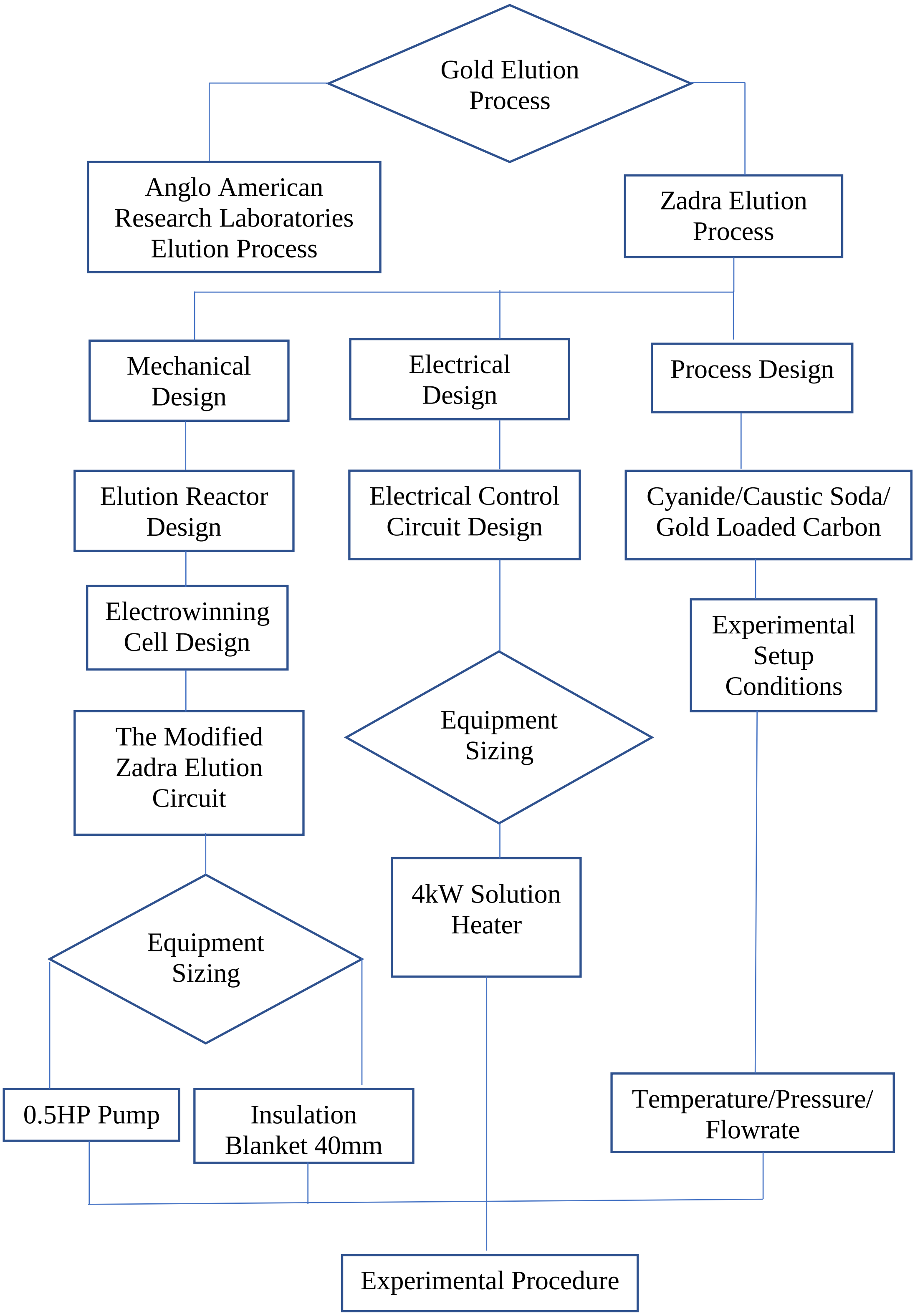
Gold Elution Process
Anglo American Research Laboratories Elution Process
Zadra Elution Process
Mechanical Design
Electrical Design
Process Design
Elution Reactor Design
Electrical Control Circuit Design
Cyanide/Caustic Soda/ Gold Loaded Carbon
Electrowinning Cell Design
Experimental Setup Conditions
The Modified Zadra Elution Circuit
Equipment Sizing
Equipment Sizing
4kW Solution Heater
0.5HP Pump
Insulation Blanket 40mm
Temperature/Pressure/ Flowrate
Experimental Procedure

3.2.1 Elution Reactor

The fabrication of the system spanned for nearly two and a half months commencing with the elution column first. The elution column made from stainless steel 2 mm plate was properly welded considering it as the high-pressure vessel. Its dimensions are 243 mm diameter by 300 mm high. It consists of a cone at the bottom with a height of 97 mm, responsible for vortex creation to enhance fluidization. At the bottom of the shell, there is a 38 mm (1.5 inch) hole for carbon and solution discharge after the experiments. The top of the vessel consists of a blank flange that can hold 4 bar (SA Gauge) pressure and a gauge pressure for pressure measurement. There is also a 1.8 bar rated safety pressure valve (Safety Angus Valve) for regulating the system pressure. A view of the elution column can be seen from Figure 3.1.

The elution reactor was designed to accommodate 2 kg of gold loaded carbon. It consists of a conically bottomed shell. The conical shape is to enhance vortex creation for fluidization and also to help the easy discharge of carbon and solution after the experiments. It also has the inlet at the bottom. The inlet pipe slants as facing downwards which directs the solution in the cone cavity to cause a proper vortex. The outlet is placed vertically upwards. The outlet pipe consists of a mesh screen in order to restrain carbon migration, and only allow the solution to circulate through the rest of the test rig. Initially, the design consisted of a heat exchanger placed along the pipe work, 300mm from the elution vessel inlet hole. Notwithstanding the fact that the elution rig was properly insulated, and the immersion heater was properly sized, upon commissioning the temperature rise of the system solution was very poor. For example, it took nearly 3hours to raise temperature from 55^0C to 60^0C. This is so, because the surface area of the heat was low. Before considering a bigger heater or increasing insulation thickness to mitigate the temperature rise problem, the position of the heater was altered. The heater is now placed directly into the elution vessel. At the bottom section, a 150mm (1.5 inch) nipple is welded to hold the elution heater. The elution heater is placed directly inside the elution vessel to increase the heating surface area of the heating element. This enables faster temperature rise.

At the opposite side of the inlet and outlet pipes, there is a hole, in which a front blanked pipe is welded. This short front blanked pipe accommodates the thermocouple for temperature measurement during the elution. Figure 3.1 shows the complete fabricated elution vessel and detailed 2D sectional view of the vessel is presented in Figure 3.2.

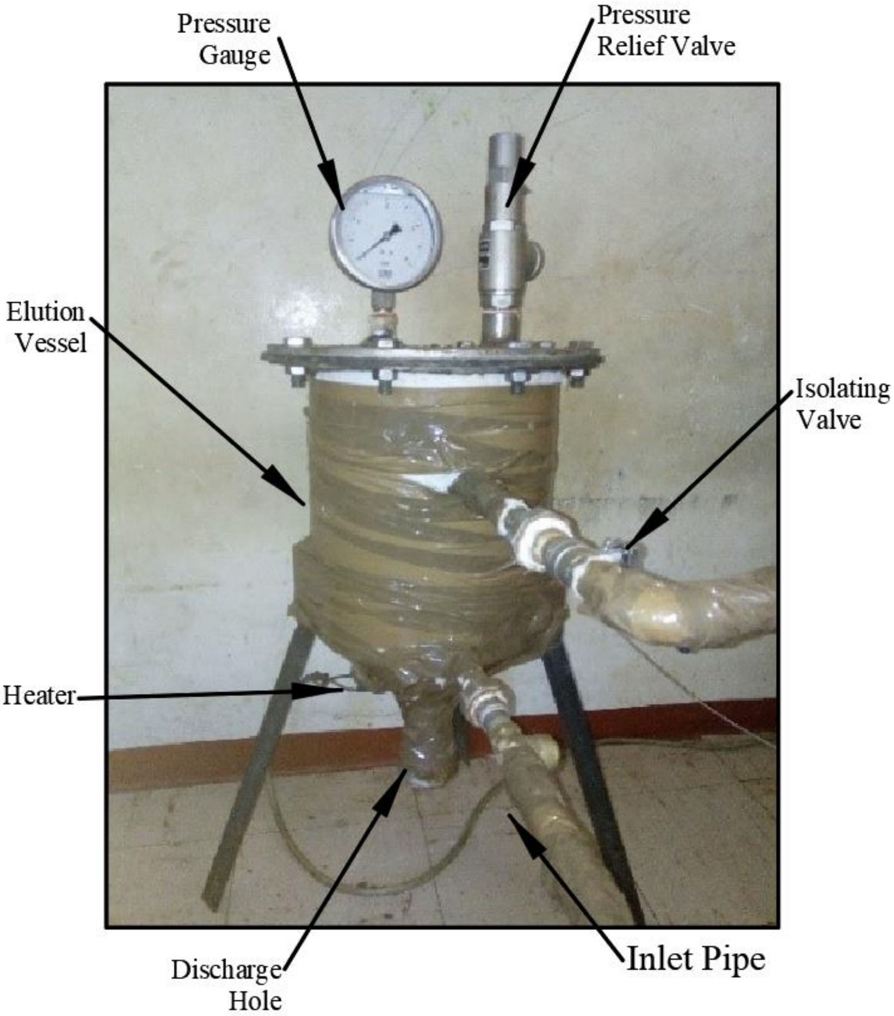

Figure 3.1: Elution pressurized vessel.

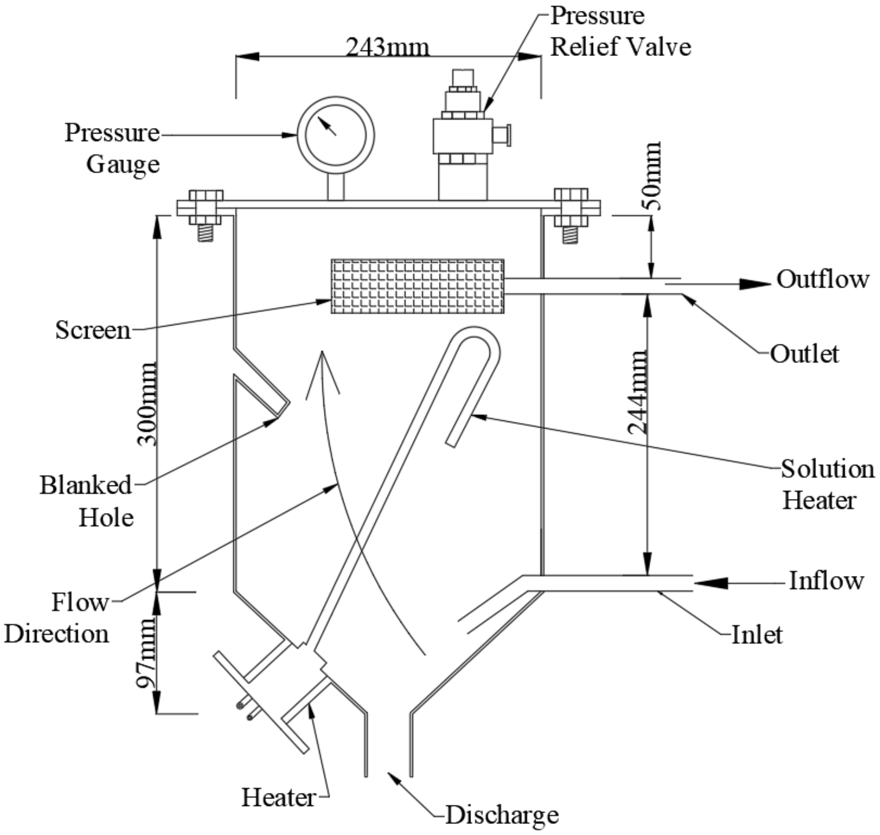

Figure 3.2: Section view of the elution vessel.

3.2.2 Electrowinning Cell

The electrowinning cell is made from an NB 150 (6 inch) mild steel pipe of height 230 mm. The cell is fabricated to accommodate two electrodes, the cathode at the bottom and the anode at the top. The cathode is placed at the bottom in order to mitigate the effects of drop out content from the wire wool during elution. As the wire wool gets loaded with gold particles, heavy laden parts of the wire wool will drop from the cathode. In such a case, if the cathode is placed on top of the anode there would be a short circuit. The electrodes are designed to be isolated from the wall of the cell to prevent short circuits. The interior of the winning cell is insulated with plastic lining made of HDPE pipe. The cell has an inlet of the solution at the bottom and outlet at the upper opposite side of the cell.

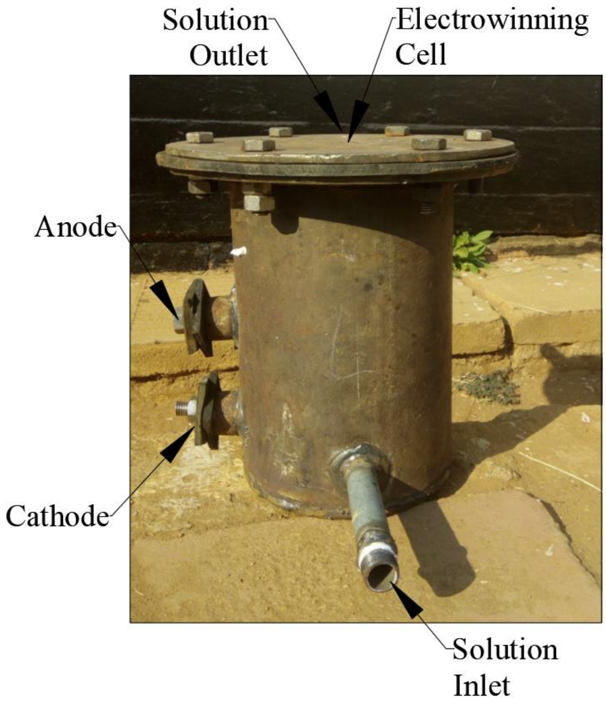

Figure 3.3: Electrowinning cell design

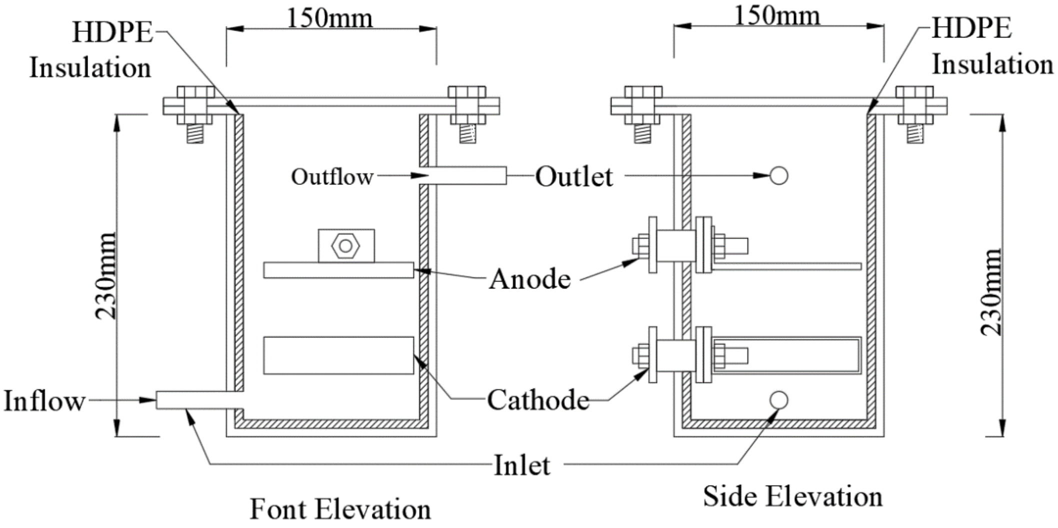

Figure 3.4: Section view through electrowinning cell design

3.2.3 Complete Assembled View of the Test Rig

These two main vessels are connected using a screw on the threaded piping system in order to allow for easy detachment, in case we would want to move the test rig from one place to another. During commission there was a leaking problem. The leaks were prevented by using thread seal tape and sealing paste. After sealing the threaded connection points the system was filled and heated to obtain 3 bar pressure and left like that for 2 hours. After this test it was observed that there was no leakage. The 3D model of the combined system of the elution test rig is shown in Figure 3.5 and Figure 3.6 above illustrates the picture of fully assembled model ready for experiments. The whole piping system including the two vessels is covered with an insulation blanket to prevent heat loss.

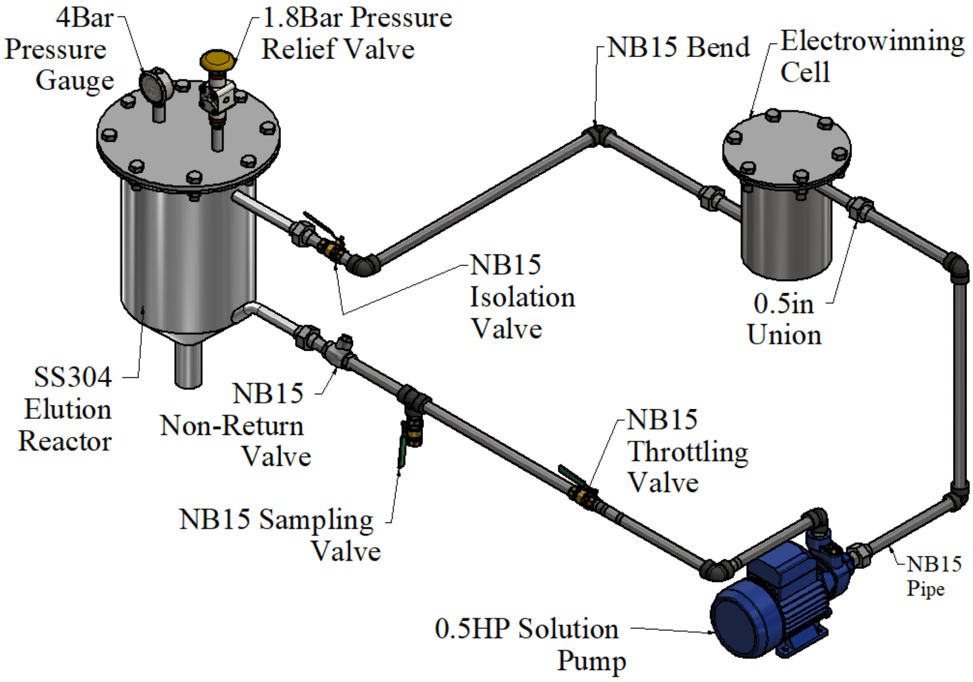

Figure 3.5: 3D model elution circuit complete

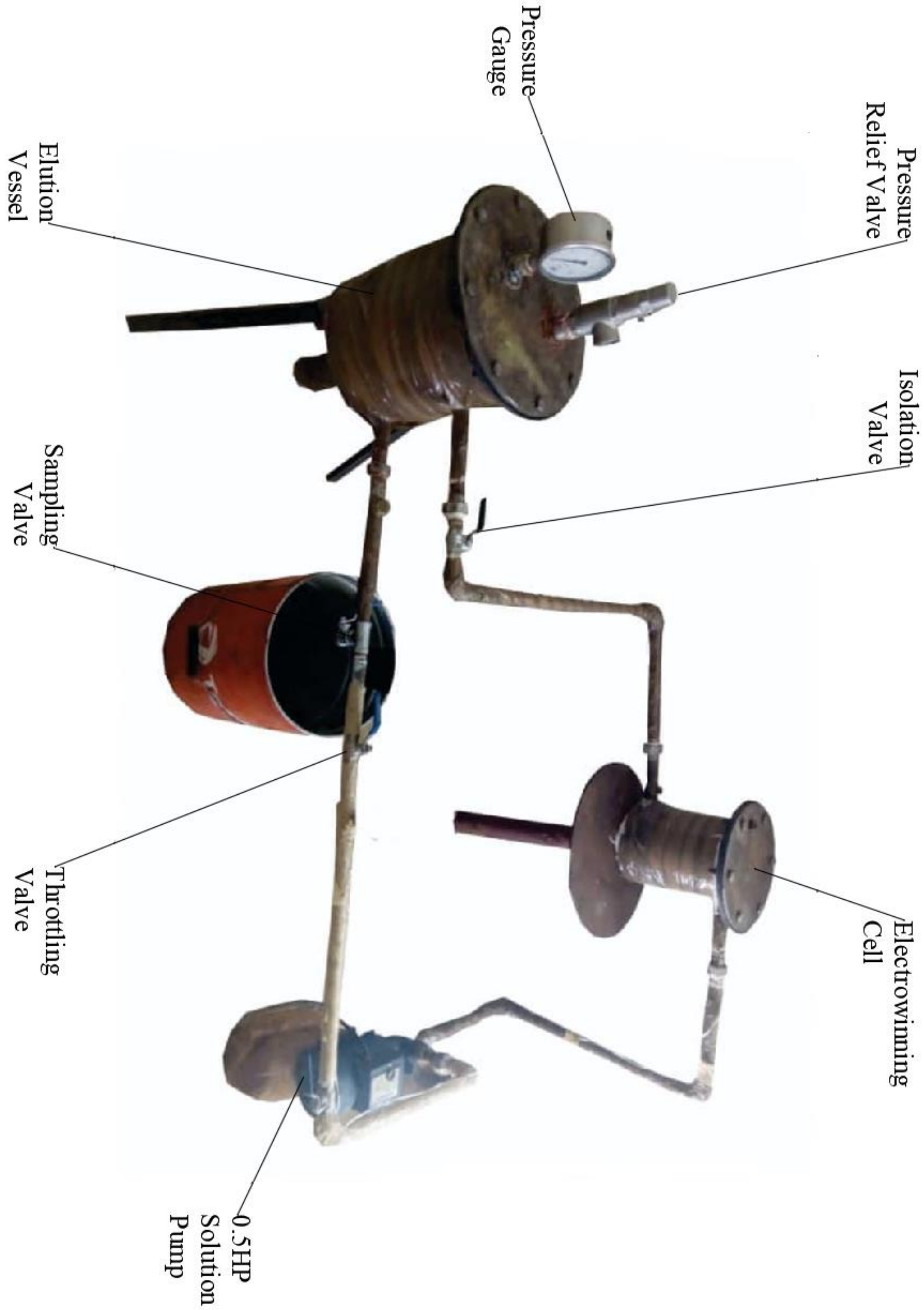

Figure 3.6: Fully assembled elution circui

3.2.4 Electrical and Control Circuitry

The electrical components that are used in the test rig are 0.5 HP pump, 4 kW immersion elution heater, two 75 Amps diodes for rectification, 220VAC-4VAC/30Amp step-down transformer, 220V contactor, K-type $0 \text{ to } 400^0C$ thermocouple, REX-C100FK02-M*EN 220VAC RKC $0 \text{ to } 400^0C$ temperature controller, Delta CTA4 series tachometer, cables and tools necessary for the work. The circuit was designed by the researcher, with the help of a class one electrician hired to wire the circuit as shown by the Figure 3.7 below. Figure 3.7 below is a complete detailed wiring diagram for the elution system. The picture of the wired components is shown in Figure 3.8. From the figure, is the contactor, labelled as K1-NC in Figure 3.7. This is the device responsible for controlling the heater. It powers the heater based on the measurements from thermocouple. The contactor gets its powering signal from the temperature controller and on the temperature controller, the input is set to determine the maximum temperature to be operated. This value is put as the set value (SV) on the controller. It monitors the process value (PV) of the contents which is transferred by the thermocouple. The thermocouple is inserted in the blocked hole, inside the elution column, filled with engine oil to enable accurate temperature measurements. On the wiring diagram for the elution system Figure 3.7, the thermocouple is connected to the temperature controller. The temperature controller is at the bottom left in Figure 3.8. At the top right corner in Figure 3.8, there is the aluminium plate used as both a heat sink and bridging plate. On it, there are two diodes that are wired to the transformer with yellow cables. Theses cables supply 4 V each to each diode, a brown cable that emerges from the plate has 4 V and forms the positive that becomes the electrowinning cell anode. In the middle of the two yellow cables is a blue 0 V pole from the transformer, which forms the cathode of the electrowinning cell. The whole circuit is powered by 220V/30Amps from the main circuit breaker.

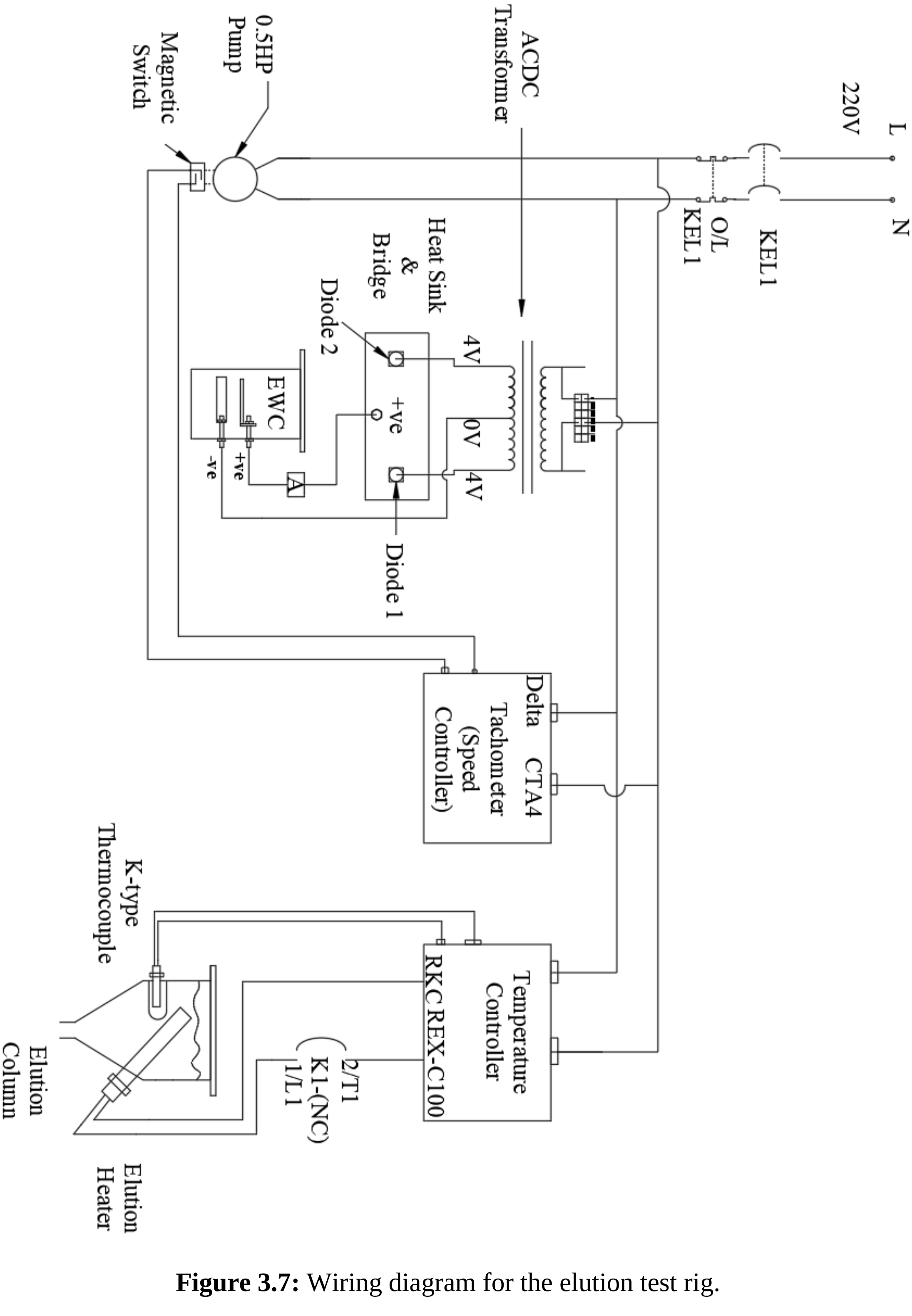

Figure 3.7: Wiring diagram for the elution test rig.

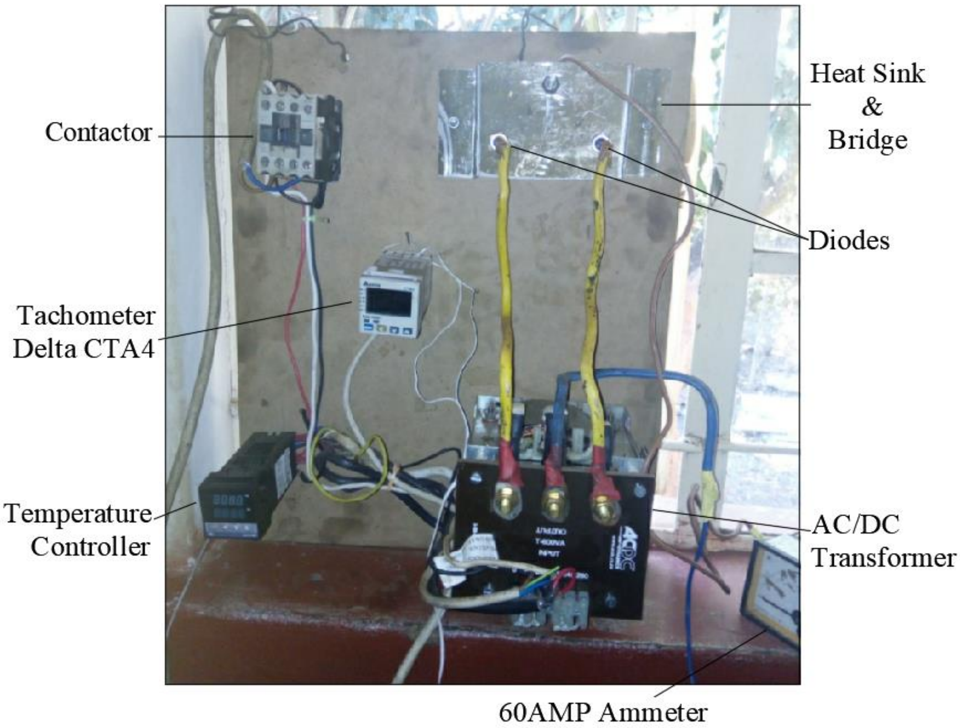

Figure 3.8: Elution system circuitry

3.3 Equipment Sizing

Below is the explanation of how the equipment was sized to suit the pilot plant for experiments.

3.3.1 Heating Element

The elution tank has the solution heater mounted from its bottom inclined inwards. This was to allow more heating surface area ratio to the volume of the liquid being heated. The total fluid in the circuit is 20 litre which is the equivalent of $0.02m^3$. This is the total volume to be occupied by the solution which includes the total volume of the two cylinders, a pump cavity and the pipework. According to the commissioning test done before the experiment, this volume was also enough to allow for sampling without reducing much solution volume for the elution process.

The full length of the pipeline is equal to 5.082 m. Using a NB 15 (0.5 inch) pipe, schedule 40 from Robor catalogue with wall thickness 2.77 mm, the inside diameter is 15.8 mm. From this, we can calculate the volume (V) of the solution inside the pipeline. From the thermophysical property tables (Cengel, 2003), properties of water (density and specific heat capacity) can be read at a mean temperature obtained in Equation 3-1. By considering the maximum average temperature of the solution after heating to be $150^0\mathrm{C}$, and the lowest average temperature at the start of the experiment to be $25^0\mathrm{C}$, the mean temperature can be given as:

$$\mathrm{T_{mean}} = \frac{150 + 25}{2} = 87.5^0\mathrm{C} \approx 90^0\mathrm{C} \tag{3.1}$$

We assume that the solution is pure water and it is incompressible where its density is constant. Also, we assume the specific heat capacity of the fluid can be approximated at average temperature of the fluid because the temperature difference is not that high. Thus, the properties will be approximated at $90^0\mathrm{C}$, $\mathrm{C_p} = 4.206\ \mathrm{kJ/kgK}$ and $\rho = 965.3\mathrm{kg/m^3}$. Using ρ and V, the mass of solution in the circuit can be determined. The power needed to increase the desired temperature rise in Watts (W), can be determined from the following formulae (Cengel, 2003).

$$\mathrm{Q} = \frac{\mathrm{mC_p\Delta T}}{\Delta \mathrm{t}} \tag{3.2}$$

$\Delta\mathrm{T}$ is the temperature difference between the average feed temperature of water which is averagely $25^0\mathrm{C}$ and our maximum intended temperature of $150^0\mathrm{C}$. Assuming a temperature rise in 1 hour;

$$\mathrm{Q} = \frac{0.02 \text{ x } 965.3 \text{ x } 4.206 \text{ x } 125}{3600}$$

$$\mathrm{P} = 2.8\mathrm{KJ/s}$$

Assuming a safety factor of 1.2, the heater power will be 3,4KW. From the formulae, the calculated heating element capacity is approximately 3.4 kW. A heater of **4kW** was suitable for the experiment to raise the temperature in approximately 1 hour.

3.3.2 Insulation Blanket

The elution vessel wall was constructed by sandwiching a hairfelt insulation blanket of thermal conductivity $k = 0.05 W/mK$ (Cengel, 2015). The initial average solution temperature is at $T_{o,i} = 25^0C$. It will be heated using a 4-kW solution heater to an average final temperature of $T_{\infty,i} = 150^0C$. The room air is at $T_{\infty,o} = 25^0C$ and the overall estimate value for natural convection coefficient at the outer surface is $h_o = 10 W/m^2K$ (Frank P. et al, 2011). The elution reactor has a height of 0.3 m and diameter of 0.243 m. Considering forced convection inside the elution reactor, we can estimate the inside convection coefficient h_i. The Figure 3.10 below shows the problem statement. It is required to draw the thermal circuit for the wall and label all temperatures, heat rates, and thermal resistance, determine the inside convection coefficient h_i and compute the insulation thickness L required to maintain the outer wall surface at a safe-to-touch temperature of $T_o = 40^0C$. The thermal circuit is shown in Figure 3.11 below;

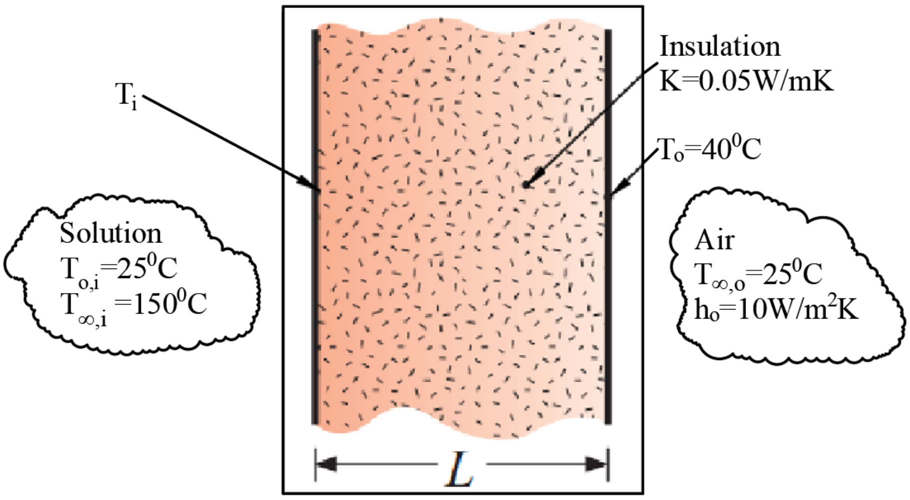

Figure 3.9: Problem illustration (Incropera, et al 2011).

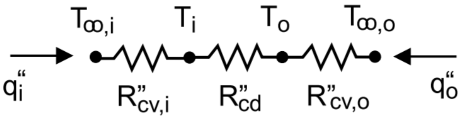

Figure 3.10: Thermal circuit (Incropera, et al 2011)

The film temperature inside the reactor

$$\mathrm{T_f} = \frac{150+25}{2} = 87.2.^0\,\mathrm{C} \approx 90^0\mathrm{C} \tag{3.3}$$

Assuming the solution is pure water and it is incompressible where its density is constant. Also, we assuming the specific heat capacity of the fluid can be approximated at average temperature of the fluid because the temperature difference is not hat high. The thermofluid properties of water at $90^0\mathrm{C}$ are derived from a table in appendix 4.

$$\mathrm{Re_d} = \rho v d/\mu = 1158690.96 \tag{3.4}$$

The critical Reynolds number for flow inside a pipe is 2300, hence flow inside elution tank is turbulent (Cengel, 2015; Incropera, et al 2011). Using Equation 3.5 below for turbulent flow in a cylinder, we compute the Nusselt number (Nu).

$$\mathrm{Nu} = h_i d/k = 0.023\mathrm{Re}_d^{0.8}\mathrm{Pr}^n \tag{3.5}$$

Where n is 0.4 for heating system. By substituting values in the equation, we get;

$$\mathrm{Nu} = h_i d/k = 1889.065$$

Using Equation 3.5 by substituting the tank diameter and the thermal conductivity of the fluid at film temperature $90^0\mathrm{C}$, we get;

$$\mathrm{h_i} = 5247.4\mathrm{W/m^2K}$$

Performing an energy balance through input and output nodes we find that shown in Figure 3.10 above we get:

$$\frac{\mathrm{T_{\infty,i} - T_i}}{\mathrm{R"_{cv,i}}} + \frac{\mathrm{T_o - T_i}}{\mathrm{R"_{cd}}} = 0$$

$$\frac{\mathrm{T_i - T_o}}{\mathrm{R"_{cd}}} + \frac{\mathrm{T_{\infty,o} - T_o}}{\mathrm{R"_{cv,o}}} = 0$$

Where thermal resistances are;

$$\mathrm{R"_{cv,i}} = \frac{1}{\mathrm{h_i}} = \frac{1}{5247.4} = 1.906 \text{ x } 10^{-4}\mathrm{m^2K/W}$$

$$\mathrm{R"_{cd}} = \frac{\mathrm{L}}{\mathrm{K}} = \frac{\mathrm{L}}{0.05}\mathrm{mK/W}$$

$$\mathrm{R"_{cv,o}} = \frac{1}{\mathrm{h_o}} = \frac{1}{10} = 0.1\mathrm{m^2K/W}$$

Therefore, solving the set of equations simultaneously, the insulation length will be;

$$\mathbf{L = 0.0366m = 37mm}$$

3.3.3 Minimum Fluidization Velocity

The minimum fluidization velocity calculation was taken from the textbook Chemical Engineering (Richardson, 2002). The most important parameter is the minimum fluidization fluid velocity of $\mathrm{U_{mf}}$ in $\mathrm{m/s}$. It is this fluid velocity which must be attained in order to overcome interparticle adhesive forces to have fluidization. This requires the input variables of fluid (liquid solution) and particle (gold loaded carbon granules). Thus, the properties will be approximated at a mean temperature $90^0\mathrm{C}$, as $\mathrm{C_p} = 4.206$ kJ/kgK and $\rho = 965.3 kg/m^3$.

The apparent density of carbon is between 250 to $650\mathrm{kg/m^3}$. Thus, averagely we may assume the apparent density to be $400\mathrm{kg/m^3}$. The bulk density is typically 90% to 91% the apparent density, and is used for sizing in gas and liquid phase applications. The bulk density of wetted gold loaded carbon granules is derived from the apparent density by the following equation (Sun & Yen, 1995);

$$\mathrm{BD} = 0.91 \text{ x } \mathrm{AD} = 0.91 \text{ x } 400 = 364\mathrm{kg/m^3} \tag{3.6}$$

Activated loaded carbon granule particle diameter is approximately $3.36\ \mathrm{mm}$ (Rogans, 2012). The calculation will be based on the method presented by (Richardson, 2002). We will determine voidage according to the following approximate equation for spheres. By considering eight closely packed spheres of diameter d in a cube of side $2\mathrm{d}$.

$$\text{Volume of spheres} = 8(\pi/6)\mathrm{d}^3 \tag{3.7}$$

$$\text{Volume of the enclosure} = (2\mathrm{d})^3 = 8\mathrm{d}^3 \tag{3.8}$$

Hence voidage,

$$\varepsilon = [8(\pi/6)\mathrm{d}^3 - 8\mathrm{d}^3]/8\mathrm{d}^3 = \mathbf{0.48} \tag{3.9}$$

From the textbook (Richardson, 2002), $\mathrm{U_{mf}}$ can be determined.

$$\mathrm{U_{mf}} = \left(1/\mathrm{K}''\right)(\varepsilon^3/S^2(1-\varepsilon)^2)(1/\mu)(-\Delta p/\mathrm{H}) \tag{3.10}$$

K'' is Kozeny's constant and generally accepted value for many circumstances for K'' is 5. Substituting $\mathrm{K}'' = 5, \mathrm{S} = 6/\mathrm{d}$ and $-\Delta\ \mathrm{P/H}$ from Equation 3.8 we get,

$$\mathrm{U_{mf}} = 0.0055\left(\varepsilon^3/(1-\varepsilon)\right)\left(\mathrm{d}^2\left(\rho_\mathrm{p} - \rho_\mathrm{f}\right)\mathrm{g}\right)/\mu \tag{3.11}$$

Substituting values, we have:

$$\mathrm{U_{mf}} = 0.0055\left(\frac{0.48^3}{(1-0.48)}\right)((2.38 \text{ x } 10^{-3})^2(1300-990.1\,)9.81)/0.577 \text{ x } 10^{-3}$$

$$\mathbf{U_{mf} = 0.035m/s}$$

From the conservation of mass principle:

$$\mathrm{A_1v_1 = A_2v_2} \qquad (3.12)$$

With $\mathrm{A_1}$ and $\mathrm{V_1}$ are the inlet pipe parameters and $\mathrm{A_2}$ and $\mathrm{V_2}$ are tank parameters. It can be calculated from this equation the pipe flow velocity as follows:

$$\mathrm{v_1} = \frac{\mathrm{A_2v_2}}{\mathrm{A_1}} = \frac{(\pi \text{ x } 0.1^2/4)\mathrm{m^2} \text{ x } 0.035\mathrm{m/s}}{(\pi \text{ x } 0.015^2/4)\mathrm{m^2}} = \mathbf{1.556m/s}$$

This is the pipe flow velocity which is related to the pump volumetric flow rate as follows;

$$\mathrm{Q = Av} \qquad (3.13)$$

$$\mathrm{Q} = (\pi \text{ x } 0.015^2/4)\mathrm{m^2} \text{ x } \frac{1.556\mathrm{m}}{\mathrm{s}}$$

$$= \mathbf{2.75 \text{ x } 10^{-4}m^3/s}$$

This translates to $\mathbf{0.99m^3/h.}$ This is an important variable in the experiment and it will be used to size a pump.

3.3.4 Pump Selection

Pump selection consists of a number of calculations in steps. The various steps are detailed below. Some material used for the calculation is taken from charts and graphs in Appendices.

3.3.4.1 Friction Head H_f for Pipe

We need to determine the equivalent pipeline, using the valves and fittings head. The actual length of the pipeline is 5.082 m and 6 x 90^0 bends of length 0.82 m each. The pipe fittings length is 4.92 m. Also available is a Tee piece of length 1.77 m. The equivalent length of the line is thus 11.77 m. Using a 12.5 mm (0.5 inch) steel pipe with line velocity of 0.576 m/s, we obtain the friction f = 0.0295 from chart WDS109 in Appendix 2. Using Darcy's equation, we obtain the friction head as follows;

$$H_f = f\frac{L}{d}\frac{V^2}{2g} \tag{3.14}$$

$$H_f = 0.0295 \text{ x } \frac{11.77}{0.025} \text{ x } \frac{0.576^2}{2 \text{ x } 9.81}$$
$$= 0.23\text{m}$$

3.3.4.2 Head Loss due to Sudden Contraction H_c from Elution Reactor to Pipe

From WDS108 Appendix 1 K_c depend on the ratio d_1/d_2. Where d_1 is the larger diameter of the tank, equal to 0.1m, and d_2 is the smaller diameter of the pipe equal to 0.015m. The resulting ratio is 16. The equivalent K_c factor is 0.45. Hence the head loss due to pipe contraction is;

$$H_c = K_c\frac{V_1^2}{2g} \tag{3.15}$$

$$H_c = 0.45 \text{ x } \frac{0.576^2}{2 \text{ x } 9.81} = 7.61 \text{ x } 10^{-3}\text{m}$$

3.3.4.3 Head Loss due to Sudden Contraction from EWC to Pipe

With K_c factor is 0.46, the H_c is calculated to be $7.78 \, x \, 10^{-3} m$.

3.3.4.4 Head Loss due to Sudden Enlargement H_e

From WDS108 Appendix 1 the head loss due to sudden enlargement will only be approximated for the tank and multiplied by two since they are of the same order as shown by the sudden contraction calculations above. The following equation gives the head loss due to sudden enlargement;

$$\mathrm{H_e} = \frac{\mathrm{V} - \mathrm{V_1}}{2\mathrm{g}} \tag{3.16}$$

$$\mathrm{H_e} = 2 \text{ x } \frac{0.576 - 0.035}{2 \text{ x } 9.81}$$
$$= 0.055\mathrm{m}$$

3.3.4.5 Total Dynamic Head

Since the static head of the system is $1.2m$, the total dynamic head is given by the sum of the above calculated head losses. This give the total dynamic head as follows;

$$\mathrm{H_m} = 1.2\mathrm{m} + 0.23\mathrm{m} + 7.61 \text{ x } 10^{-3}\mathrm{m} + 7.78 \text{ x } 10^{-3}\mathrm{m} + 0.055\mathrm{m}$$

$$\mathrm{H_m} = \mathbf{1.5m}$$

A pump can now be selected using the flow velocity of $0.576m/s$ and total dynamic head of $1.5\,m$. Using the pump performance system curves in Appendix 3, assuming the efficiency of the pump to be 71%, the power required for the pump is given by the following equation;

$$\mathrm{P} = \frac{\rho_f \mathrm{Q} \mathrm{H_m} \mathrm{g}}{1000\eta} \tag{3.17}$$

With η as the efficiency from system curves and Q is the volumetric flow rate.

$$\mathrm{P} = \frac{990.1 \text{ x } 9.81 \text{ x } 0.283 \text{ x } 10^{-3} \text{ x } 1.5}{1000 \text{ x } 0.71}$$

$$\mathrm{P} = 0.005\mathrm{KW}$$

Applying safety factor of about 25%, for a range of 0 to 11KW, we get the power to be;

$$P = 1.25 \text{ x } 0.005$$

$$= \mathbf{0.06kW}$$

Thus, considering what is available on the market, a **0.37kW** or **0.5HP** circulating pump is suitable for the test rig.

3.5 Material for Experiment

For the experiment to proceed, reagents and loaded carbon were gathered. The reagents included caustic soda and cyanide. The purpose of caustic soda was to exothermically react with water and add a temperature spike that also enables a faster temperature rise until the caustic soda is completely saturated in the solution. It is also very essential in order to lower the pH of the solution to 11, which is a conducive environment for elution. Cyanide is important in forming strong ions for better electroplating during winning in the electrowinning cell.

3.6 Experimental Set Up Conditions for Elution System

Here we will present the method employed to control the system flow rate, pressure and temperature during the experiments.

3.6.1 Flow Rate Control

On flow rate measurement, the method relies upon the pump affinity laws for centrifugal pumps. The affinity laws for centrifugal pumps describe the impact of changes in speed or impeller diameter on pump flow, head and horsepower (Whitesides, 2012).

They are useful tools in deriving quickly the performance when changes are made on the pump due to either change in rotation speed on the rotor, or when a variable speed drive (VSD) is used for flow variations. This in particular also works in the same principle when a throttle valve is used to vary the flow rate of the liquid being pumped. The affinity laws according to (Whitesides, 2012) state that:

1. Flow will change directly when there is a change in speed or diameter of the impeller
2. Heads will change as the square of a change in speed or diameter of impeller
3. Horsepower will change as the cube of a change in speed or diameter of impeller

Using the first affinity law, as we throttle our valve to vary flow rate, the flow reduces because the weight of the water being pumped has reduced. In turn the rotational speed of the rotor reduces thereby resulting in less current being drawn by the rotor. In order for us to calculate the flow rate at such a particular throttle, we can measure the rotation speed of the impellor using the tachometer, and use the first law to calculate the flow rate. This relationship depends on the maximum rotational speed of 2850 rpm that delivers 42 l/min from the pump nameplate. The mathematical expression of the above first relations is given in Equation 3.16 below as:

$$\frac{\mathrm{Q_1}}{\mathrm{Q_2}} = \frac{\mathrm{d_1}}{\mathrm{d_2}} = \frac{\mathrm{N_1}}{\mathrm{N_2}} \tag{3.18}$$

Where Q is flow rate in l/min, d is diameter in m, and N is rotational speed in rpm. Using this equation together with the tachometer in place we can configure and measure the rotation speed. By throttling the ball valve for different flow rates, we reduce the speed of the rotor. Consequently, we obtain a lower rotation speed that enables us to calculate the new flow rate that corresponds to the new rotation speed. Elution process possess a difficulty in measuring flow rate even at the commercial level because of the temperature in the fluid, and the corrosiveness of the solution.

By this, it becomes more expensive to purchase a flow meter that can handle high temperatures of 130^0C at the same time corrosive resistant. The advantages of the flowrate measuring method are that the fluid is in contact with the rotating component that perfumes energy conversion of the fluid to kinetic energy, Water pressure rotates the measured rotor and Each drop of liquid passing through goes through rotating rotor. Each cycle or rotation of the rotor supplies a defined quantity of liquid to the discharge. Although the method seems so accurate, it has to be taken into consideration that there is a degree of error. With this in mind, the purpose of this exercise is to come up with approximate flow rates that can give us a clear picture of the effects it has on elution. The rotational speed can be determined from name plate data with maximum flow rate $Q_1 = 42l/min$ at rotation speed $N_1 = 2850rpm$. If we throttle our valve and read a rotation speed of the rotor of $N_2 = 1430rpm$, the new flow rate is given as;

$$\frac{\mathrm{Q_1}}{\mathrm{Q_2}} = \frac{\mathrm{d_1}}{\mathrm{d_2}} = \frac{\mathrm{N_1}}{\mathrm{N_2}}$$

$$\mathrm{Q_2} = \frac{\mathrm{Q_1 N_2}}{\mathrm{N_1}}$$

$$\mathrm{Q_2} = \frac{42 * 1430}{2850} = 21 \text{ l/min}$$

Using the same method, results in Table3.1 below were obtained for three different flow diversions. The corresponding results were converted to m^3/h. Using the pipe diameter just after the pump and flow velocity, the corresponding Reynolds' numbers were determined for each flow. These Reynolds' numbers for the three unique conditions were taken under atmospheric pressure and an ambient temperature of 32^0C.In case of more accurate flow measurement, other methods can be employed at a more advanced stage.

Table 3.1: Flow rates results and corresponding Reynolds number

Valve position	RPM	Flow rate (l/min)	Flow rate (m^3/h)	Pipe Dia.	Flow velocity (m/s)	Re
Full open	1445	21.3	0.000355	0.015	2.01	37608
½ close	1245	18.3	0.000306	0.015	1.73	32403
¾ close	918	13.5	0.000226	0.015	1.28	23892

3.4.2 Temperature Control

The system temperature is electronically controlled using a K-type thermocouple and a temperature controller. The thermocouple is connected to the temperature Proportional, Integral, Derivative (PID) controller. The required temperature per each experiment is configured on the temperature PID controller by programming it. The PID output is connected to a contactor. The contactor is connected to the heating element. See Figure 3.11 above. By controlling the contactor on and off it maintains the required temperature by the temperature controller. The control philosophy is a closed loop circuit including a sensor (K-type thermocouple), a temperature PID controller (Rex-C100), measured variable (heated solution), and an actuator (contactor).

3.4.3 Pressure Control

The system pressure is mechanically controlled using a pressure gauge and a pressure relief valve. Three system pressure values used for the experiment are 1.0bar, 1.5bar and 2.0bar. To vary these pressure values, the researcher varies the pressure relief valve setting to a different setting position to achieve the desired value. In order to get a high pressure inside the system, the lock nut is unscrewed first, then screw clockwise the pressure setting nut. The spring inside the valve compresses the plunger so that it allows pressure to escape at high values. In order to get a low pressure inside the system, the pressure setting nut is unscrewed counter clockwise. The spring inside the valve decompresses the plunger to allow for pressure to escape at lower values.

3.5 Experimental Conditions

Below is the Table 3.2 illustrating the summary of the conditions that are implemented during the main experiments. The conditions have been derived from temperature, flow rate and pressure setting procedures performed prior to the main experiment execution. The control measurement employed are made to achieve repeatable results. Temperature variable effect, pressure variable effect and flow rate variable effect are measured at least three times to assure repeatability and accuracy of the elution test rig.

Table 3.2: Experimental conditions for temperature test

Flow rate	**Temperature**	**Pressure**
37608 Re	110	1.5 Bar
37608 Re	120	1.5 Bar
37608 Re	130	1.5 Bar

Table 3.3: Experimental conditions for pressure test

Flow Rate	**Temperature**	**Pressure**
37608 Re	120	1.0 Bar
37608 Re	120	1.5 Bar
37608 Re	120	2.0 Bar

Table 3.4: Experimental conditions for flow rate test

Flow Rate	**Temperature**	**Pressure**
37608 Re	120	1.5 Bar
32403 Re	120	1.5 Bar
23892 Re	120	1.5 Bar

3.6 Experimental Procedure

Below are steps followed during each experiment in order;

1. Weigh 2 kg of gold loaded carbon and load in the elution column.
2. Weigh 50 g of caustic soda and load in the elution column.
3. Weigh 25 g of cyanide and load in the elution column.
4. Load 50 g of wire wool in the electrowinning cell on the cathode terminal.
5. Add water in the elution column, 100mm height above the outlet and the electrowinning cell, 50 mm above the outlet and close.
6. Make sure the whole circuit, including the pipework, is filled with water.
7. Prime the pump by unscrewing the plug on the priming chamber, make sure bubbles of air are vented out until the priming chamber is filled with water.
8. Pour engine oil inside the blanked hole of the elution column and place the thermocouple nob inside.
9. Open the isolating valve and throttling valve to the required opening and switch on the main circuit breaker, and start the test.
10. Set the Set Value on temperature controller to the required maximum operating temperature
11. Set the pressure relief valve to suit desired pressure for a particular experiment.
12. Note time is taken to reach the desired temperature and start taking samples at that desired temperature through the sampling valve.
13. Take samples every 2-hour interval, to achieve 4 samples for the next 6 hours.
14. Perform stage 13 for the next 6-hours and stop the elution.
15. Take samples to the laboratory on the GBC 933 AA machine and get results.

3.7 Summary

The above described methodology was used to perform the experiments. These experiments followed the same order to avoid any form of error on the outcome. The main important points to note were the time taken to reach maximum temperature per every test, and the gold concentration in gram per ton for each test. The gold concentration results were obtained from Homestake laboratories Pvt Ltd. and stamped certificates were issued to prove the authenticity of the outcomes. A GBC 933 AA machine was used to measure gold concentration results from the samples at a cost. The table of results and corresponding graphical representations are well articulated in the next chapter 4.

CHAPTER 4
RESULTS AND DISCUSSIONS

4.1 Overview

In this chapter the researcher will detail the explanations of the results obtained from the experiments. Under **heading 4.1.1**, the repeatability of the experiment is explained. It is explained together with a table of results to show how agreeable the outcomes were. Under **heading 4.1.2, 4.1.3, and 4.1.4** are the test results discussions. These discussions include pressure, temperature and flow rate test results respectively. The corresponding laboratory results for the graphs explained in this chapter are found in Appendix 4 to 6. Finally, **heading 4.2** is the summary of the chapter. The discussions in this chapter pertain to modified Zadra elution system, which includes elution and electrowinning happening simultaneously.

4.1.1 Repeatability of the Experiment

In Table 4.1 below, there is an agreement amongst the measurands under the same conditions of the experiments. The conditions used to verify the repeatability of the experiments are flow rate of 37608 Re, temperature of 120^0C and pressure of 1.5 bar. Each experiment with the same conditions was conducted for 7 hours. Samples were collected in a 2-hour interval and tested at the laboratory. Comparing the results, from first to third test under the same conditions it can be seen that the results in grams per ton are agreeing as shown by a very small standard deviation. The degree of agreement shown verifies the repeatability of the experiment.

Table 4.1: Repeatability test results

Conditions	Test 1	Test 2	Test 3	Standard Deviation
Flow rate: 37608 Re Temp 120^0C Pressure 1.5 bar	2.61g/t	2.29g/t	2.52g/t	0.13
	1.48g/t	1.59g/t	1.44g/t	0.06
	1.11g/t	1.09g/t	1.13g/t	0.02
	0.62g/t	0.48g/t	0.5g/t	0.06

4.1.2 Effect of Pressure on Elution

Figure 4.1 shows the general behaviour of the reactants. It is the expected trend that gold concentration decreases as the process progresses. As the reaction occurs, gold is eluted from the carbon and electroplated on the electrowinning cell. As is in the conventional methods, in the early stages of the process, gold concentration should be high when a sample is tested. As the elution process progresses, the electrowinning cell becomes more cathodic, as it attracts more gold on it. Gold concentration starts decreasing since mass is being transferred from the carbon to the electrowinning cell. In any case, if the reaction shows an increase on gold concentration during the elution process, the condition is unacceptable (Deventer & Merwe, 1994). Under all three pressure variables gold concentration decreased over the course of the process. Of cause the rate of decrease was different, owing to the difference in pressure conditions for each experiment.

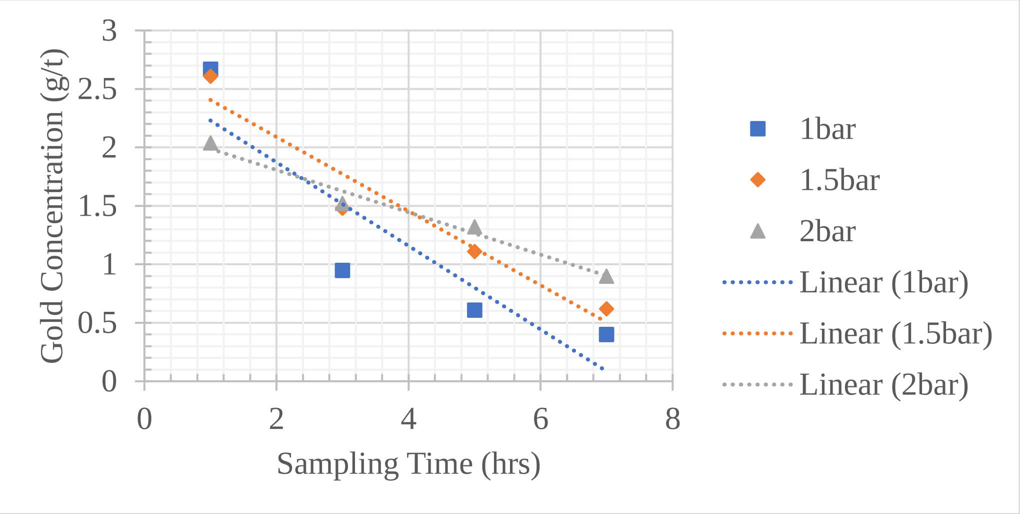

Figure 4.1: Pressure test graph

This conforms with the changes that take place in a conventional Zadra elution process. From Figure 4.2 it can be seen that the gold concentration change at high pressures is lower than gold concentration change at low pressures.

As the system pressure increases gold accumulation in the electrowining cell decreases. Thus, we have more gold concentration in the solution at high pressures. To further clarify this, a linearity graph in Appendix 7 has been prepared for each pressure variable.

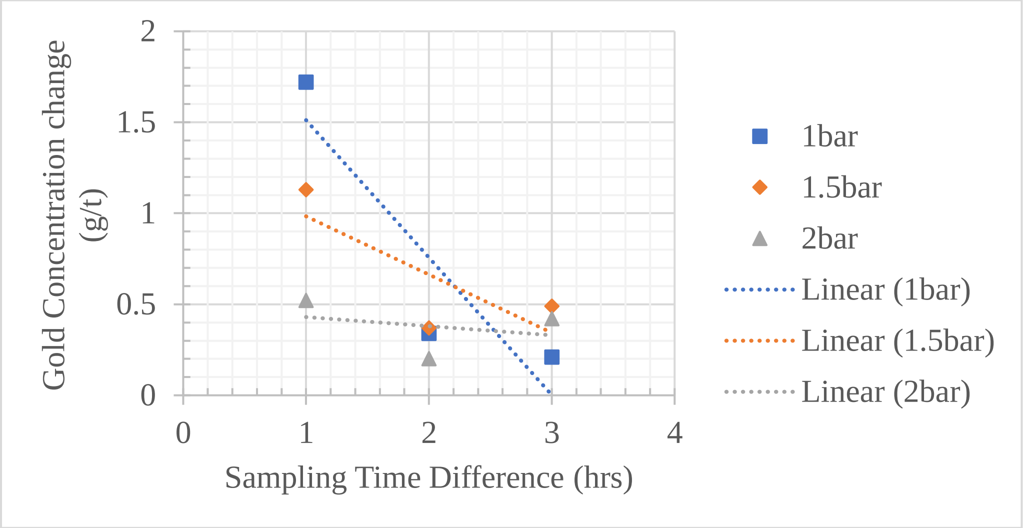

Figure 4.2: Gold concentration change versus pressure difference graph

The linear equations attached show different gradients that depict the sloppiness of the line. The steeper the line, the greater the change in gold concentration per pressure variable. The steepest gradient is -0.3575 for 1 bar which gives the highest gold concentration change, followed by the steeper gradient of -0.317 for 1.5 bar. The 2-bar pressure gives the lowest gold concentration change with a gradient of -0.181. From chapter 2 **heading 2.3.1**. Jeffrey, et al, (2009) purported that the gold loading capacity on carbon decreases with increasing in pressure. At high pressure 5 bar (0.5MPa), the rate of desorption is approximately 96% (Xinhai Mining) for about 12 to 14 hours, faster than the conventional system that takes 20 hours (Wang, 2017). The information obtained from these researches was not derived from a reactor under fluidisation. The results obtained in this work was done for in a fluidised bed reactor, hence pressure values obtained for high stripping rates are lower than those purported in the previous works. Fluidisation changes reaction dynamics. In a conventional packed bed reactor that has been researched by many scholars, more energy would be required to achieve more pressure for fast elution processes. Under the fluidised reactor, the energy required to achieve low pressure values is low. This presents a net positive result on cost of production during.

4.1.3 Effect of Temperature on Elution

Figure 4.3 shows the general behaviour of the reactants. It is the expected trend that gold concentration decreases as the process progresses. As the reaction occurs, gold is eluted from the carbon and electroplated on the electrowinning cell. As is in the conventional methods, in the early stages of the process, gold concentration should be high when a sample is tested. As the elution process progresses, the electrowinning cell becomes more cathodic, as it attracts more gold on it. Gold concentration starts decreasing since mass is being transferred from the carbon to the electrowinning cell.

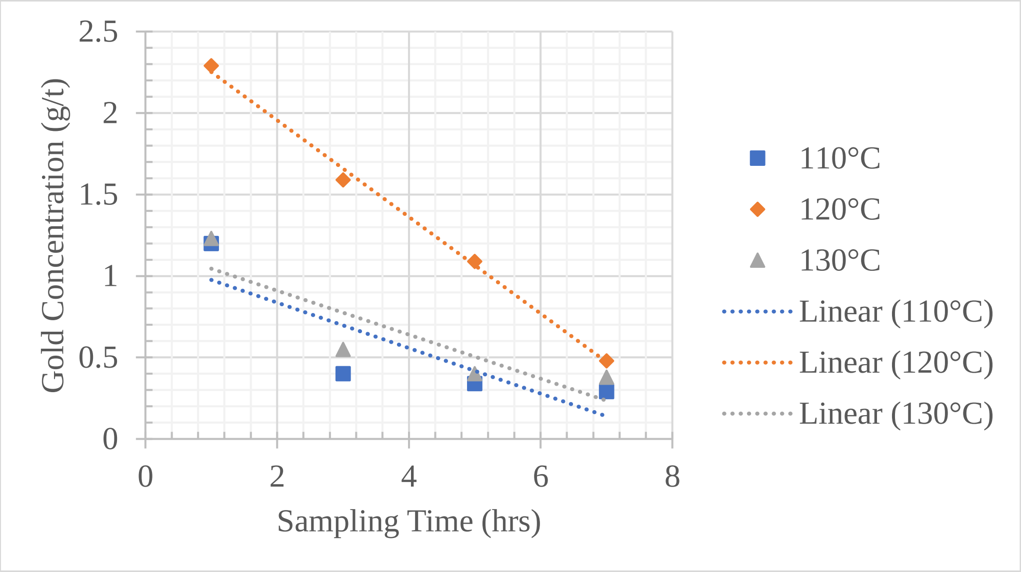

Figure 4.3: Temperature test graph

In any case, if the reaction shows an increase on gold concentration during the elution process, the condition is unacceptable (Deventer & Merwe, 1994;Wang Monica, 2017). Under all three temperature variables gold concentration decreased over the course of the process. Of cause the rate of decrease was different, owing to the difference in temperature

conditions for each experiment. This conforms with the changes that take place in a conventional Zadra elution process. Figure 4.3 shows the expected general behaviour of the reactants. Under all three temperature variables gold concentration decreases over the course of the process. This justifies the feasibility of the changes made from the conventional methods. From the Figure 4.4 below it can be observed that gold concentration change increases with increase in temperature as evinced by variations between $110^{0}\mathrm{C}$ and $120^{0}\mathrm{C}$. These variations are well articulated from the linearity graphs for each particular temperature. The linearity graph for temperature in Appendix 8 shows that the steeper the gradient of the line, the greater the gold concentration change in a reaction under a particular temperature. The negative sign in the linear equation shows the decrease in concentration of gold during the elution process. For $110^{0}\mathrm{C}$, the gradient is less sloppy at -0.1395. The steeper gradient at $120^{0}\mathrm{C}$ is -0.2965. This agrees with information articulated in chapter 2 under **heading 2.3.1**. Elution rate at $180^{0}\mathrm{C}$ is 8 times faster than at $90^{0}\mathrm{C}$ at atmospheric pressure (Jeffrey, et al, 2009). According to Jeffrey, et al, (2009) the gold loading capacity on carbon decreases with increasing in temperature. At high temperature the rate of desorption is approximately 96% (Xinhai Mining) for about 12 to 14 hours, faster than the conventional system that takes 20 hours (Wang, 2017). Modified high temperature Zadra process has been implemented by other organisations, operating at $140^{0}\mathrm{C}$ decreasing elution time to about 12 hours (Feng, et al, 2003). Although this is in agreement with previous studies, it must also be accepted that the experiments were conducted under fluidised bed condition. Owing to the loaded carbon used and the alkaline chemistry of the loaded carbon, some differences would be expected. This includes the difference in behaviour of elution at $130^{0}\mathrm{C}$. The effect of temperature under a flow rate of 37608 Re and pressure 1.5 bar shows a significantly low elution characteristic comparable to that at $110^{0}\mathrm{C}$. From the studied literature, this behaviour can be attributed to the sensitivity of the aurocyanide complex to
high temperatures. Under **heading 2.3.1.1**, information is well articulated that explain the behaviour of aurocyanide complex during elution. Two sets of equations, Equations 2.5, 2.6 and 2.7, and Equations 2.8 and 2.9 explain the routes through which cyanide is decomposed at low and high temperature. According to Merwe (1993), cyanide decomposition is gradual

at low temperature. At higher temperatures hydrolysis reaction is more significant, while at low temperatures the dominant reaction is that of catalytic oxidation. Hence, hydrolysis becomes the main mechanism for cyanide and gold loss (Merwe, 1993) at high temperature. The decomposition of the aurocyanide complex results in cyanide and gold loss giving a low gold concentration in sample. **Figure 4.4 in chapter 2** shows cyanide profiles for elution at different temperatures (Merwe, 1993). It is clear that at high temperature of 130^0C there is a tendency of cyanide decomposition in the solution. Although elution is efficient at higher temperatures, cyanide critical operating temperature becomes an important and a major limiting factor to operating temperature. The researcher could not find the critical temperature for cyanide decomposition to compare with results, but using **Figure 2.4.5 in chapter 2**, Merwe (1993) shows that at 150^0C decomposition is active.

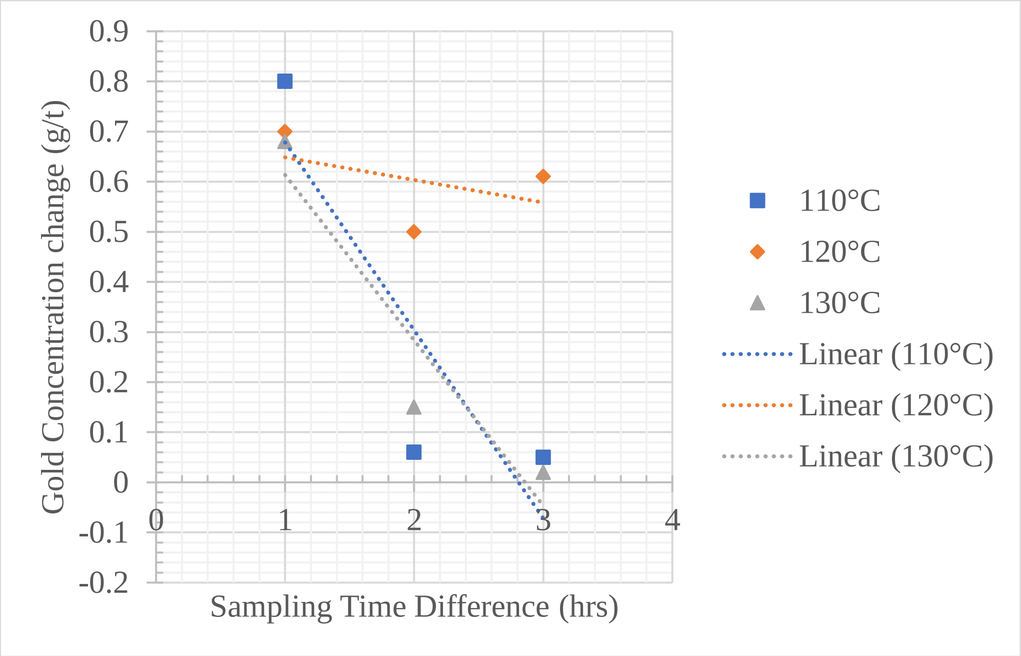

Figure 4.4: Gold concentration change versus temperature difference graph

4.1.4 Effect of Flow Rate on Elution

Figure 4.5 shows the general behaviour of the reactants. It is expected that gold concentration decreases as the process progresses. As the reaction occurs, gold is eluted from the carbon and electroplated on the electrowinning cell. In the early stages of the process, gold concentration should be high when a sample is tested. As the elution process progresses, the electrowinning cell becomes more cathodic, as it attracts more gold on it. Gold concentration starts depleting in the solution since mass is being transferred from the carbon to the solution, finally on the cathode plate of the electrowinning cell. In any case, if the reaction shows an increase in gold concentration during the elution process, the condition is unacceptable (Deventer & Merwe, 1994). During flow rate test, only two flow diversions of $32403\ Re$ and $37608\ Re$ conformed to the expectations of the reaction. Flow rate $23892\ Re$ presented an anomalous behaviour. Flow rate is key to elution since it is responsible for two key fundamental factors that affect elution process. These are heat and mass transfer. Convective heat transfer ensures a uniform temperature distribution across the fluid. The fluid has an approximately high convective heat transfer coefficient of $5247.4\mathrm{W/m^2K}$ as calculated in chapter 3 under heading 3.4.2.

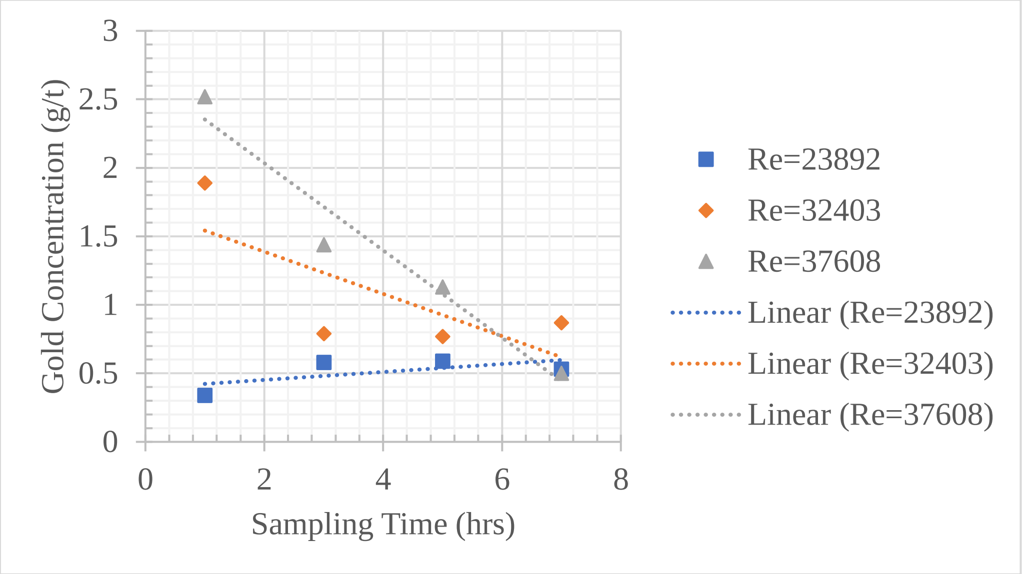

Figure 4.5: Flow rate test graph

Aurocyanide chemical species will migrate through the micropore of carbon by diffusion, into the solution, and electroplated on the cathode plate in the electrowinning.

This happens through a process of mass transfer process. During this experiment, increase in flow rate caused an increase in gold concentration change in the solution. Figure 4.6 shows that flow rate 37608 Re gives increased gold concentration change than 32403 Re. From Appendix 9, at flow rate 37608 Re we have a gradient of -0.3185 while flow rate 32403 Re we have a gradient of -0.154. These gradients show the steepness of the graphs which conforms to the gold concentration changes. The differences in rate concentration changes are due to the differences in rate of transfer of mass and transfer of heat. Essential fundamental example which shows increased flow velocity increases mass transfer rate is that of a home humidifier. At high flow velocity, the room quickly gets warm as water vapour species are carried into a dry air environment. In that same token, a fluidised system is good in that it promotes increased diffusivity of the aurocyanide ion from within the micropores of carbon into the solution due to turbulence (Sun & Yen, 1995).

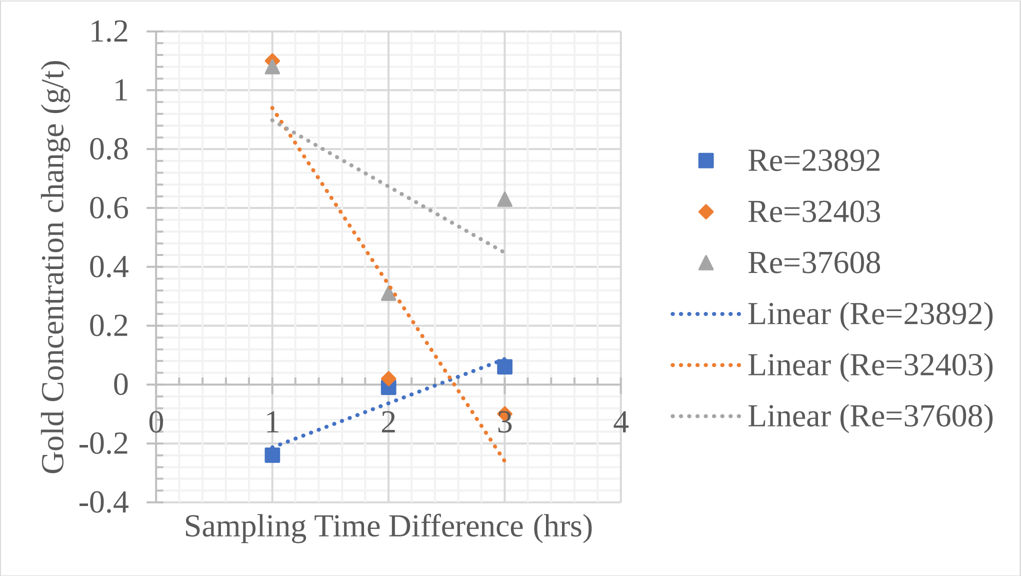

Figure 4.6: Gold concentration change versus flow rate difference graph

Flow rate is important in reactions, especially ones that are conducted in vertical reactors. It is more fundamental in the elution process during solution circulation in the circuit. This easy of flow increases with increase in fluidisation as shown from the results obtained.

At low flow rate of 23892 Re, there is a unique phenomenon. It shows that during the course of the elution process, gold eluted into the solution has not been properly electroplated. We know for sure that elution has been occurring because the two conditions of temperature 120^0C and pressure of 1.5 bar do favour the forward reaction of elution. Furthermore, after testing samples in the laboratory, we find gold concentrates in the solution to prove that mass transfer of species from carbon into the solution has occurred. There is a slight increase in concentration, and a sudden constant concentration of gold in the solution. From the linear graph, the gradient is positive suggesting gold is not being electroplated. Therefore, the researcher can only attribute the reaction dynamic to the electrowinning cell response to the flow rate. Further tests are suggested to verify the conditions.

4.2 Summary

The chapter gave detailed result discussions. The discussions depended on the information reviewed in chapter two. Chapter four discussed the effect of pressure, temperature and flow to elution. The effect of pressure to elution showed that as it is increased, there is also an increase of gold concentration in the solution. Gold concentration increases in the solution with increase in temperature. According to the investigation carried, it showed that this increase is only within a limited range of temperature. At temperature of 130^0C gold concentration decreases. Chapter 4 discussed the effect of fluidised bed reactor. This section showed how fluidisation yields good results during elution.

CHAPTER 5

CONCLUSIONS AND RECOMMENDATIONS

5.1 Overview

Investigation of the effect of temperature, pressure and flow rate on modified Zadra gold elution process was conducted at Near East University Northern Republic of Turkish Cyprus. Conclusions and recommendations have been drawn after the study. These are explained in this chapter under the following **headings 5.2** and **5.3.**

5.2 Conclusion

The effect of temperature, pressure and flow rate on the modified Zadra elution process was investigated. To proper conclusion of the effect of these parameters it must be noted that the experiments performed were based on the Zadra elution system. The Zadra elution system comprises of the elution vessel, in which elution takes place and the electrowinning, in which electroplating of gold happens. These two vessels are in a single circuit which includes a pump, pipe line and fittings. This is the design shown in **Figure 3.0.1 of chapter 3 heading 3.2.3**. Furthermore, the conditions employed for both the elution column, and the electrowinning cell are a true replica of the conditions employed at large scale. These conditions include the parameters investigated on the elution side. On the electrowinning side these conditions include the cathode and anode voltage of 4V, using a tailor-made transformer for electrowinning process specifically. The current used of 75A is also a true replica of the one at large scale.

Firstly, it showed that there is a decrease in gold concentration change as pressure increases. The conventional Zadra elution system has the gold concentration change increasing as pressure increases. This study has given a different process behaviour due to the presents of fluidisation. Owing to this, the reaction kinetics have shifted to favour the forward reaction at low pressure. Operating at low pressure, achieving good results means we have saved on material costs, process cost, and enhanced safety precautions. At high pressure, the process is hazardous. At low pressure the process is safe. The net positive effect of this is both on efficiency and cost of the elution process.

Secondly it can be concluded that, as temperature increases gold concentration change increases. This agrees with information well-articulated in chapter 2. This is more clearer considering the 110^0C and the 120^0C temperature variable. At 120^0C the process experiences an increased gold concentration change than at $110^0C.$ Thus, temperature is important during the fluidised Zadra elution process. Considering that the process was fluidised, the reaction dynamics at 130^0C were unexpected. But using the information from chapter 2, it can be concluded that the low gold concentration change tendency is attributed to aurocyanide decomposition. This is primarily because the aurocyanide complex is sensitive to high temperatures.

Thirdly, flow rate showed that as it is increased, so does fluidisation, the gold concentration change increases in the solution. The fluidised Zadra elution process responded as expected considering the net positive effect of fluidised bed reactors to mass and heat transfer. It can be concluded that at low flowrate of $23892\ Re$ the reaction was unexpected. Challenges to make solid conclusions are attributed to the fact that, at this flow rate, the process may have different responses from the two chambers i.e. elution chamber and electrowinning chamber. Previous studies have shown that at low flow rates, under packed bed, elution occurs. Thus, at any flow rate above the minimum flow rate used for packed bed reactors mass transfer should occur. In this case further recommendations will be made for future studies.

Finally, the researcher used tailing carbon for the experiments. The tailings carbon obtained after main elution process has low gold loading capacity. It is difficult to extract the small proportions of gold from this carbon (Sun & Yen, 1995). From the research done, samples of gold concentrates were drawn. This shows that the process is able to extract the small proportions under fluidised conditions.

5.3 Recommendations

After evaluating the conclusions made in this chapter, it is clear that fluidisation causes a change in reaction dynamics. Pressure parameter gave a different response to the results, compared with its behaviour on previous studies and conventional method. Flow rate at $23892\ Re$ gave unexpected results as well. As previously highlighted before, the study was focused on the effect of these parameters on the complete modified Zadra elution system. For future studies, it is recommended to separate the two Zadra elution chambers, analysing the elution process separately from the electrowinning cell. This will help to make further better conclusions on the effect of each parameter on each process. These conclusions can therefore be married to each other for optimisation of the process.

Furthermore, as the researcher has eluded in the conclusion section, it is difficult to extract the small proportions of gold from this carbon (Sun & Yen, 1995). For future studies, the researcher recommends to use full loaded carbon with a high gold grade. With loaded carbon, samples give better results for analysing gold concentration changes and extraction efficiency for each parameter.

Only four samples were drawn for each experiment. It is recommended to increase number of samples collected per elution run. With the funding limitations experienced during this research, the flow rate measuring instrument was only enough to give an idea as to what happens with change in flow rate. It is equally important to draw conclusions on the flow rate regimes at specific given values, hence the need for proper accurate measuring instrument.

REFERENCES

Adams, M. D. (1994). The elution of gold from activated carbon at room temperature using sulphide solutions. *The Journal of the South African Institute of Mining an Metallurgy*, (August), 187–198.

Barker, J. J. (1965). Heat transfer in fluidized beds, *57*(5), 33–39. https://doi.org/10.1016/0032-5910(78)80089-8

Butt, J. B. (1960). Chemical engineering plant design. *Chemical Engineering Science*, *13*(2), 93. https://doi.org/10.1016/0009-2509(60)80030-9

Cengel, Y. A. (2003). Heat Transfer: A Practical Approach. *Mc Graw-Hill*, 785–841.

Cengel, Y. A. (2015). Heat Transfer ; 2nd Edition, *2th*(c), 474–532.

Davidson, R. J. (1974). The mechanism of gold adsorption on activated charcoal. *Journal of the South African Institute of Mining and Metallurgy*, (November), 67–76.

Deventer, J. S. J. Van, & Merwe, P. F. Van Der. (1994). Factors affecting the elution of gold cyanide from activated carbon, *7*(I), 71–86.

Espiell, F., Roca, A., Cruells, M., & Núñez, C. (1988). Gold desorption from activated carbon with dilute NaOH/organic solvent mixtures. *Hydrometallurgy*, *19*(3), 321–333. https://doi.org/10.1016/0304-386X(88)90038-2

Frank P. Incropera, Bergman, Theodore L. Arienne S. Lavine, D. P. D. (2011). *Fundamentals of Heat and Mass Transfer*. (D. P. D. Frank P. Incropera, Bergman, Theodore L. Adrienne S. Lavine, Ed.) (7th Edition). John Wiley & Sons ISBN 13 978-

0470-50197-9. https://doi.org/10.15713/ins.mmj.3

Gray, D. E. (1999). A quantitative study into carbon-in-pulp adsorption operations a quantitative study into carbon-in-pulp, (April), 54.

Merwe, P. F. Van Der. (1993). The effect of temperature on the desorption cyanide from activated carbon of gold, *221*, 99–113.

Mickley, H. S., & Trilling, C. a. (1949). Heat Transfer Characteristics of Fluidized Beds. *Industrial & Engineering Chemistry*, *41*(6), 1135–1147. https://doi.org/10.1021/ie50474a007

Mular, A. L., Halbe, D. N., & Barratt, D. J. (2002). *Mineral Processing Plant Design, Practice, and Control. Proceedings* (Vol. 1, 2).

Rhodes, M. (2008). *Introduction to Particle Technology: Second Edition*. *Introduction to Particle Technology: Second Edition*. https://doi.org/10.1002/9780470727102

Richardson, J. M. C. & J. F. (2002). *Chemical engineering* (Vol. 2).

Rogans, J. (2012). Activated Carbon In Gold, (June), 1–34.

Snyders, C. A., Bradshaw, S. M., Akdogan, G., & Eksteen, J. J. (2015). Factors affecting the elution of Pt , Pd and Au cyanide from activated carbon. *Minerals engineering*, *80*, 14–24. https://doi.org/10.1016/j.mineng.2015.06.013

Stanley, G. . (1987). The Extractive Metallurgy of Gold in South Africa, *2*, 1–544.

Sun, T. M., & Yen, W. T. (1995). A reactor model for gold elution from activated carbon with caustic cyanide solution. *Canadian Metallurgical Quarterly*, *34*(4), 303–310.

https://doi.org/10.1016/0008-4433(95)00020-X

Ubaldini, S., Fornari, P., Massidda, R., & Abbruzzese, C. (1998). An innovative thiourea gold leaching process. *Hydrometallurgy*, *48*(1), 113–124. https://doi.org/10.1016/S0304-386X(97)00076-5

Ubaldini, S., Massidda, R., Vegliò, F., & Beolchini, F. (2006). Gold stripping by hydro-alcoholic solutions from activated carbon: Experimental results and data analysis by a semi-empirical model. *Hydrometallurgy*, *81*(1), 40–44. https://doi.org/10.1016/j.hydromet.2005.10.004

Van Den Berg, R., Petersen, F. W. (2000). Inhibition of pregrobbing phenomenon in gold ores. *Proceedings of the V International Conference on Clean Technologies for the Mining Industry*, (December), 329–338.

Van Deventer, J. S. J., & Liebenberg, S. P. (2003). The role of cyanide in the multi-component elution of cyanide complexes from activated carbon. *The European Journal of Mineral Processing and Environmental Protection*, *3*(3), 1303–1868.

Wang Monica. (2017). Desorption Electrolysis System, Electrolysis Equipment, Gold Electrowinning Process - Xinhai. Retrieved October 3, 2017, from http://www.xinhaimining.com/product/gold/desorption-electrolysis-system

Whitesides, I. R. W. (2012). Basic Pump Parameters and the Affinity Laws, *125*.

APPENDICES

Appendix 1a: Valves/ Fittings/ Head Losses

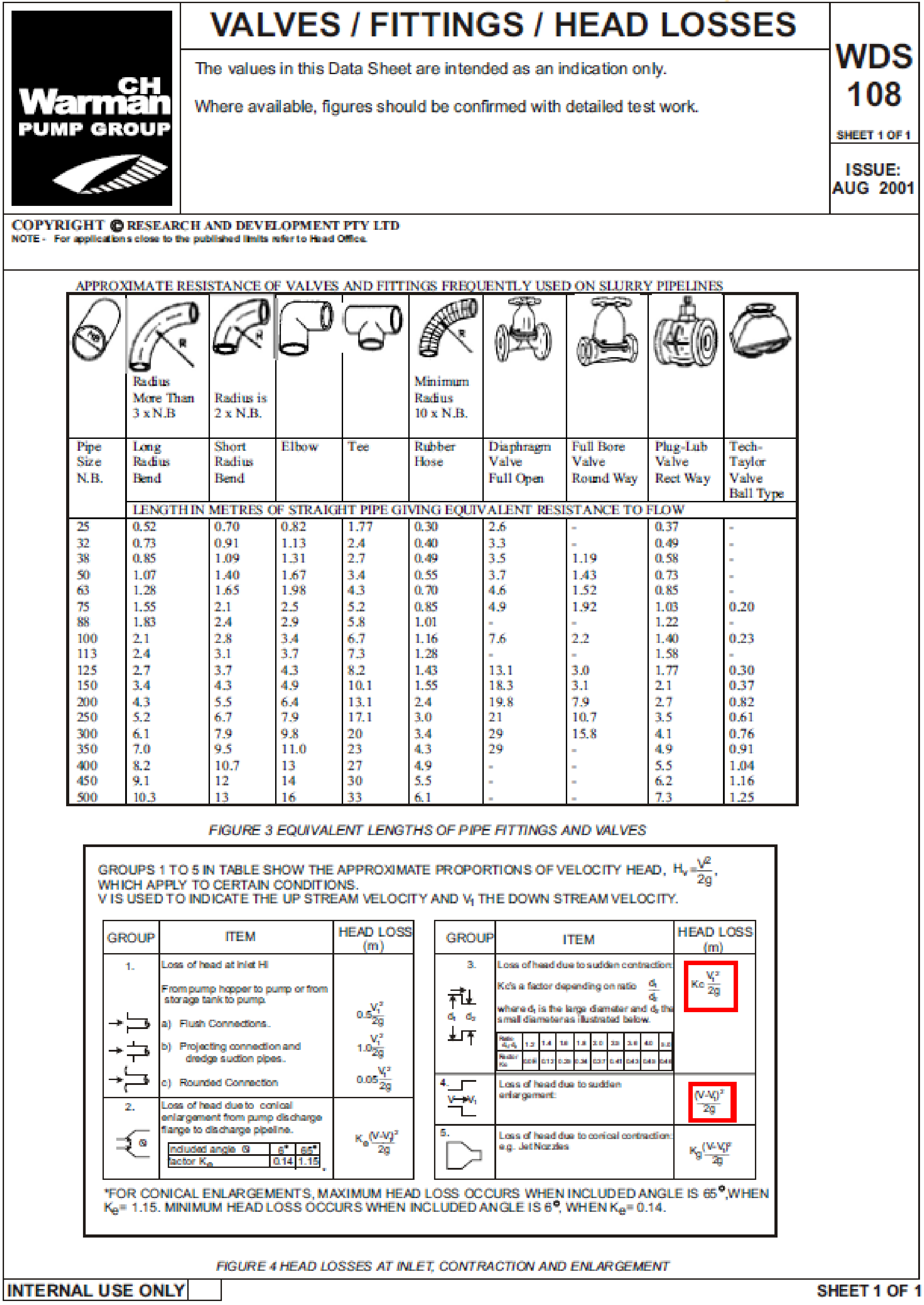

CH Warman
PUMP GROUP

VALVES / FITTINGS / HEAD LOSSES

The values in this Data Sheet are intended as an indication only.

Where available, figures should be confirmed with detailed test work.

WDS 108

SHEET 1 OF 1

ISSUE:
AUG 2001

NOTE - For applications close to the published limits refer to Head Office.

APPROXIMATE RESISTANCE OF VALVES AND FITTINGS FREQUENTLY USED ON SLURRY PIPELINES

	Radius More Than 3 x N.B	Radius is 2 x N.B.			Minimum Radius 10 x N.B.				
Pipe Size N.B.	Long Radius Bend	Short Radius Bend	Elbow	Tee	Rubber Hose	Diaphragm Valve Full Open	Full Bore Valve Round Way	Plug-Lub Valve Rect Way	Tech-Taylor Valve Ball Type
	LENGTH IN METRES OF STRAIGHT PIPE GIVING EQUIVALENT RESISTANCE TO FLOW								
25	0.52	0.70	0.82	1.77	0.30	2.6	-	0.37	-
32	0.73	0.91	1.13	2.4	0.40	3.3	-	0.49	-
38	0.85	1.09	1.31	2.7	0.49	3.5	1.19	0.58	-
50	1.07	1.40	1.67	3.4	0.55	3.7	1.43	0.73	-
63	1.28	1.65	1.98	4.3	0.70	4.6	1.52	0.85	-
75	1.55	2.1	2.5	5.2	0.85	4.9	1.92	1.03	0.20
88	1.83	2.4	2.9	5.8	1.01	-	-	1.22	-
100	2.1	2.8	3.4	6.7	1.16	7.6	2.2	1.40	0.23
113	2.4	3.1	3.7	7.3	1.28	-	-	1.58	-
125	2.7	3.7	4.3	8.2	1.43	13.1	3.0	1.77	0.30
150	3.4	4.3	4.9	10.1	1.55	18.3	3.1	2.1	0.37
200	4.3	5.5	6.4	13.1	2.4	19.8	7.9	2.7	0.82
250	5.2	6.7	7.9	17.1	3.0	21	10.7	3.5	0.61
300	6.1	7.9	9.8	20	3.4	29	15.8	4.1	0.76
350	7.0	9.5	11.0	23	4.3	29	-	4.9	0.91
400	8.2	10.7	13	27	4.9	-	-	5.5	1.04
450	9.1	12	14	30	5.5	-	-	6.2	1.16
500	10.3	13	16	33	6.1	-	-	7.3	1.25

FIGURE 3 EQUIVALENT LENGTHS OF PIPE FITTINGS AND VALVES

GROUPS 1 TO 5 IN TABLE SHOW THE APPROXIMATE PROPORTIONS OF VELOCITY HEAD, $H_v = \frac{V^2}{2g}$, WHICH APPLY TO CERTAIN CONDITIONS.
V IS USED TO INDICATE THE UP STREAM VELOCITY AND V_1 THE DOWN STREAM VELOCITY.

GROUP	ITEM	HEAD LOSS (m)
1.	Loss of head at inlet HI From pump hopper to pump or from storage tank to pump.	
	a) Flush Connections.	$0.5\frac{V_1^2}{2g}$
	b) Projecting connection and dredge suction pipes.	$1.0\frac{V_1^2}{2g}$
	c) Rounded Connection	$0.05\frac{V_1^2}{2g}$
2.	Loss of head due to conical enlargement from pump discharge flange to discharge pipeline. Included angle θ: 6° / 65° factor K_e: 0.14 / 1.15 *	$K_e\frac{(V-V_1)^2}{2g}$

GROUP	ITEM	HEAD LOSS (m)
3.	Loss of head due to sudden contraction: Kc is a factor depending on ratio $\frac{d_1}{d_2}$ where d_1 is the large diameter and d_2 the small diameter as illustrated below. Ratio d_1/d_2: 1.2, 1.4, 1.6, 1.8, 2.0, [illegible], 3.0, 4.0, 5.0 Factor Kc: 0.08, 0.17, 0.26, 0.34, 0.37, 0.41, 0.43, [illegible], [illegible]	$Kc\frac{V_1^2}{2g}$
4.	Loss of head due to sudden enlargement:	$\frac{(V-V_1)^2}{2g}$
5.	Loss of head due to conical contraction: e.g. Jet Nozzles	$K_g\frac{(V-V_1)^2}{2g}$

*FOR CONICAL ENLARGEMENTS, MAXIMUM HEAD LOSS OCCURS WHEN INCLUDED ANGLE IS 65°, WHEN K_e = 1.15. MINIMUM HEAD LOSS OCCURS WHEN INCLUDED ANGLE IS 6°, WHEN K_e = 0.14.

FIGURE 4 HEAD LOSSES AT INLET, CONTRACTION AND ENLARGEMENT

INTERNAL USE ONLY

SHEET 1 OF 1

Appendix 1b: Warman pipe friction chart

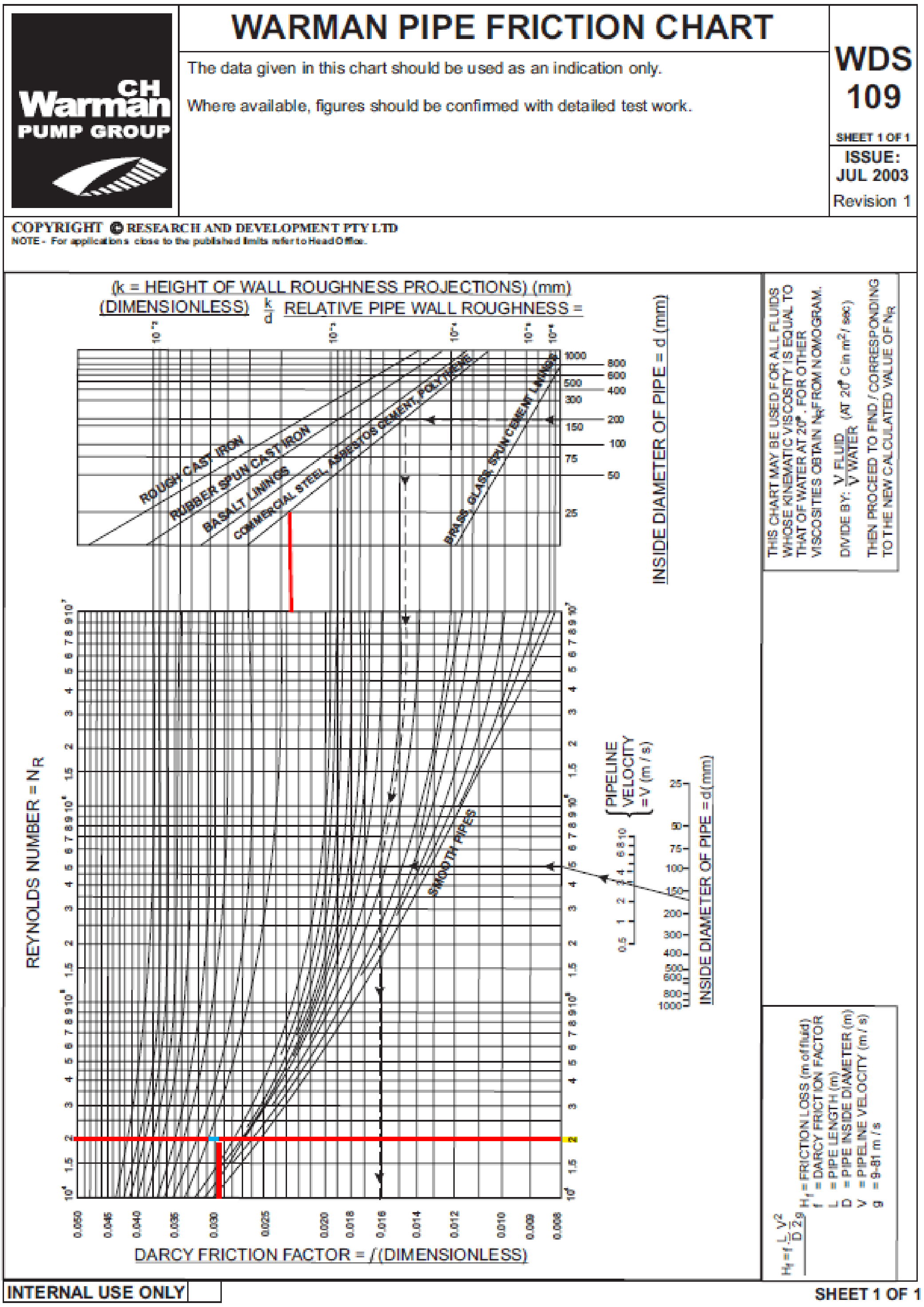

CH Warman PUMP GROUP

WARMAN PIPE FRICTION CHART

The data given in this chart should be used as an indication only.

Where available, figures should be confirmed with detailed test work.

WDS 109

SHEET 1 OF 1

ISSUE: JUL 2003

Revision 1

NOTE - For applications close to the published limits refer to Head Office.

THIS CHART MAY BE USED FOR ALL FLUIDS WHOSE KINEMATIC VISCOSITY IS EQUAL TO THAT OF WATER AT 20°. FOR OTHER VISCOSITIES OBTAIN N_R FROM NOMOGRAM.

DIVIDE BY: $\frac{V \text{ FLUID}}{V \text{ WATER}}$ (AT 20° C in m²/sec)

THEN PROCEED TO FIND / CORRESPONDING TO THE NEW CALCULATED VALUE OF N_R

$$H_f = f \frac{L}{D} \frac{V^2}{2g}$$

H_f = FRICTION LOSS (m of fluid)
f = DARCY FRICTION FACTOR
L = PIPE LENGTH (m)
D = PIPE INSIDE DIAMETER (m)
V = PIPELINE VELOCITY (m / s)
g = 9·81 m / s

INTERNAL USE ONLY

SHEET 1 OF 1

Appendix 2: Characteristic curves and performance data

CHARACTERISTIC CURVES AND PERFORMANCE DATA 60 Hz n= 3450 min⁻¹ HS= 0 m

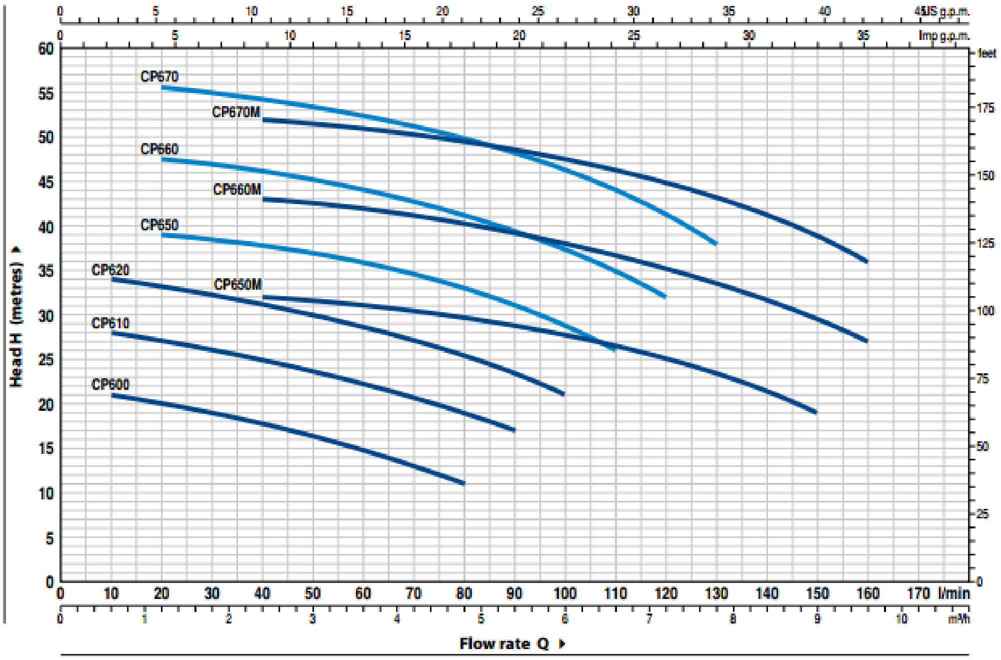

MODEL		POWER (P2)			Q													
					m³/h	0	0.6	1.2	2.4	3.6	4.8	5.4	6.0	6.6	7.2	7.8	9.0	9.6
Single-phase	**Three-phase**	**kW**	**HP**	▲	l/min	**0**	**10**	**20**	**40**	**60**	**80**	**90**	**100**	**110**	**120**	**130**	**150**	**160**
CPm 600	**CP 600**	0.37	0.50	**IE2**	**H** metres	22	21	20	18	15	11							
CPm 610	**CP 610**	0.60	0.85			28.5	28	27	25	22	19	17						
CPm 620	**CP 620**	0.75	1	**IE3**		35	34	33	31	28.5	25.5	23.5	21					
CPm 650	**CP 650**	1.1	1.5			40	–	39	38	36	33.1	31.2	28.8	26				
CPm 660	**CP 660**	1.5	2			48	–	47.5	46	44	41	39.5	37.5	35	32			
CPm 670	**CP 670**	2.2	3			56	–	55.5	54.5	52.5	50	48.5	46.5	44	41.5	38		
CPm 650M	**CP 650M**	1.1	1.5			33	–	–	32	31	30	29	28	26.5	25	23	19	
CPm 660M	**CP 660M**	1.5	2			44	–	–	43	42	40	39	38	37	35.5	34	29.5	27
CPm 670M	**CP 670M**	2.2	3			53	–	–	52	51	49.5	48.5	47.5	46.5	45	43.5	39	36

Q = Flow rate **H** = Total manometric head **HS** = Suction height

Tolerance of characteristic curves in compliance with EN ISO 9906 Grade 3B.

▲ Performance class of the three-phase motor (IEC 60034-30-1)

Appendix 3: Properties of saturated water

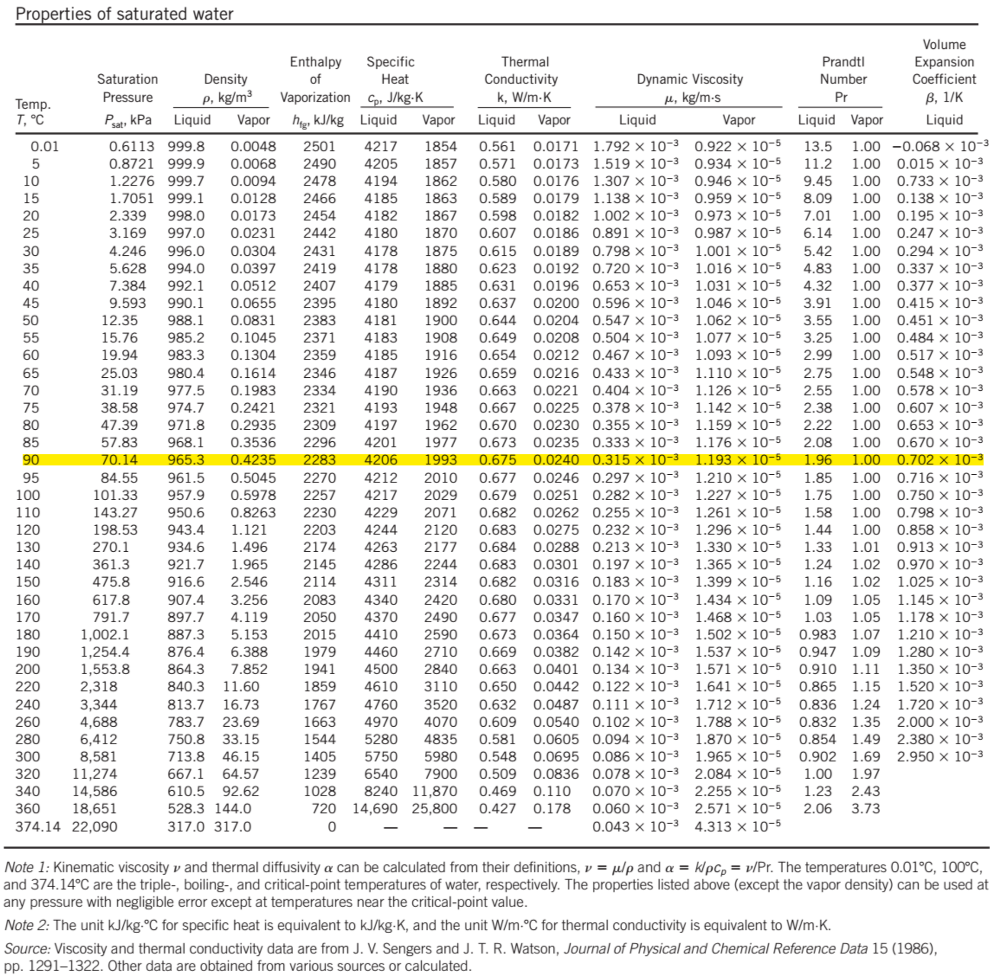

Properties of saturated water

Temp. T, °C	Saturation Pressure P_{sat}, kPa	Density ρ, kg/m³ Liquid	Density ρ, kg/m³ Vapor	Enthalpy of Vaporization h_{fg}, kJ/kg	Specific Heat c_p, J/kg·K Liquid	Specific Heat c_p, J/kg·K Vapor	Thermal Conductivity k, W/m·K Liquid	Thermal Conductivity k, W/m·K Vapor	Dynamic Viscosity μ, kg/m·s Liquid	Dynamic Viscosity μ, kg/m·s Vapor	Prandtl Number Pr Liquid	Prandtl Number Pr Vapor	Volume Expansion Coefficient β, 1/K Liquid
0.01	0.6113	999.8	0.0048	2501	4217	1854	0.561	0.0171	1.792×10^{-3}	0.922×10^{-5}	13.5	1.00	-0.068×10^{-3}
5	0.8721	999.9	0.0068	2490	4205	1857	0.571	0.0173	1.519×10^{-3}	0.934×10^{-5}	11.2	1.00	0.015×10^{-3}
10	1.2276	999.7	0.0094	2478	4194	1862	0.580	0.0176	1.307×10^{-3}	0.946×10^{-5}	9.45	1.00	0.733×10^{-3}
15	1.7051	999.1	0.0128	2466	4185	1863	0.589	0.0179	1.138×10^{-3}	0.959×10^{-5}	8.09	1.00	0.138×10^{-3}
20	2.339	998.0	0.0173	2454	4182	1867	0.598	0.0182	1.002×10^{-3}	0.973×10^{-5}	7.01	1.00	0.195×10^{-3}
25	3.169	997.0	0.0231	2442	4180	1870	0.607	0.0186	0.891×10^{-3}	0.987×10^{-5}	6.14	1.00	0.247×10^{-3}
30	4.246	996.0	0.0304	2431	4178	1875	0.615	0.0189	0.798×10^{-3}	1.001×10^{-5}	5.42	1.00	0.294×10^{-3}
35	5.628	994.0	0.0397	2419	4178	1880	0.623	0.0192	0.720×10^{-3}	1.016×10^{-5}	4.83	1.00	0.337×10^{-3}
40	7.384	992.1	0.0512	2407	4179	1885	0.631	0.0196	0.653×10^{-3}	1.031×10^{-5}	4.32	1.00	0.377×10^{-3}
45	9.593	990.1	0.0655	2395	4180	1892	0.637	0.0200	0.596×10^{-3}	1.046×10^{-5}	3.91	1.00	0.415×10^{-3}
50	12.35	988.1	0.0831	2383	4181	1900	0.644	0.0204	0.547×10^{-3}	1.062×10^{-5}	3.55	1.00	0.451×10^{-3}
55	15.76	985.2	0.1045	2371	4183	1908	0.649	0.0208	0.504×10^{-3}	1.077×10^{-5}	3.25	1.00	0.484×10^{-3}
60	19.94	983.3	0.1304	2359	4185	1916	0.654	0.0212	0.467×10^{-3}	1.093×10^{-5}	2.99	1.00	0.517×10^{-3}
65	25.03	980.4	0.1614	2346	4187	1926	0.659	0.0216	0.433×10^{-3}	1.110×10^{-5}	2.75	1.00	0.548×10^{-3}
70	31.19	977.5	0.1983	2334	4190	1936	0.663	0.0221	0.404×10^{-3}	1.126×10^{-5}	2.55	1.00	0.578×10^{-3}
75	38.58	974.7	0.2421	2321	4193	1948	0.667	0.0225	0.378×10^{-3}	1.142×10^{-5}	2.38	1.00	0.607×10^{-3}
80	47.39	971.8	0.2935	2309	4197	1962	0.670	0.0230	0.355×10^{-3}	1.159×10^{-5}	2.22	1.00	0.653×10^{-3}
85	57.83	968.1	0.3536	2296	4201	1977	0.673	0.0235	0.333×10^{-3}	1.176×10^{-5}	2.08	1.00	0.670×10^{-3}
90	70.14	965.3	0.4235	2283	4206	1993	0.675	0.0240	0.315×10^{-3}	1.193×10^{-5}	1.96	1.00	0.702×10^{-3}
95	84.55	961.5	0.5045	2270	4212	2010	0.677	0.0246	0.297×10^{-3}	1.210×10^{-5}	1.85	1.00	0.716×10^{-3}
100	101.33	957.9	0.5978	2257	4217	2029	0.679	0.0251	0.282×10^{-3}	1.227×10^{-5}	1.75	1.00	0.750×10^{-3}
110	143.27	950.6	0.8263	2230	4229	2071	0.682	0.0262	0.255×10^{-3}	1.261×10^{-5}	1.58	1.00	0.798×10^{-3}
120	198.53	943.4	1.121	2203	4244	2120	0.683	0.0275	0.232×10^{-3}	1.296×10^{-5}	1.44	1.00	0.858×10^{-3}
130	270.1	934.6	1.496	2174	4263	2177	0.684	0.0288	0.213×10^{-3}	1.330×10^{-5}	1.33	1.01	0.913×10^{-3}
140	361.3	921.7	1.965	2145	4286	2244	0.683	0.0301	0.197×10^{-3}	1.365×10^{-5}	1.24	1.02	0.970×10^{-3}
150	475.8	916.6	2.546	2114	4311	2314	0.682	0.0316	0.183×10^{-3}	1.399×10^{-5}	1.16	1.02	1.025×10^{-3}
160	617.8	907.4	3.256	2083	4340	2420	0.680	0.0331	0.170×10^{-3}	1.434×10^{-5}	1.09	1.05	1.145×10^{-3}
170	791.7	897.7	4.119	2050	4370	2490	0.677	0.0347	0.160×10^{-3}	1.468×10^{-5}	1.03	1.05	1.178×10^{-3}
180	1,002.1	887.3	5.153	2015	4410	2590	0.673	0.0364	0.150×10^{-3}	1.502×10^{-5}	0.983	1.07	1.210×10^{-3}
190	1,254.4	876.4	6.388	1979	4460	2710	0.669	0.0382	0.142×10^{-3}	1.537×10^{-5}	0.947	1.09	1.280×10^{-3}
200	1,553.8	864.3	7.852	1941	4500	2840	0.663	0.0401	0.134×10^{-3}	1.571×10^{-5}	0.910	1.11	1.350×10^{-3}
220	2,318	840.3	11.60	1859	4610	3110	0.650	0.0442	0.122×10^{-3}	1.641×10^{-5}	0.865	1.15	1.520×10^{-3}
240	3,344	813.7	16.73	1767	4760	3520	0.632	0.0487	0.111×10^{-3}	1.712×10^{-5}	0.836	1.24	1.720×10^{-3}
260	4,688	783.7	23.69	1663	4970	4070	0.609	0.0540	0.102×10^{-3}	1.788×10^{-5}	0.832	1.35	2.000×10^{-3}
280	6,412	750.8	33.15	1544	5280	4835	0.581	0.0605	0.094×10^{-3}	1.870×10^{-5}	0.854	1.49	2.380×10^{-3}
300	8,581	713.8	46.15	1405	5750	5980	0.548	0.0695	0.086×10^{-3}	1.965×10^{-5}	0.902	1.69	2.950×10^{-3}
320	11,274	667.1	64.57	1239	6540	7900	0.509	0.0836	0.078×10^{-3}	2.084×10^{-5}	1.00	1.97	
340	14,586	610.5	92.62	1028	8240	11,870	0.469	0.110	0.070×10^{-3}	2.255×10^{-5}	1.23	2.43	
360	18,651	528.3	144.0	720	14,690	25,800	0.427	0.178	0.060×10^{-3}	2.571×10^{-5}	2.06	3.73	
374.14	22,090	317.0	317.0	0	—	—	—	—	0.043×10^{-3}	4.313×10^{-5}			

Note 1: Kinematic viscosity ν and thermal diffusivity α can be calculated from their definitions, $\nu = \mu/\rho$ and $\alpha = k/\rho c_p = \nu/\mathrm{Pr}$. The temperatures 0.01°C, 100°C, and 374.14°C are the triple-, boiling-, and critical-point temperatures of water, respectively. The properties listed above (except the vapor density) can be used at any pressure with negligible error except at temperatures near the critical-point value.

Note 2: The unit kJ/kg·°C for specific heat is equivalent to kJ/kg·K, and the unit W/m·°C for thermal conductivity is equivalent to W/m·K.

Source: Viscosity and thermal conductivity data are from J. V. Sengers and J. T. R. Watson, *Journal of Physical and Chemical Reference Data* 15 (1986), pp. 1291–1322. Other data are obtained from various sources or calculated.

Appendix 4a: First pressure test results

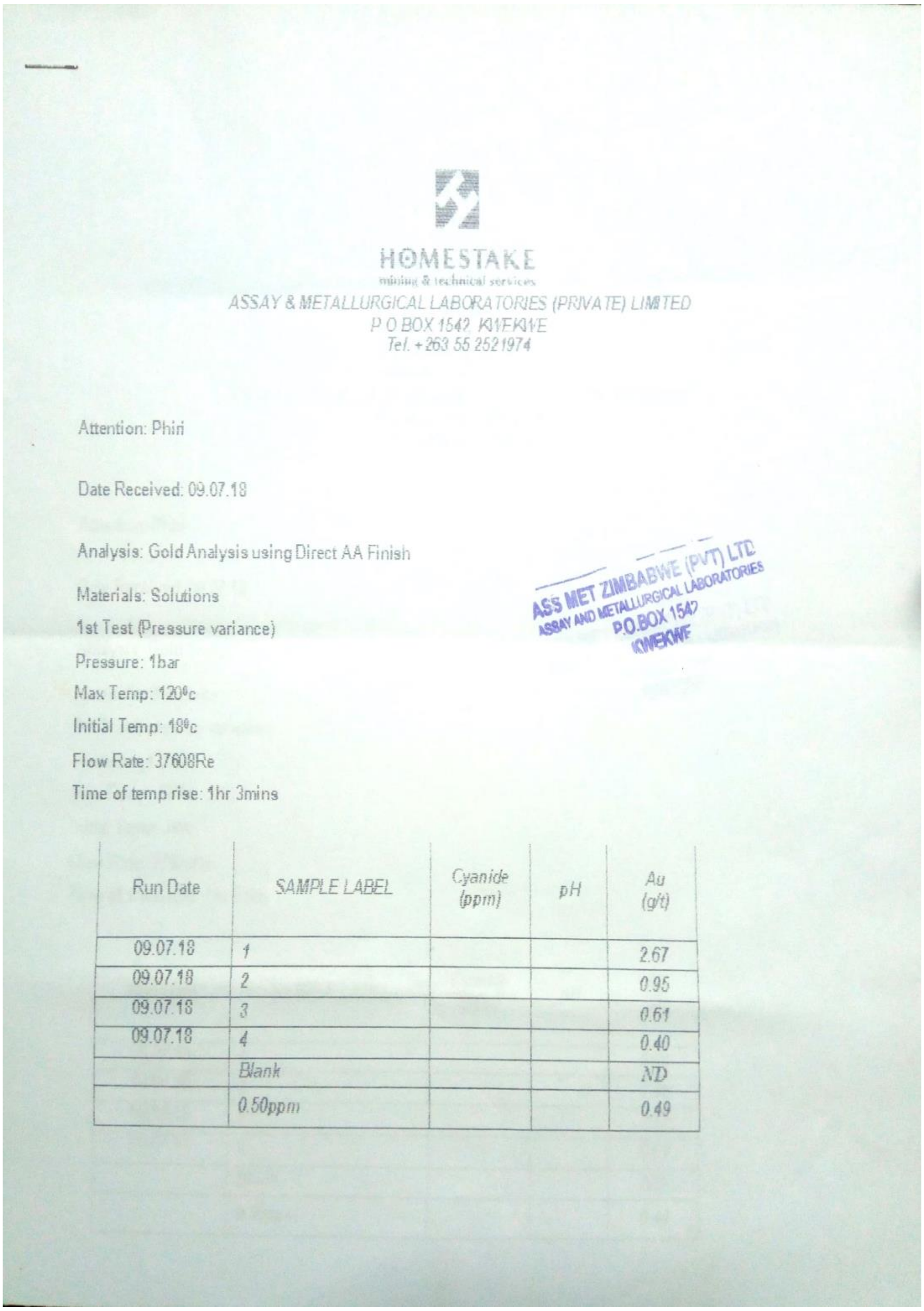

HOMESTAKE
mining & technical services
ASSAY & METALLURGICAL LABORATORIES (PRIVATE) LIMITED
P O BOX 1542 KWEKWE
Tel. +263 55 2521974

Attention: Phiri

Date Received: 09.07.18

Analysis: Gold Analysis using Direct AA Finish

Materials: Solutions

1st Test (Pressure variance)

Pressure: 1bar

Max Temp: 120^{0}c

Initial Temp: 18^{0}c

Flow Rate: 37608Re

Time of temp rise: 1hr 3mins

ASS MET ZIMBABWE (PVT) LTD
ASSAY AND METALLURGICAL LABORATORIES
P.O.BOX 1542
KWEKWE

Run Date	SAMPLE LABEL	Cyanide (ppm)	pH	Au (g/t)
09.07.18	1			2.67
09.07.18	2			0.95
09.07.18	3			0.61
09.07.18	4			0.40
	Blank			ND
	0.50ppm			0.49

Appendix 4b: Second pressure test results

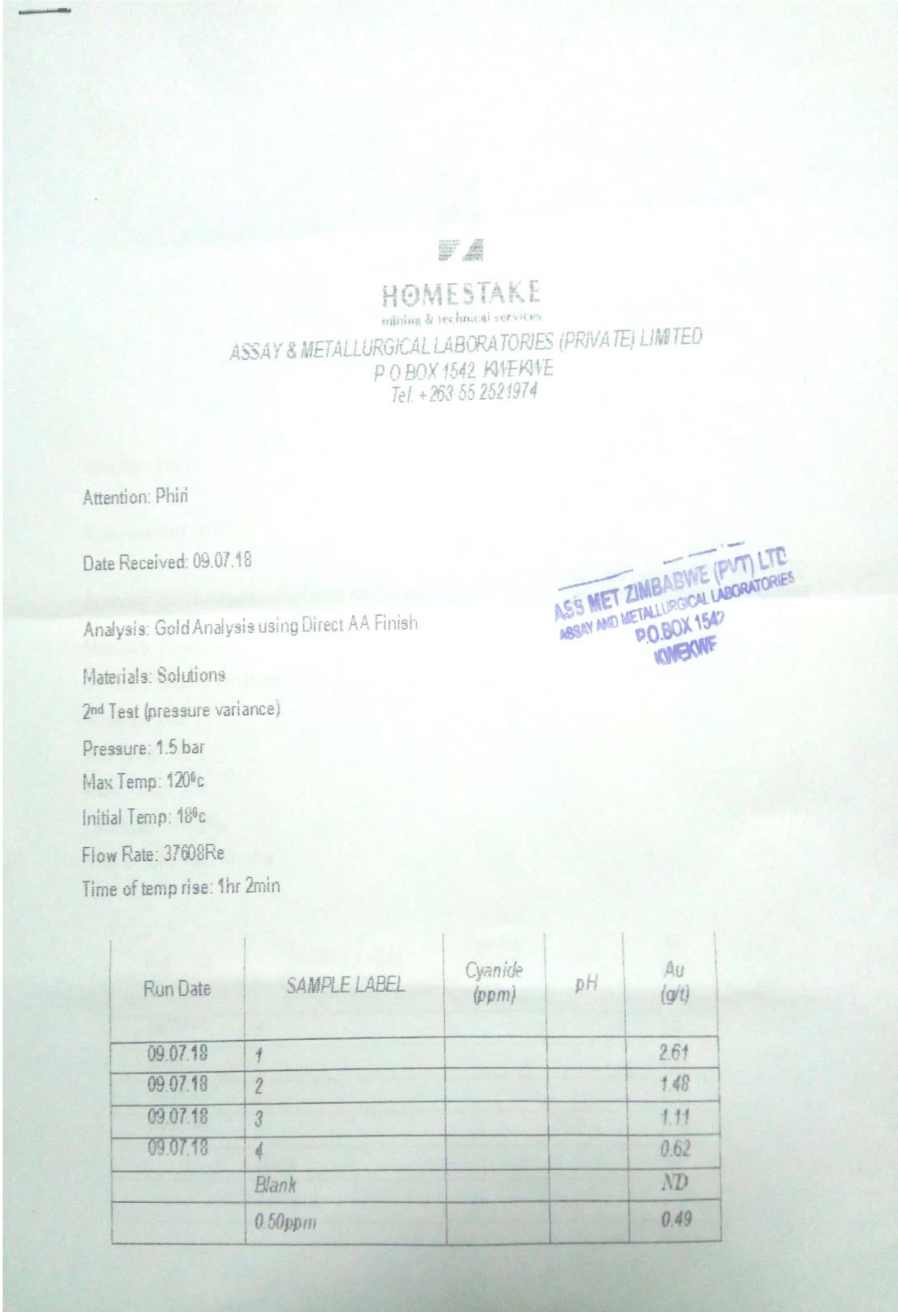

HOMESTAKE
mining & technical services
ASSAY & METALLURGICAL LABORATORIES (PRIVATE) LIMITED
P O BOX 1542, KWEKWE
Tel. +263 55 2521974

Attention: Phiri

Date Received: 09.07.18

ASS MET ZIMBABWE (PVT) LTD
ASSAY AND METALLURGICAL LABORATORIES
P.O.BOX 1542
KWEKWE

Analysis: Gold Analysis using Direct AA Finish

Materials: Solutions

2nd Test (pressure variance)

Pressure: 1.5 bar

Max Temp: 120^{0}c

Initial Temp: 18^{0}c

Flow Rate: 37608Re

Time of temp rise: 1hr 2min

Run Date	SAMPLE LABEL	Cyanide (ppm)	pH	Au (g/t)
09.07.18	1			2.61
09.07.18	2			1.48
09.07.18	3			1.11
09.07.18	4			0.62
	Blank			ND
	0.50ppm			0.49

Appendix 4c: Third pressure test results

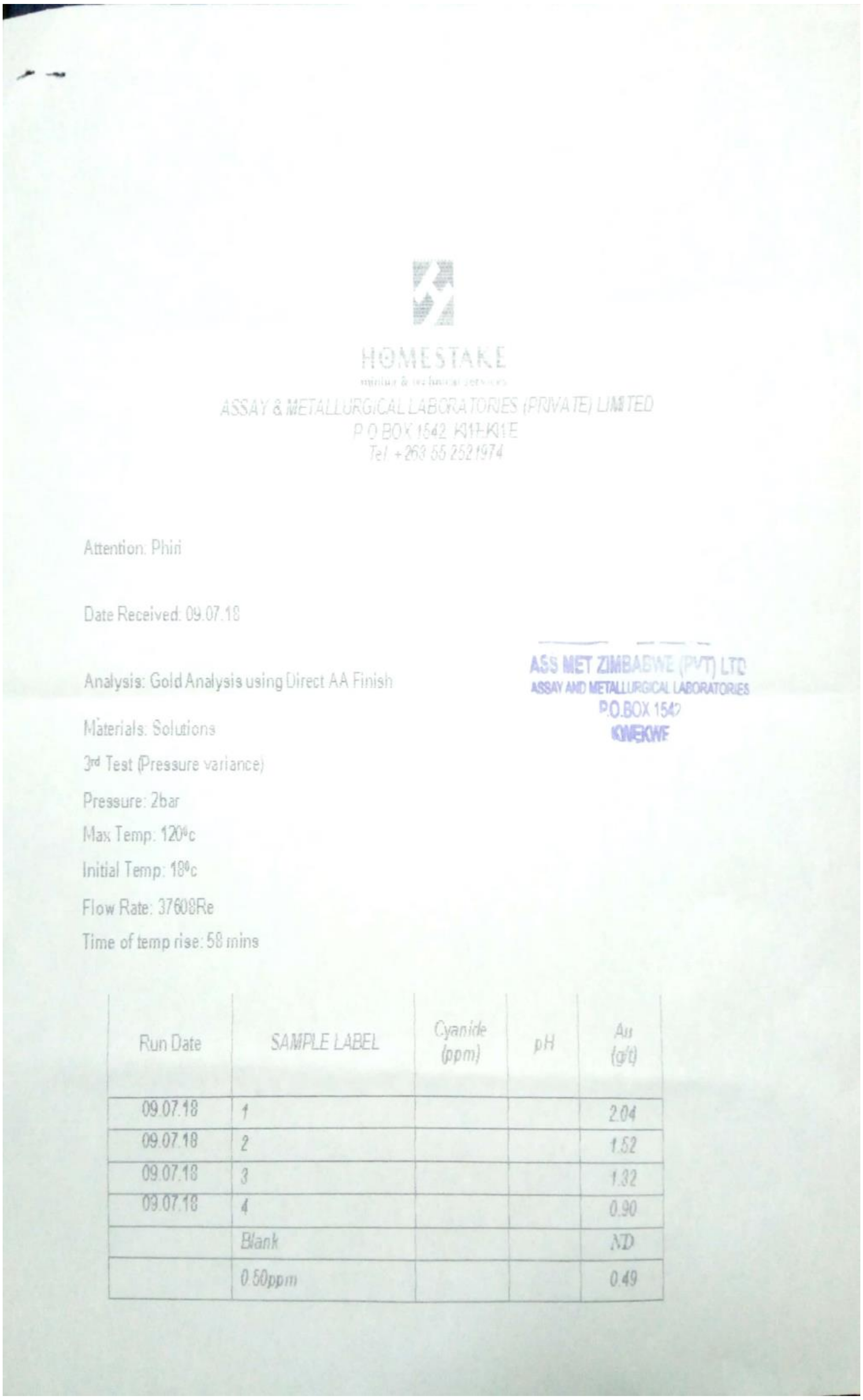

HOMESTAKE
mining & technical services
ASSAY & METALLURGICAL LABORATORIES (PRIVATE) LIMITED
P O BOX 1542, KWEKWE
Tel. +263 55 2521974

Attention: Phiri

Date Received: 09.07.18

Analysis: Gold Analysis using Direct AA Finish

ASS MET ZIMBABWE (PVT) LTD
ASSAY AND METALLURGICAL LABORATORIES
P.O.BOX 1542
KWEKWE

Materials: Solutions

3rd Test (Pressure variance)

Pressure: 2bar

Max Temp: 120^{0}c

Initial Temp: 18^{0}c

Flow Rate: 37608Re

Time of temp rise: 58 mins

Run Date	SAMPLE LABEL	Cyanide (ppm)	pH	Au (g/t)
09.07.18	1			2.04
09.07.18	2			1.52
09.07.18	3			1.32
09.07.18	4			0.90
	Blank			ND
	0.50ppm			0.49

Appendix 5a: First temperature test results

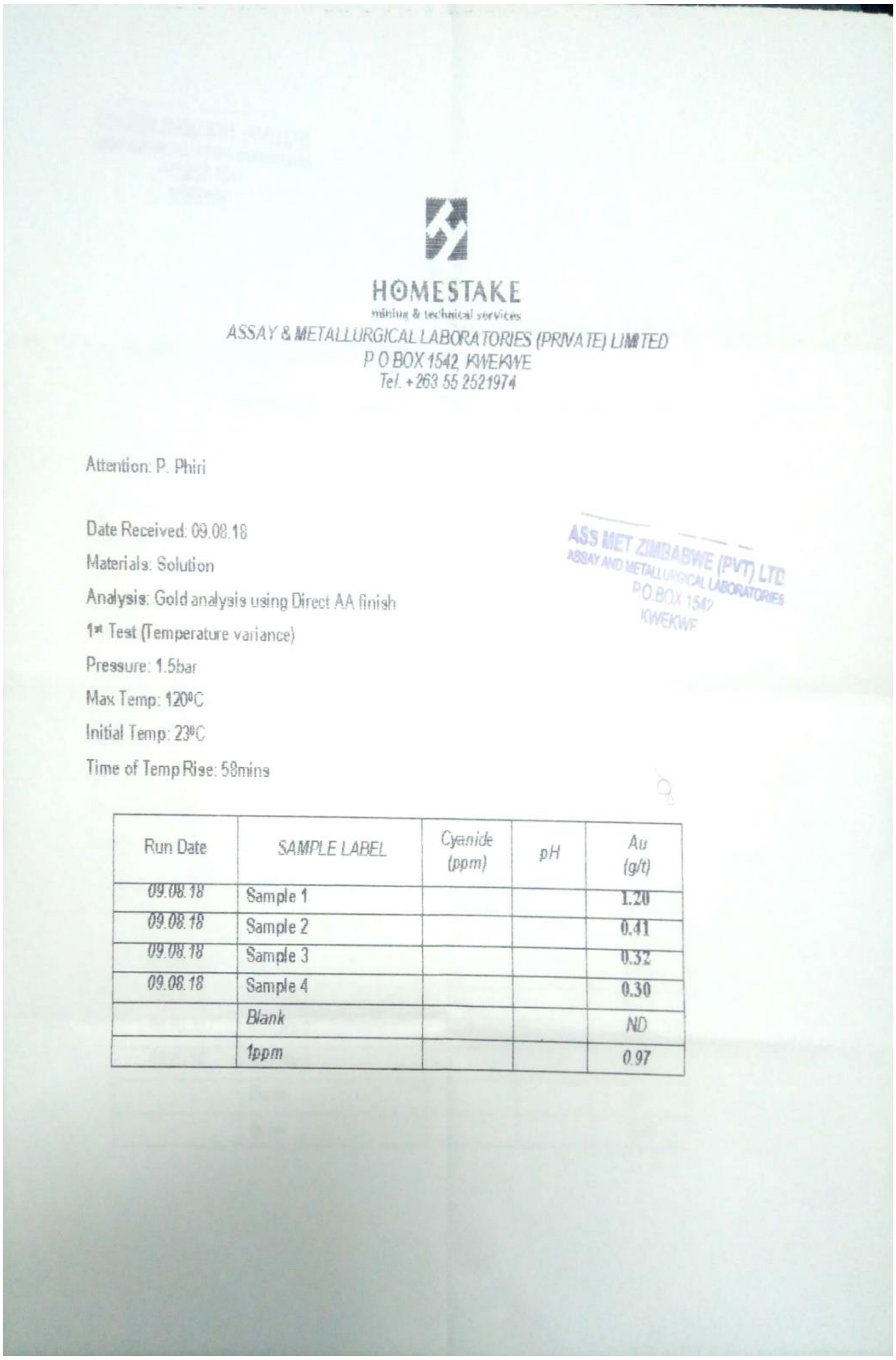

HOMESTAKE
mining & technical services
ASSAY & METALLURGICAL LABORATORIES (PRIVATE) LIMITED
P O BOX 1542, KWEKWE
Tel. +263 55 2521974

ASS MET ZIMBABWE (PVT) LTD
ASSAY AND METALLURGICAL LABORATORIES
P.O.BOX 1542
KWEKWE

Attention: P. Phiri

Date Received: 09.08.18
Materials: Solution
Analysis: Gold analysis using Direct AA finish
1st Test (Temperature variance)
Pressure: 1.5bar
Max Temp: 120°C
Initial Temp: 23°C
Time of Temp Rise: 58mins

Run Date	SAMPLE LABEL	Cyanide (ppm)	pH	Au (g/t)
09.08.18	Sample 1			1.20
09.08.18	Sample 2			0.41
09.08.18	Sample 3			0.32
09.08.18	Sample 4			0.30
	Blank			ND
	1ppm			0.97

Appendix 5b: Second temperature test results

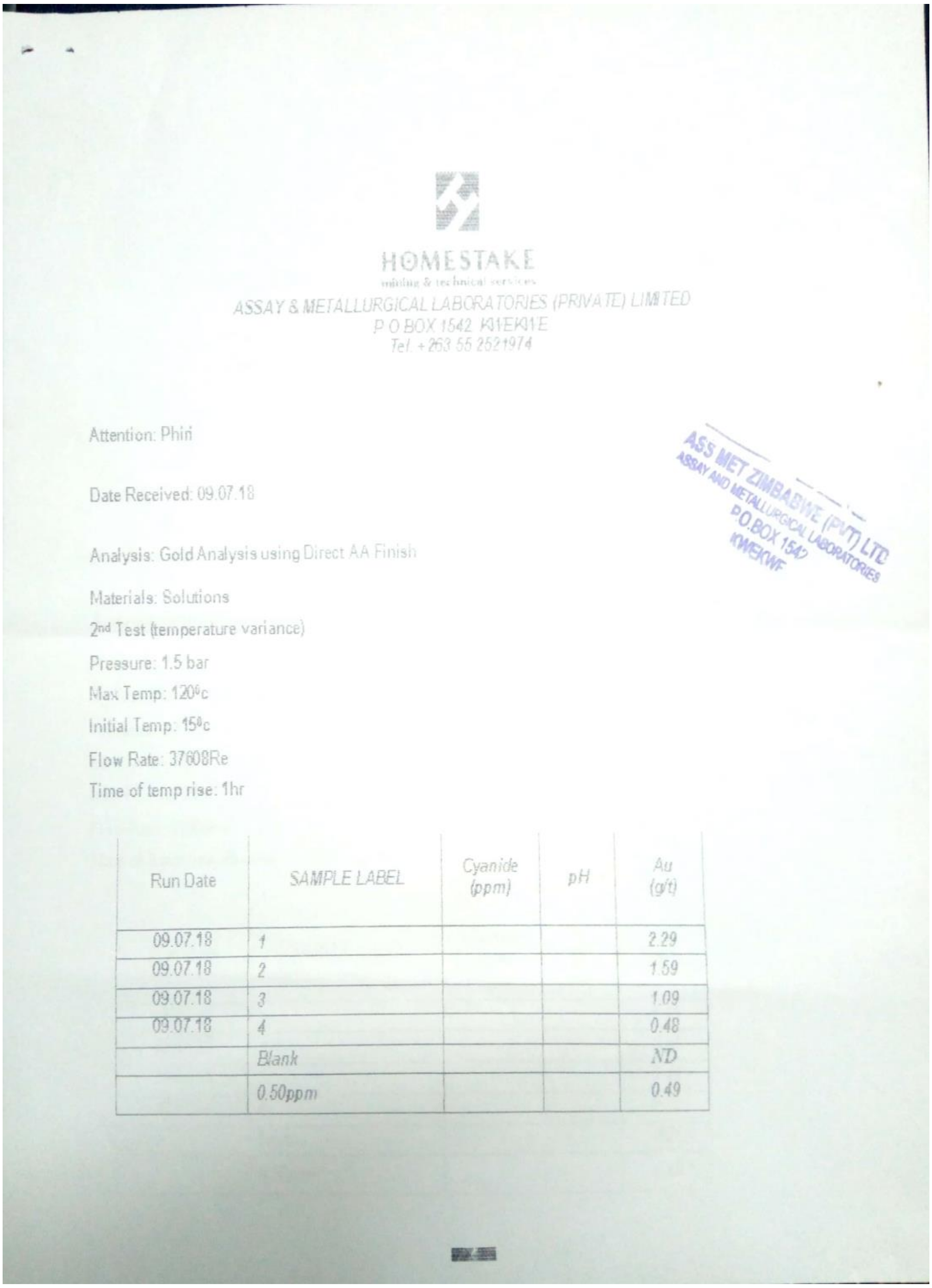

HOMESTAKE
mining & technical services
ASSAY & METALLURGICAL LABORATORIES (PRIVATE) LIMITED
P O BOX 1542 KWEKWE
Tel. +263 55 2521974

ASS MET ZIMBABWE (PVT) LTD
ASSAY AND METALLURGICAL LABORATORIES
P.O.BOX 1542
KWEKWE

Attention: Phiri

Date Received: 09.07.18

Analysis: Gold Analysis using Direct AA Finish

Materials: Solutions

2nd Test (temperature variance)

Pressure: 1.5 bar

Max Temp: 120⁰c

Initial Temp: 15⁰c

Flow Rate: 37608Re

Time of temp rise: 1hr

Run Date	SAMPLE LABEL	Cyanide (ppm)	pH	Au (g/t)
09.07.18	1			2.29
09.07.18	2			1.59
09.07.18	3			1.09
09.07.18	4			0.48
	Blank			ND
	0.50ppm			0.49

Appendix 5c: Third temperature test results

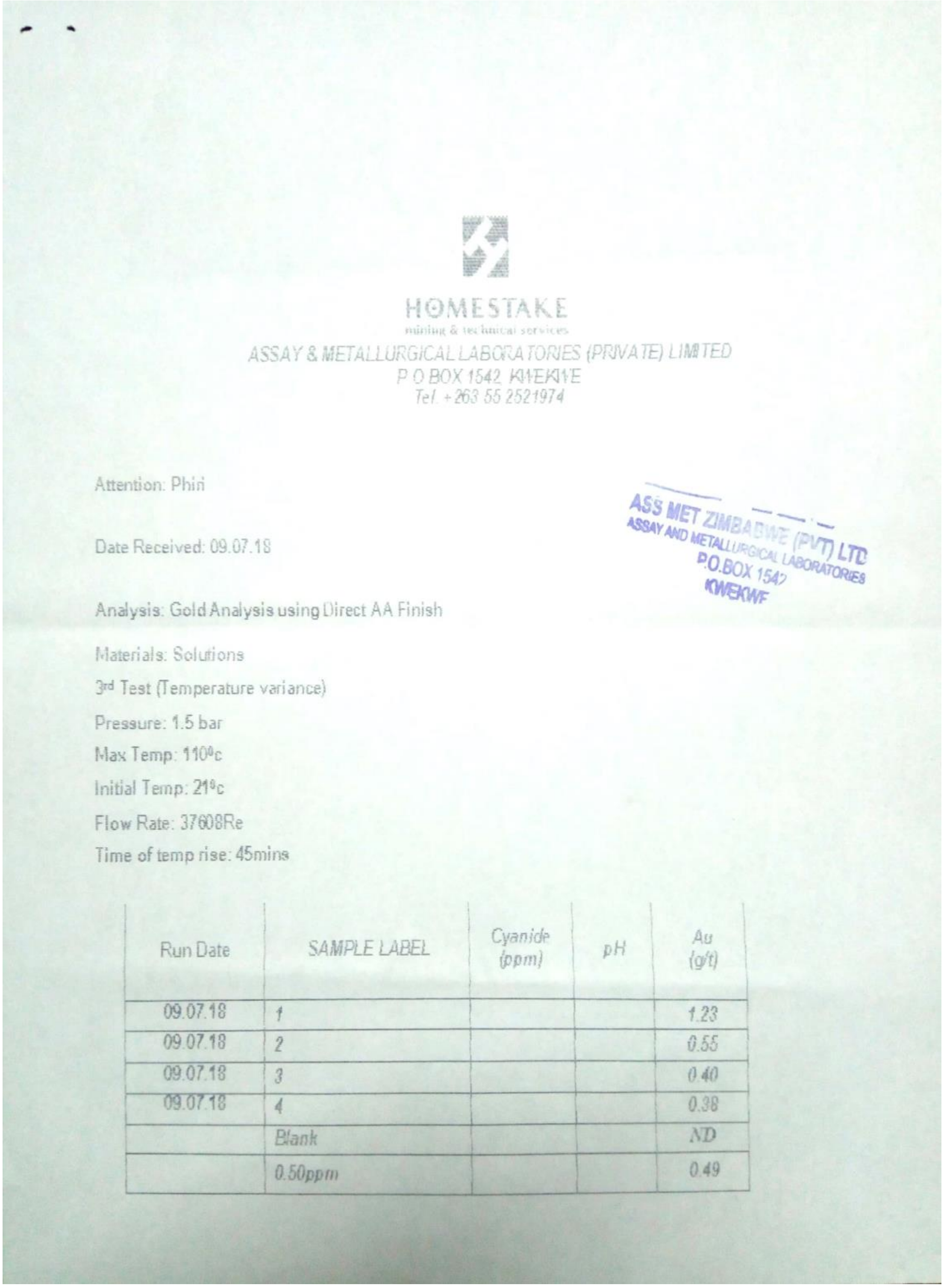

HOMESTAKE
mining & technical services
ASSAY & METALLURGICAL LABORATORIES (PRIVATE) LIMITED
P O BOX 1542, KWEKWE
Tel. +263 55 2521974

Attention: Phiri

Date Received: 09.07.18

ASS MET ZIMBABWE (PVT) LTD
ASSAY AND METALLURGICAL LABORATORIES
P.O.BOX 1542
KWEKWE

Analysis: Gold Analysis using Direct AA Finish

Materials: Solutions

3rd Test (Temperature variance)

Pressure: 1.5 bar

Max Temp: 110⁰c

Initial Temp: 21⁰c

Flow Rate: 37608Re

Time of temp rise: 45mins

Run Date	SAMPLE LABEL	Cyanide (ppm)	pH	Au (g/t)
09.07.18	1			1.23
09.07.18	2			0.55
09.07.18	3			0.40
09.07.18	4			0.38
	Blank			ND
	0.50ppm			0.49

Appendix 6a: First flow rate test results

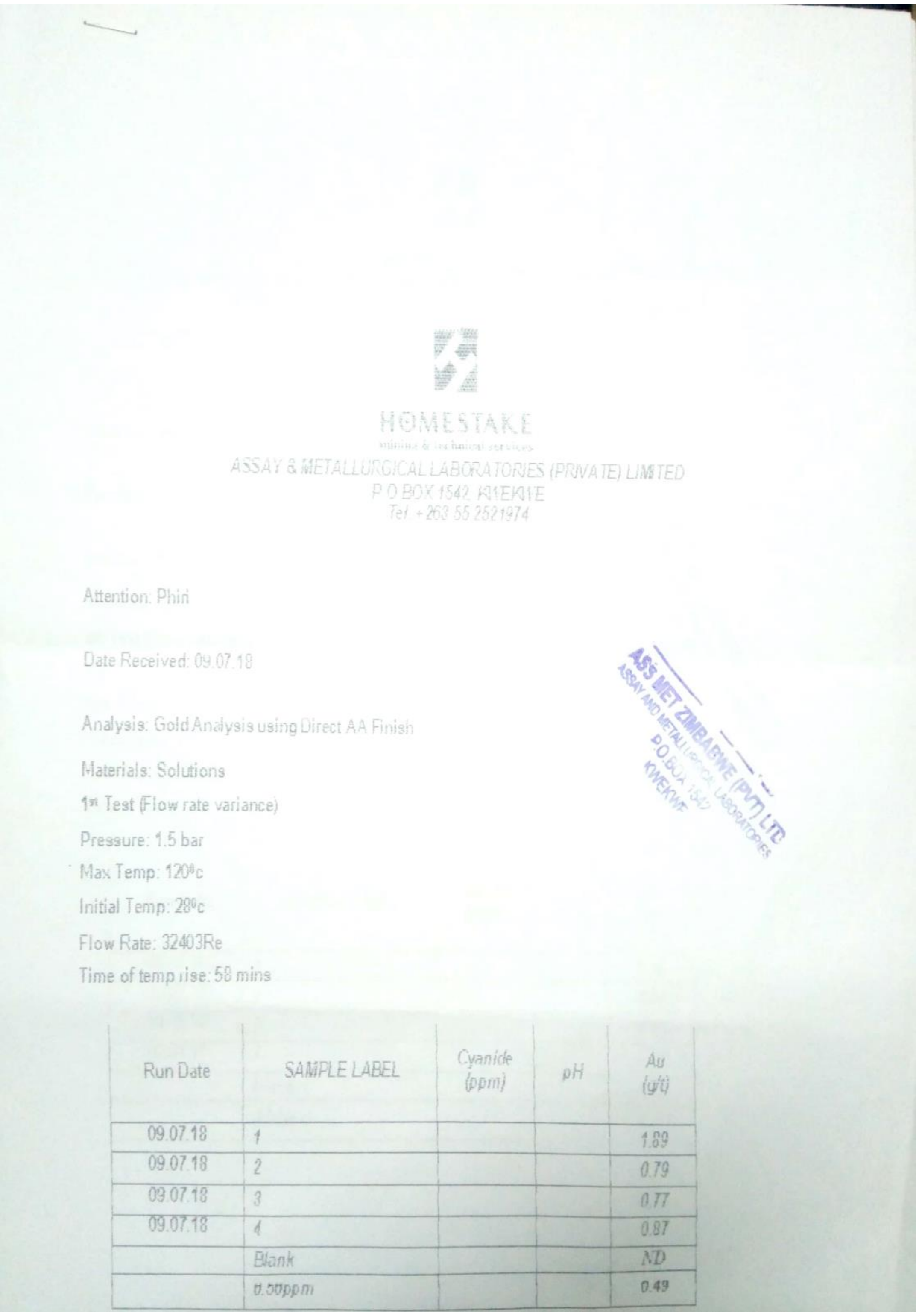

HOMESTAKE
mining & technical services
ASSAY & METALLURGICAL LABORATORIES (PRIVATE) LIMITED
P O BOX 1542, KWEKWE
Tel. +263 55 2521974

Attention: Phiri

Date Received: 09.07.18

Analysis: Gold Analysis using Direct AA Finish

Materials: Solutions

1st Test (Flow rate variance)

Pressure: 1.5 bar

Max Temp: 120^{0}c

Initial Temp: 28^{0}c

Flow Rate: 32403Re

Time of temp rise: 58 mins

ASS MET ZIMBABWE (PVT) LTD
ASSAY AND METALLURGICAL LABORATORIES
P.O.BOX 1542
KWEKWE

Run Date	SAMPLE LABEL	Cyanide (ppm)	pH	Au (g/t)
09.07.18	1			1.89
09.07.18	2			0.79
09.07.18	3			0.77
09.07.18	4			0.87
	Blank			ND
	0.50ppm			0.49

Appendix 6b: Second flow rate test results

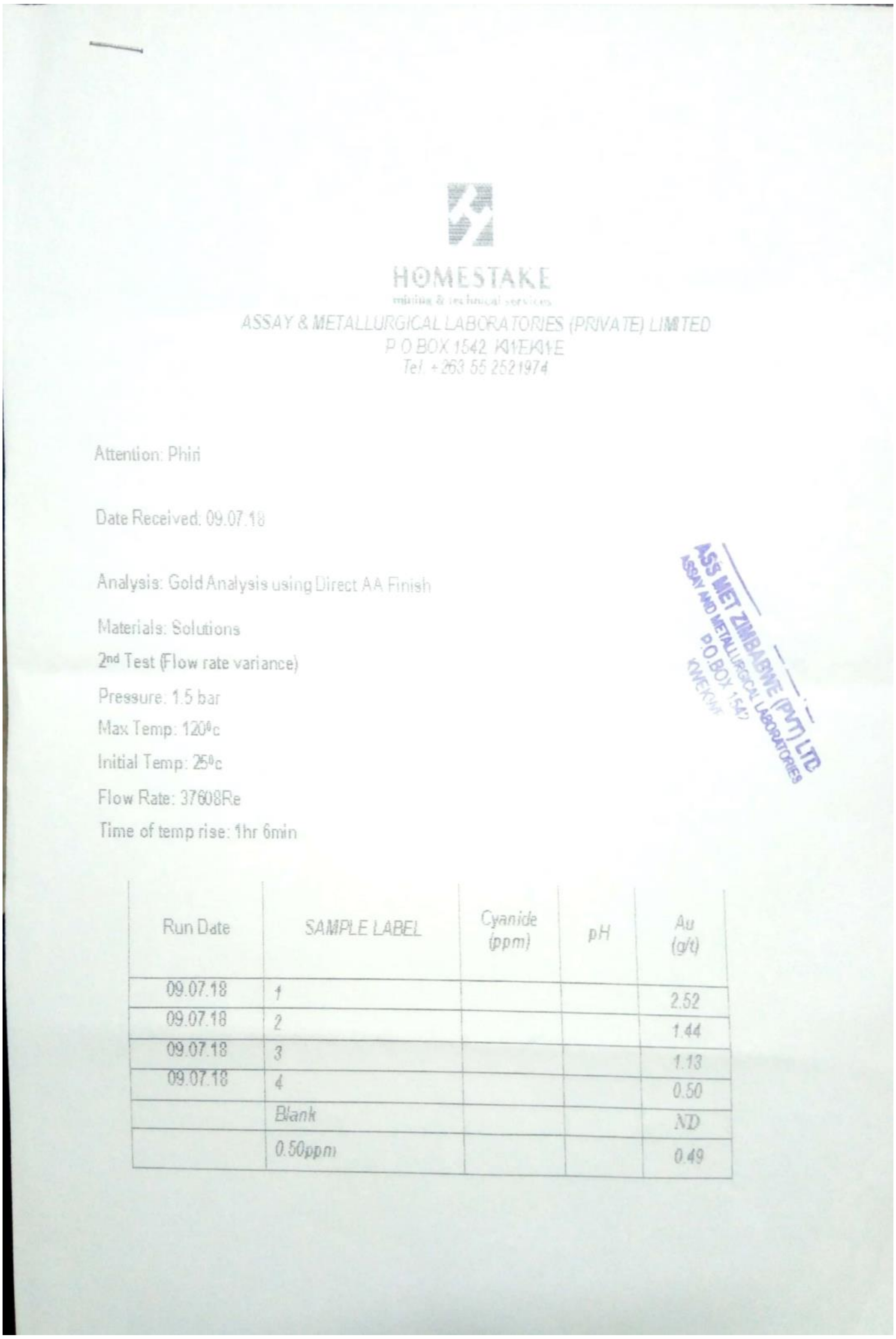

HOMESTAKE
mining & technical services
ASSAY & METALLURGICAL LABORATORIES (PRIVATE) LIMITED
P O BOX 1542 KWEKWE
Tel. +263 55 2521974

Attention: Phiri

Date Received: 09.07.18

Analysis: Gold Analysis using Direct AA Finish

Materials: Solutions

2nd Test (Flow rate variance)

Pressure: 1.5 bar

Max Temp: 120^{0}c

Initial Temp: 25^{0}c

Flow Rate: 37608Re

Time of temp rise: 1hr 6min

ASS MET ZIMBABWE (PVT) LTD
ASSAY AND METALLURGICAL LABORATORIES
P.O.BOX 1542
KWEKWE

Run Date	SAMPLE LABEL	Cyanide (ppm)	pH	Au (g/t)
09.07.18	1			2.52
09.07.18	2			1.44
09.07.18	3			1.13
09.07.18	4			0.50
	Blank			ND
	0.50ppm			0.49

Appendix 6c: Third flow rate test results

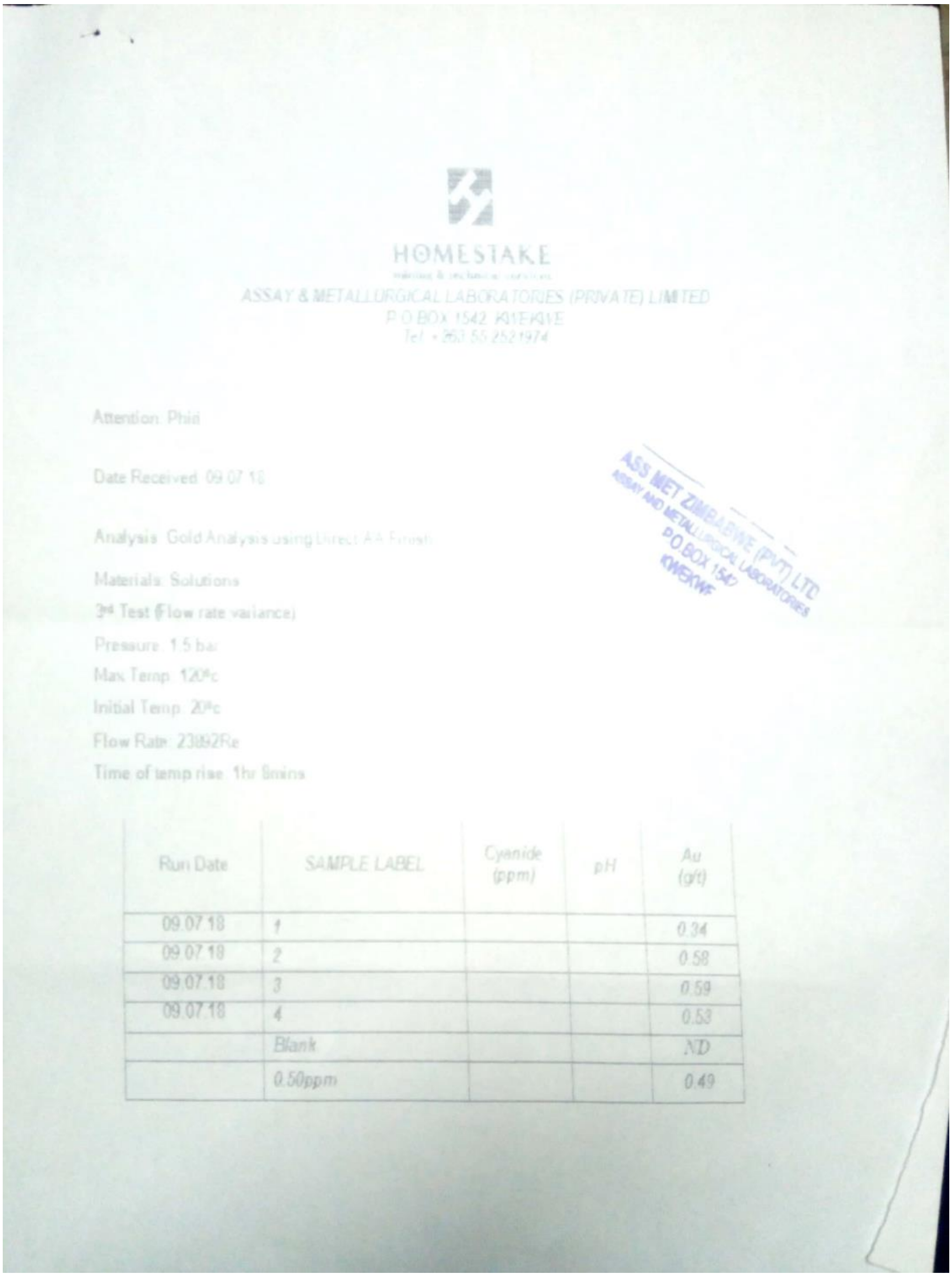

HOMESTAKE
mining & technical services
ASSAY & METALLURGICAL LABORATORIES (PRIVATE) LIMITED
P.O.BOX 1542 KWEKWE
Tel: +263 55 2521974

ASS MET ZIMBABWE (PVT) LTD
ASSAY AND METALLURGICAL LABORATORIES
P.O.BOX 1540
KWEKWE

Attention: Phiri

Date Received: 09.07.18

Analysis: Gold Analysis using Direct AA Finish

Materials: Solutions

3rd Test (Flow rate variance)

Pressure: 1.5 bar

Max Temp: 120°c

Initial Temp: 20°c

Flow Rate: 23892Re

Time of temp rise: 1hr 8mins

Run Date	SAMPLE LABEL	Cyanide (ppm)	pH	Au (g/t)
09.07.18	1			0.34
09.07.18	2			0.58
09.07.18	3			0.59
09.07.18	4			0.53
	Blank			ND
	0.50ppm			0.49

Appendix 7: Pressure linearity graphs

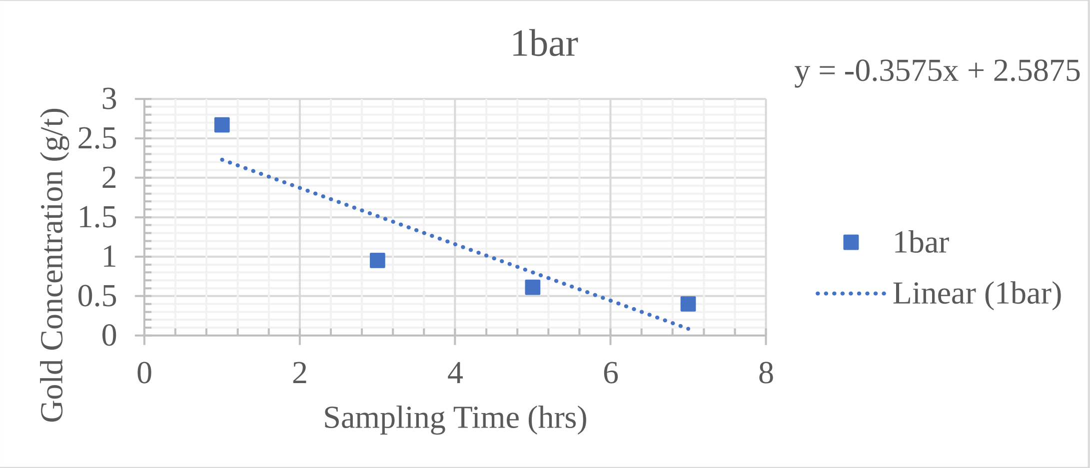

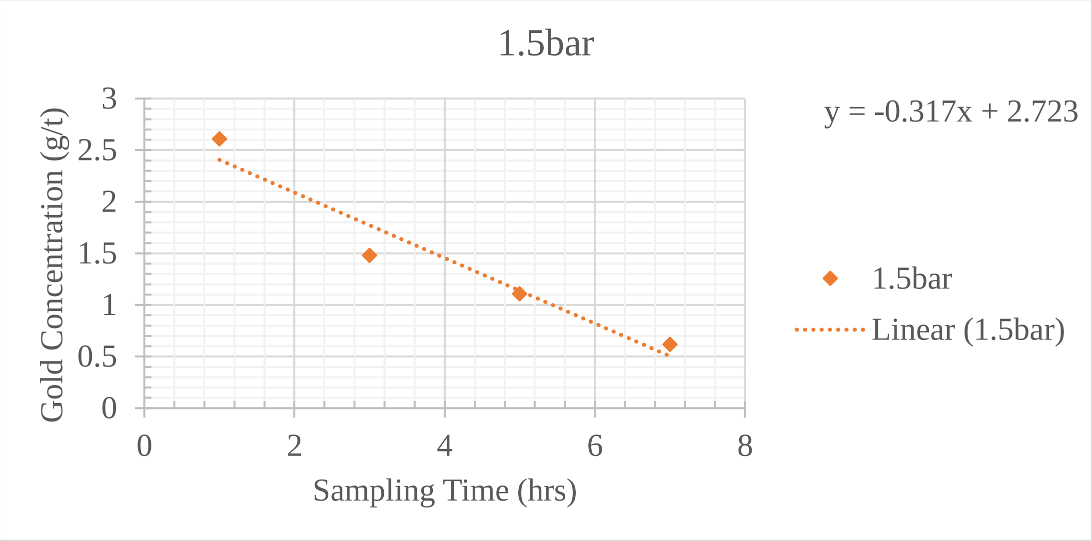

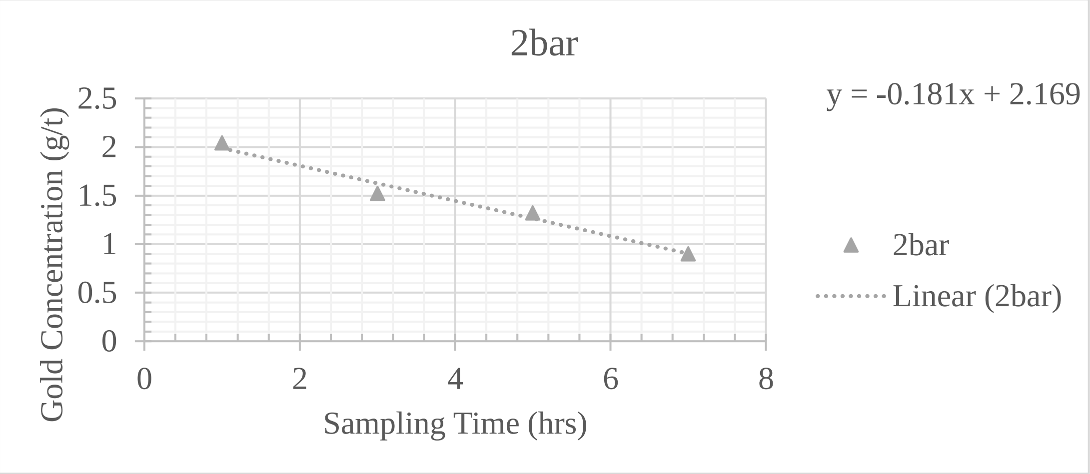

Appendix 8: Temperature linearity graphs

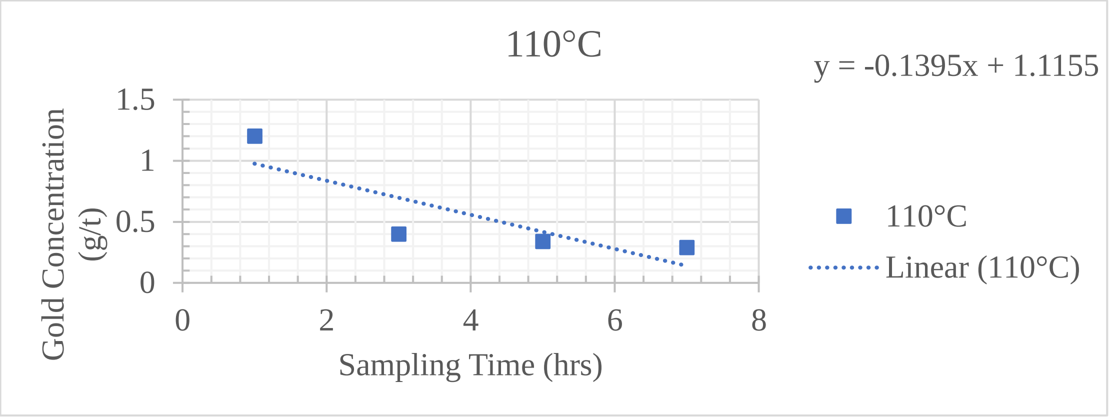

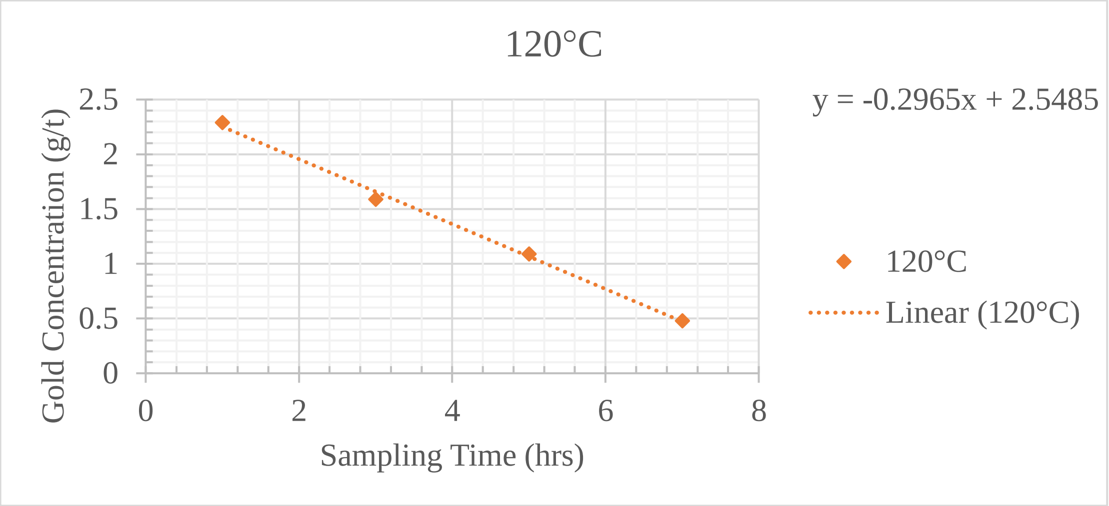

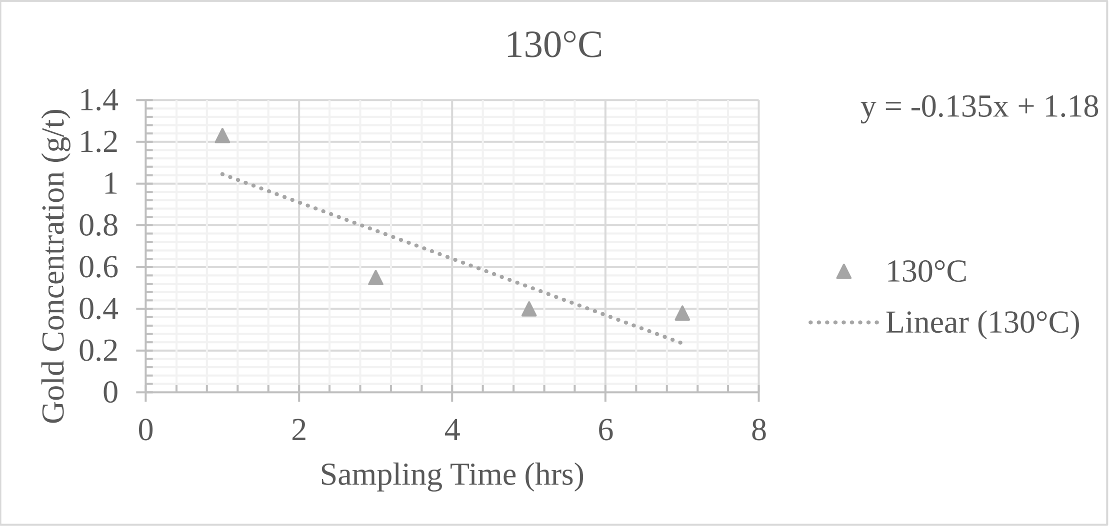

Appendix 9: Flow rate linearity graphs